12-2006

Computer Modeling of Tennessee Valley Authority's Coal Based Power Plant at Kingston to Predict the Effluent to Emory River

Bratendu Bagchi
University of Tennessee - Knoxville

To the Graduate Council:

I am submitting herewith a dissertation written by Bratendu Bagchi entitled "Computer Modeling of Tennessee Valley Authority's Coal Based Power Plant at Kingston to Predict the Effluent to Emory River." I have examined the final electronic copy of this dissertation for form and content and recommend that it be accepted in partial fulfillment of the requirements for the degree of Doctor of Philosophy, with a major in Chemical Engineering.

Paul R. Bienkowski, Major Professor

We have read this dissertation and recommend its acceptance:

Robert M. Counce, Naresh B. Handagama, Chris Cox

Accepted for the Council:

Carolyn R. Hodges

Vice Provost and Dean of the Graduate School

(Original signatures are on file with official student records.)

To the Graduate Council:

I am submitting herewith a dissertation written by Bratendu Bagchi entitled "Computer Modeling of Tennessee Valley Authority's Coal Based Power Plant at Kingston to Predict the Effluent to Emory River." I have examined the final electronic copy of this dissertation for form and content and recommend that it be accepted in partial fulfillment of the requirements for the degree of Doctor of Philosophy, with a major in Chemical Engineering.

Paul R.Bienkowski

Major Professor

We have read this dissertation
and recommend its acceptance:

Robert M.Counce

Naresh B.Handagama

Chris Cox

Accepted for the Council:

Linda Painter

Interim Dean of Graduate Studies

(Original signatures are on file with official student records)

Computer Modeling of Tennessee Valley Authority's Coal Based Power Plant at Kingston to Predict the Effluent to Emory River

A Dissertation

Presented for the Doctor of Philosophy Degree

The University of Tennessee, Knoxville

Bratendu Bagchi

December 2006

DEDICATION

This work is dedicated

to my family & friends

who matter to me so much

ACKNOWLEDGEMENTS

I am grateful to my major professor Dr. Paul R. Bienkowski for the guidance and help from time to time and for his contribution in the scholarly merit of this dissertation. I would like to express my gratitude to Dr. Naresh B. Handagama for the help in formulating my research ideas and for critically reviewing my experimental designs and results. I would like to thank Dr. Chris Cox, who in addition to serving on my committee, conceptualized various experimental concepts for a large portion of my research. I would also like to thank Dr. Robert M. Counce for serving on my committee and for useful advice on my dissertation. Last but not the least, I want to express my gratitude to Dr. Alice Layton, Dr. Paul Frymier and Shawn Hawkins for various help in conducting my biotechnical experiments. Various scholars at the Center for Environmental Biotechnology also helped me a great deal in my "bench top" experiments. Drs. George Southworth and Joanna McFarlane helped me a lot to put together my mercury experiments and analysis.

Finally, I want to thank my parents and wife for instilling in me the confidence required to achieve this goal.

ABSTRACT

In the wake of stringent environmental regulations, this research studies ash pond discharge to the river by Kingston Power plant. Currently 1296 MGD of fresh water from the Emory river via plant intake is used in condenser cooling. 40 MGD of ash sluice water containing ammonium compounds, mercury compounds, phosphates, Arsenic, Selenium, etc, is discharged to the plant intake via the ash pond for recycle back as sluice water into the plant. Ammonia slip from SCR unit is responsible for the ammonia and mercury comes from the coal. The research addresses the methodology to predict pollutants in the ash pond discharge and optimize the overall water consumption from its current usage by using the pinch analysis method and recycle. A generic model focusing particularly on ammonia and mercury discharge is developed using ChemCAD simulator backed by actual data from the Kingston Power plant. The research reveals that mercury either elemental or oxidized tends to adsorb on the ash surface ($K_D \sim 10000$ mL g^{-1}). It is found in this work that in the presence of ammonia, mercury desorption follows a complex equation, due to the ammonia mercury interaction. About 70% of the ammonia slip is captured as ammonium compounds adsorbed on the fly ash surface and destroyed biologically in the pond. The ammonia destruction is modeled as Monod equation. On an average, the volatile suspended solid increases from 2 to 5.2 mg/l during the experimental residence time of 17 days suggesting a nitrification process responsible for ammonia breakdown. The model can be used to estimate ammonia, nitrates, phosphates, and mercury in the effluent to the river. The model can also form a basis for future research to (i) analyse Arsenic and Selenium; (ii) the effect of pH and Loss of Ignition on mercury

desorption from the ash; (iii) assist in designing any treatment scheme deemed necessary at a future date by providing effluent data based on coal feed and process conditions.

EXECUTIVE SUMMARY

Coal based power plants face stringent environmental regulations that are expected to become more stringent in the future. A major environmental impact concern faced by the Tennessee Valley Authority (TVA) is the ash pond discharge to the river. The fly ash captured in coal combustion process after coal burning contains ammonia (and its compounds such as ammonium bisulfate), mercury (and its compounds), phosphates, arsenic and selenium in addition to other constituents, that is hydraulically conveyed to the ash pond. There are two main water streams at TVA's Kingston Power plant; 1296 million gallons per day (MGD) of fresh water used as the condenser cooling water (CCW), is not an environmental issue and 40 MGD of spent water released to the river via an ash pond and a stilling pond, which is of particular concern. Emission control retrofits; SCR and FGD transfers some air pollutants into the aqueous phase that is transported to the ash pond. SCRs introduce ammonia into the fly ash while FGDs trap oxidized mercury. TVA is spending billions of dollars for installing SCR and FGD units to reduce the air pollutants NOx and SOx in the flue gas. Currently, the main constituents of concern in the ash pond are (i) ammonia due to ammonia slip from SCR, (ii) mercury and its compounds desorbing from ash into water and (iii) arsenic and selenium desorbing from ash into water. Also, TVA strives to reduce fresh water usage while maintaining compliance with all current and future emission and effluent regulations. This research develops a model to help reduce waste water discharge, while minimizing the usage of fresh water. The model is developed through computer simulation in ChemCAD backed by experimental data. TVA's Kingston plant, does not have FGD

units, is the source of data for this work. The model developed, however is generic for power plants that also include FGD units. This research focuses especially on ammonia and mercury. Further work will be performed to analyse the kinetics of arsenic (As) and selenium (Se) in the ash pond. Also, the effect of pH and Loss of Ignition (LOI) on mercury desorption from the ash will be studied as future work. The ammonia is destroyed biologically in the pond and is modeled with a Monod type kinetic equation with half saturation constant of 84 mg/l. On an average, the volatile suspended solid (VSS) increased from 2 to 5.2 mg/l during the experimental residence time of 17 days confirming occurance of the nitrification process in the ash pond. The mercury desorption from ash is inhibited in presence of ammonia in the ash pond and follows a complex equation, which is used in building the ChemCAD model. The mercury and ammonia concentration prediction from the model based on these experimentally determined equation is within 15% of the measured value. The model developed in this work with these kinetic constants will assist in estimating the ammonia, nitrates, phosphates, mercury in the ash pond water stream. The model developed forms a basis for future research that focuses on arsenic and selenium. The computer model will also assist in designing any treatment scheme deemed necessary at a future date by providing effluent data based on a particular coal feed and process conditions. This research addresses the means to reduce and optimize the overall water consumption from its current usage by using the pinch analysis method and recycle of the pond water.

TABLE OF CONTENTS

LIST OF TABLES

LIST OF FIGURES

LIST OF PLATES

NOMENCLATURE

μ_m / μ_{max}	=	Maximum specific growth rate, hr^{-1}
r_{su}	=	Substrate utilization rate, $kg/m^3.hr$
X	=	Biomass concentration, mg/l
S	=	Concentration of growth-limiting substrate in solution, mg/l
K_s	=	Substrate concentration at one-half the maximum growth rate, mg/l
Y	=	Maximum yield coefficient, mg/mg
U_{DN}	=	Specific denitrification rate, lb NO_3-N/lb MLVSS.d
U'_{DN}	=	Overall denitrification rate
DO	=	Dissolved Oxygen
AOB	=	Ammonia Oxidizing Bacteria
UBC	=	Un Burnt Carbon
FGD	=	Flue Gas Desulphurization unit
ESP	=	Electro Static Precipitator
SCR	=	Selective Catalytic Reduction unit
WSO	=	Water-system optimization
ω^0_A	=	Initial concentration of mercury in ash
ω_A	=	Concentration of mercury in ash at time t
C_{NH3}	=	Concentration of ammonia

CHAPTER 1.0

INTRODUCTION

1.1 Current Concerns in Coal Industry

The purpose of this research is total water usage minimization and optimization while meeting current and anticipated future regulations on water effluent. Simulating the flow and reactions of the major toxic and deleterious elements and compounds in the sluice water from a typical coal based power plant in general and TVA's Kingston Power Plant will allow achievement of this goal. Water pinch analysis can be performed and water usage in the plant can be reduced based on the pinch analysis. Kingston Fossil Plant is located on Watts Bar Reservoir near Kingston, Tennessee. At the time it was finished in 1955, Kingston was the largest coal-burning power plant in the world, a distinction it held for more than a decade.

The Research Goal is to model the power plant, including the combustion and flue gas air pollution control path [APCD] path in ChemCAD, so that the composition of the effluent can be predicted. Figure 1.1 provides a schematic of a particular unit of the Kingston power plant. There are four units of 130 MW capacity and five units of 175 MW capacity. The stream descriptions are shown in Table 1.1. The stream description shows ammonia and NOx information and gross stream information. The amount of mercury in the emission will be predicted by the model.

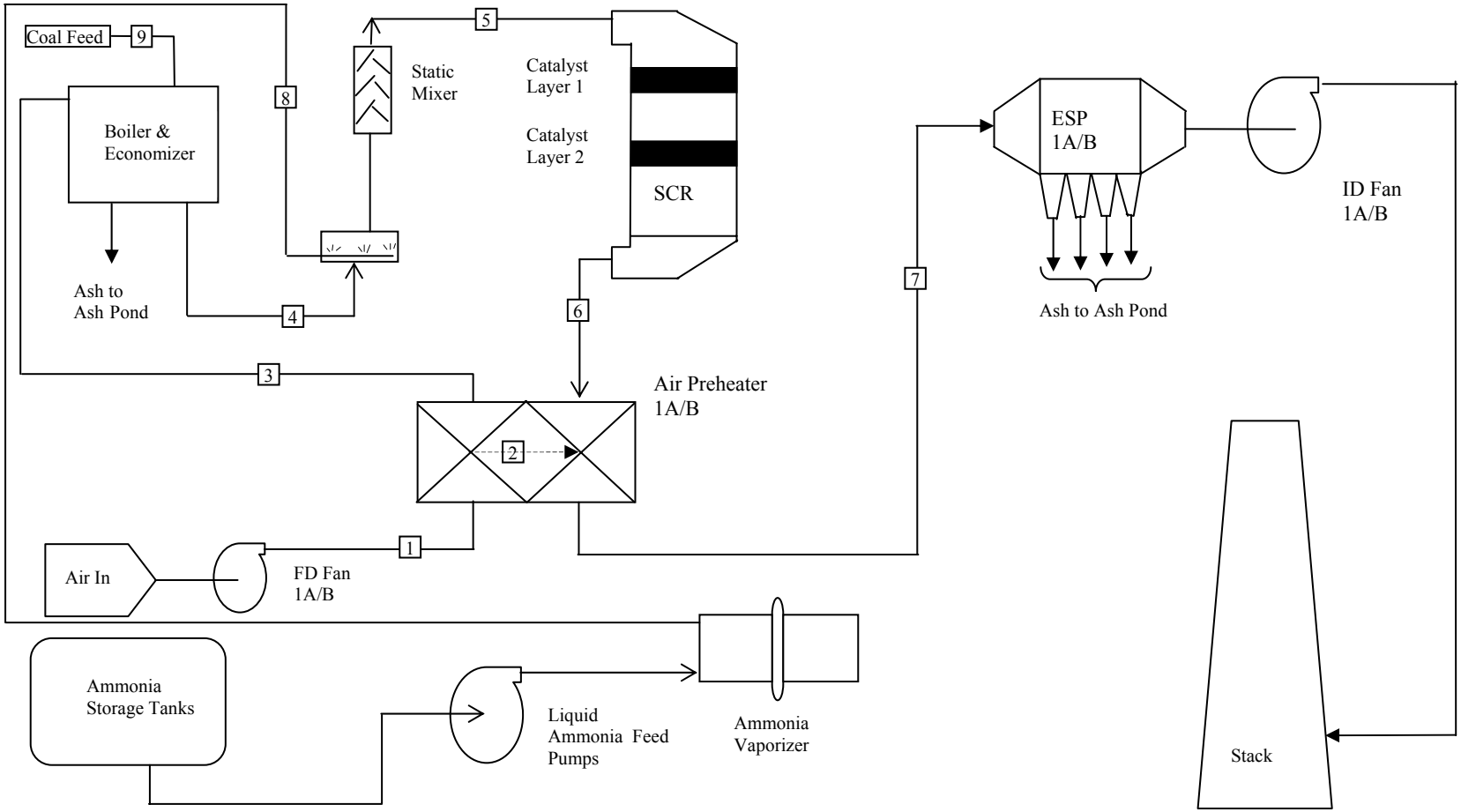

Figure 1.1: Schematic of Kingston power plant

Table 1.1: Stream description of schematic shown in Figure 1

	Stream 1	Stream 2	Stream 3	Stream 4	Stream 5	Stream 6	Stream 7	Stream 8	Stream 9
Description	APH air inlet	APH air leakage	APH air to boiler	Economizer outlet gas	SCR inlet Flue gas	APH inlet Flue gas	APH outlet Flue gas	NH_3+ Air to injection	Coal Feed
Temperature (^{0}F)	120 (116)	120 (116)	590 (600)	615 (650)	615 (650)	623 (659)	272 (288)	100	
Press., (in. w.g.)	3.1(7.2)	-4.4 (-12.7)	1.7(4)	-3.0 (-5.7)	-3.7 (-9.7)	-4.4 (-12.7)	-5.9 (-16.1)	25.4	
Flow (acfm), x 10^5	0.912(1.88)	0.085 (.22)	2.97 (6.17)	3.27 (7.04)	3.37 (7.21)	3.47 (7.48)	1.3 (2.834)	0.0448 (.0456)	
Flow (lb/hr), x 10^5	3.65 (7.69)	0.375 (0.925)	6.55 (13.53)	7.18 (14.88)	7.38 (15.08)	7.53 (15.38)	4.14 (8.61)	0.195 (0.197)	~0.95 (~1.25)
NOx (ppmv)	-	-	-	469(482)	456(475)	44.7(46.5)	40.5(41.4)	-	
NH_3 (lb/hr)	-	-	-	0	183(389)	0.7(1.5)	0.3(0.7)	183(389)	
Particulate(lb/hr)	-	-	-	5100 (11000)	5100 (11000)	5100 (11000)	2550 (5500)	-	

Notes:-

1. All flows are for one unit of 70 MW.
2. Mass flow rates of NOx assume 95% as NO and 5% as NO_2.
3. **Numbers within parenthesis are for 140 MW unit**

1.1.1 Brief Process Description

Refer to the schematic diagram in Figure 1.1 in conjunction with this description. Coal is pulverized into a fine powder and injected into the boiler where it is combusted. The combustion of coal, heats highly treated demineralized water in a boiler, changing phase of the water into gaseous steam. The steam, under tremendous temperature and pressure, throttle into a turbine, where the force of the expanding steam spins the turbine blades. The turbine spins a magnet inside copper coils in a generator to produce the flow of electrons called electricity. After leaving the turbine, the low pressure steam passes over tubes filled with river water in a condenser where the steam is condensed and reverts to water condensate. This condensate is recycled to the boiler. River water for condenser cooling, used to condense the low pressure steam, is returned to the river at a slightly elevated temperature within compliance with environmental regulations. The turbine, other associated equipment, the steam circuit, and the water flow lines for steam condenser are not shown in the schematic, as they will not be dealt with in this study. The condenser water requirement is based on heat duty and can be reduced only if the heat duty is reduced. As the heat duty reduction is not envisaged in this study, the condenser water requirement is not included in the current water usage minimization study. Flue gas from coal combustion contains CO_2, NOx and SOx as well as other constituents. The flue gas passes through the Selective Catalyst Reduction Unit (SCR) for NOx control. Ammonia is injected into the flue gas stream and introduced into the SCR, where in presence of vanadium-titanium catalyst NOx is converted to harmless nitrogen and water. The SCR catalyst also converts 70% of the mercury according to a study[43]. The flue gas

stream then passes through the air preheater, where it cools down from 623^0F to 272^0F by heating the ambient air fed to the boiler. The flue gas then passes through the Electrostatic Precipitator (ESP), where the particulate solids are ionized and separated from the flue gas stream. Almost all the ammonia and its salts and majority of the oxidized mercury are separated in the ESP with fly ash. Oxidized mercury being more soluble than elemental form is separated easily in ESP and FGD. The treated flue gas is then discharged to the atmosphere. The ash collected at the boiler bottom during combustion is the bottom ash and the ash collected in the ESP is the fly ash. The bottom ash and the fly ash are collected by sluice water collection system and routed to the ash pond. The river water is first collected in underground sumps and the sluice water portion is pumped to boiler to collect the bottom ash and to the SCR and ESP to collect the fly ash. About 40 million gallons per day of water goes to the ash pond containing mainly fly ash and bottom ash. Kingston generates about 10 billion kilowatt-hours of electricity a year, enough to supply more than 700,000 homes. TVA has spent more than $2.5 billion on emissions controls at its fossil-fuel plants to ensure that this power supply is generated as cleanly as possible, consistent with efficiency. To reduce SO2 emissions all nine units use a blend of low-sulfur coal. To reduce NOx, Units 1 through 4 and Unit 9 use combustion controls and boiler optimization. Units 5 through 8 use low-NOx burners. Selective Catalytic Reduction units are installed to further control NOx emissions from all nine units.

1.2 Research Proposal

TVA is contemplating measures and procedures to deal with the various future problems that may arise due to the presence of pollutants in the ash pond, which can reach regulated levels if not properly controlled.

The materials that are dealt with in this research are ammonia and ammonium salts in the ash, phosphate salts in the ash and mercury in the ash. Currently arsenic and selenium are also materials of concern, which will be dealt with as future work. The source of the ash is from the boiler and the electrostatic precipitator (ESP). The boiler ash is washed by sluice water from boiler bottom. The fly ash is sucked by sluice water from ESP bottom and is transported by water. The fly ash and the bottom ash are conveyed through different routes into the ash pond. Refer to Figure-1.2 for details of the water flow rate to the ash pond, Emory River/Clinch River at Kingston power plant. Approximately, 6.8 MGD of bottom ash sluice water, about 25.2 MGD of fly ash sluice water and about 8 MGD of miscellaneous cooling and washing water flows into the ash pond. In the ash pond the ash settles and the clear water devoid of majority of the ash (suspended solid) flows into the Watts Bar lake which connects to the Emory River. The condenser cooling water amounting to about 1297 MGD is released to the Clinch river. Unlike, the ash sluice water, the condenser cooling water is clean. The condenser cooling water picks up heat from the condenser and hence its temperature will be normally 9^0F to 18^0F higher than ambient. The ash sluice water coming to the ash pond is contaminated with ammonia, nitrates, mercury, As, Se, etc, in varying proportions depending on the

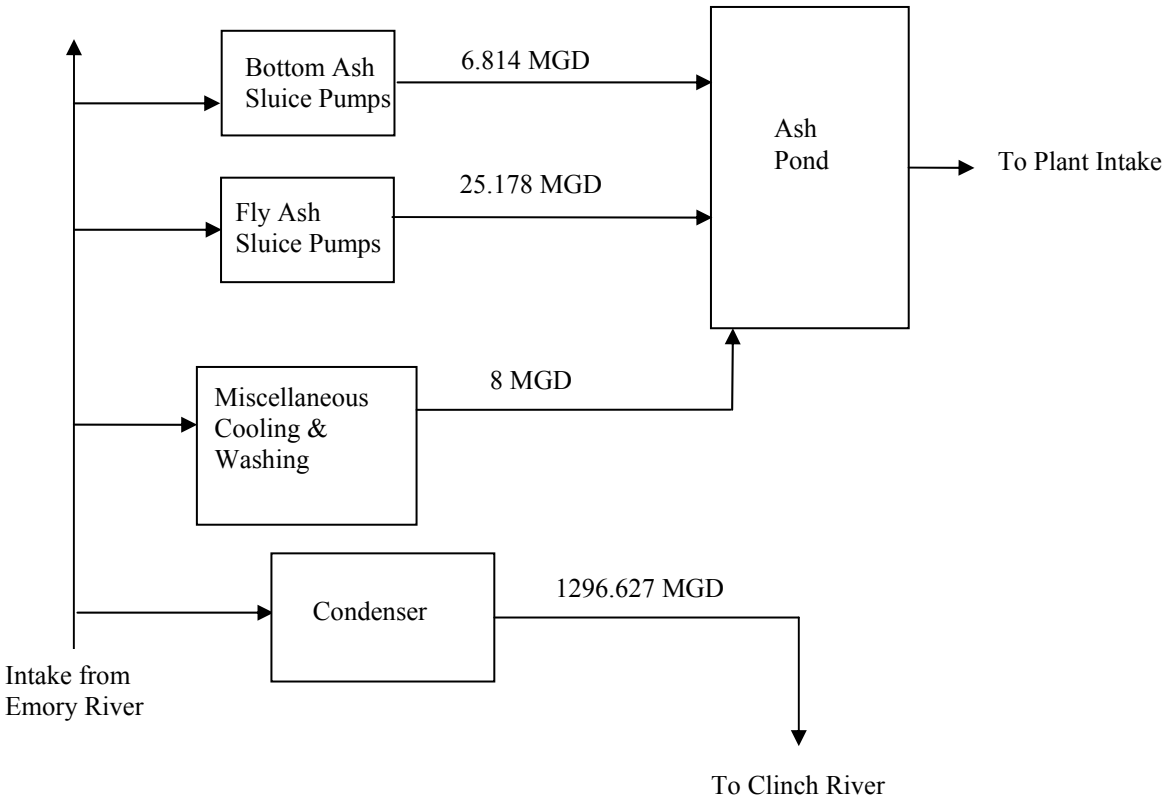

Figure 1.2: Block diagram of water distribution inside Kingston power plant

coal composition. The settled ash mainly consists of Silicon dioxide (SiO_2), Aluminum oxide (Al_2O_3), Ferric oxide (Fe_2O_3) and Calcium oxide (CaO). The pond water analysis (Table-1.2) shows significant amount of nitrogen as ammonia or ammonium salt (TKN) present in the water. Ammonia is present as various ammonium salts and partially dissociates into ammonium ion or ammonia depending on the pH of water. Presence of ammonia in river water even in very low concentration (~ 0.2 ppm) can kill fish in the river. As coal contains significant amounts of phosphorus, a great deal of it is present in fly ash and is likely to be removed in the ESP and will report to the ash pond. In the ash pond it will exist as PO_4^{3-} ion. The presence of phosphate and nitrate ion (formed after nitrification) will assist in algae growth. The presence of algae can reduce dissolved oxygen concentration during daytime and affect fish growth and respiration. The water analysis of the bottom ash to pond (Table-1.3) shows mercury in it. Mercury is a component in coal and the mercury coming to the pond adsorbed on the ash is desorbed from the ash into the water. A computer model can predict the amount of ammonia, nitrate (NOx), mercury and algae in the overflow water from the ash pond to the Emory river during different times of the day and year. In order to predict these constituents in the ash pond effluent, kinetic data of the ammonia breakdown and mercury desorption from the ash is studied, and is then incorporated in the model. This project envisages modeling the entire power plant including the ash pond to predict ammonia, nitrate and mercury and ensure they are contained within the stipulated limits. Table 1.4 furnishes the Toxics release inventory in pounds at Kingston in 2004. It shows the amount of mercury, selenium, arsenic, ammonia and host of other compounds released in air, water,

Table-1.2: Analysis of ash pond (as furnished by TVA)

Data Report Number: 040924-172235
Report of Results: Environmental

TENNESSEE VALLEY AUTHORITY
CENTRAL LABORATORIES SERVICES
1101 Market Street, PSC 1B-C
Chattanooga, Tennessee 37402-2801
Phone: (423) 876 - 4318 • Fax: (423) 876 - 4137

Shipping Address:
Chickamauga Power Service Center
North Side Chickamauga Reservation
Chattanooga, Tennessee 37415

Customer Address:

Phone: Not Available
Fax : Not Available
E-Mail:

Location Code: KIF
Field ID: POND #1
Sample Description: WATER FROM POND #1

Sample ID: AE15196 **LRF ID:** 04090207
Matrix: Water **Reg:** RCRA
Date Collected: 09/15/2004
Time Collected: 0:00 EST
Date Received: 09/02/2004
Time Received: 11:01
Project Manager: Randall L. Howell

Analyte	CAS Number[1]	Result	Units	MDL[2]	Analysis Date	Analysis Time	Analyst	Method Reference
Ammonia as N	7664-41-7	< MDL	mg/L	0.01	09/22/2004	12:27	ADP	EPA 350.1
Nitrate-Nitrite as N		0.38	mg/L	0.01	09/22/2004	12:27	ADP	EPA 353.2
Total Kjeldahl Nitrogen		0.14	mg/L	0.02	09/21/2004	13:58	GMP	EPA 351.2
Sulfur, Total	7704-34-9	20	ppm	0.14	09/24/2004	5:03	CLS	IC
Mercury, Total	7439-97-6	< MDL	mg/L	0.0001	09/23/2004	14:57	CLS	EPA 7470A
Non-Filterable Residue		110.	mg/L	1.	09/17/2004	10:24	AJH	EPA 160.2
Filterable Residue		210.	mg/L	10.	09/20/2004	13:57	AJH	EPA 160.1

Sample Comments: None

Table-1.3: Analysis of bottom ash to pond (As furnished by TVA)

Data Report Number: 040924-172235
Report of Results: Environmental

TENNESSEE VALLEY AUTHORITY
CENTRAL LABORATORIES SERVICES
1101 Market Street, PSC 1B-C
Chattanooga, Tennessee 37402-2801
Phone: (423) 876 - 4318 • Fax: (423) 876 - 4137

Shipping Address:
Chickamauga Power Service Center
North Side Chickamauga Reservation
Chattanooga, Tennessee 37415

Customer Address:

Phone: Not Available
Fax : Not Available
E-Mail:

Sample ID: AE15194 **LRF ID:** 04090207
Matrix: Water **Reg:** RCRA
Date Collected: 09/15/2004
Time Collected: 0:00 EST
Location Code: KIF
Date Received: 09/02/2004
Field ID: 1 THRU 5 BOTTOM ASH TO POND
Time Received: 11:01
Sample Description: BOTTOM ASH WATER FROM UNIT 1 THRU 5
Project Manager: Randall L. Howell

Analyte	CAS Number[4]	Result	Units	MDL[2]	Analysis Date	Analysis Time	Analyst	Method Reference
Ammonia as N	7664-41-7	< MDL	mg/L	0.01	09/22/2004	12:27	ADP	EPA 350.1
Nitrate-Nitrite as N		0.59	mg/L	0.01	09/22/2004	12:27	ADP	EPA 353.2
Total Kjeldahl Nitrogen		2.0	mg/L	0.02	09/21/2004	13:58	GMP	EPA 351.2
Sulfur, Total	7704-34-9	9	ppm	0.14	09/24/2004	3:30	CLS	IC
Mercury, Total	7439-97-6	0.0002	mg/L	0.0001	09/23/2004	14:52	CLS	EPA 7470A
Non-Filterable Residue		520.	mg/L	1.	09/17/2004	10:24	AJH	EPA 160.2
Filterable Residue		160.	mg/L	10.	09/20/2004	13:56	AJH	EPA 160.1

Sample Comments: None

Table 1.4: Toxics release inventory of TVA (Source: TVA website)

2004 data

All amounts are in pounds.

Chemical	**Air[1]**	**Water[2]**	**Land[3]**	**Off-Site Disposal[4]**	**Total Releases[5]**
Arsenic Compounds	299	9,227	45,239	0	54,765
Barium Compounds	867	41,700	582,700	0	625,267
Chromium Compounds	501	717	93,890	1	95,109
Cobalt Compounds	131	0	39,472	0	39,603
Copper Compounds	404	3,706	121,070	0	125,180
Lead Compounds	315	0	51,049	12	51,376
Manganese Compounds	728	0	130,870	0	131,598
Mercury Compounds	450	0	231	0	681
Nickel Compounds	511	0	80,290	0	80,801
Selenium Compounds	11,201	2,459	6,716	0	20,376
Vanadium Compounds	474	6,525	182,380	0	189,379
Zinc Compounds	1,506	1,740	121,130	0	124,376
Hydrochloric Acid (aerosol)	4,150,006	0	0	0	4,150,006
Hydrogen Fluoride	490,006	0	0	0	490,006

Table 1.4: Continued

Chemical	Air[1]	Water[2]	Land[3]	Off-Site Disposal[4]	Total Releases[5]
Sulfuric Acid (aerosol)	1,004,006	0	0	0	1,004,006
Ammonia	1,306	76	0	0	1,383
Nitrate Compounds	0	0	0	0	0
TOTALS	5,662,794	66,151	1,455,088	12	7,184,045

[1] "Air" indicates emissions that come out of the stack, commonly known as flue gas.

[2] "Water" indicates emissions that have been placed in an on-site holding pond and then discharged to the local waterway following all state and local permit requirements, commonly called aqueous waste or effluent.

[3] "Land" indicates ash that has been put in ponds or stacked dry in a pile on-site.

[4] "Off-site disposal" indicates ash used for such things as driveways and fill for industrial parks.

[5] Total 2004 releases represent a decrease of 292,437 pounds from 2003. Releases decreased primarily due to a decrease in coal combustion and a switch to western coal.

land and off-site disposal. As per PISCES Water Characterization Field Study[39], the freshwater criteria at 100 mg/l and 550 mg/l hardness for ammonia release is 0.4 mg/l. To put things in perspective, 40 Million Gallons per Day of ash pond water having 0.4 ppm ammonia released from the ash pond into the river, 48565 lbs per year of ammonia can be released. Whereas the amount of ammonia released to water in 2004 was 76 lbs and the total ammonia released in air and water together was 1383 lbs.

Hence, the ammonia release to the environment is much less than it is allowed. The general water quality criteria from TDEC[1] mentions the limits set for some of the most commonly occurring toxic substances, and among them the limit set for mercury is 2 µg/l. Therefore, with 40 MGD water flow from the ash pond, the mercury that can be released is 242.8 lbs per year. The mercury released by TVA in 2004 was 450 in air, 231 lbs per year in land and none in water. The total mercury released in the environment is 681 lbs/year. With the installation of the SCR and running it all round the year will transfer the majority of the total mercury to the water and that is why the real concern arises as the limit of 2 µg/l in effluent prescribed by TDEC is expected to cross.

1.3 Research Goals and Objective

The main goal of this research is the reduction of pollutants at the waste water discharge to the river. A generic model of a coal based power plant is developed to predict the constituents of water discharge and the flue gas at the stack. The model developed is generic; the input parameters of which can be changed by the user/researcher according to the plant under investigation. The recent concerns of coal based power plant and ash ponds are; ammonia, mercury, arsenic and selenium.

Ammonia and mercury are studied in this work. The following described goals pertinent to each of these species.

1.3.1 Ammonia

Ammonia is used as a reagent to reduce NOx in the SCR. The "ammonia slip" caused by unreacted ammonia in the SCR results in ammonia in the flue gas duct system . This ammonia is adsorbed on fly ash surface and thereby routed to the ash pond via the ESP and/or FGD[49]. Within the APCD fly ash flight path ammonium bi sulfate (ABS) is formed and adsorbed on fly ash surface and gets transported to the ash pond. This transfer of "unreacted ammonia" from the gaseous phase to the liquid phase is causing concern to the power plant where SCR unit is installed. The objective of the present work is to effectively model the ammonia-N emission and ammonia/ammonium breakdown in the ash pond based on experimental study of nitrification kinetic. The model results can then be used to predict the ammonia content at the outfall of the plant for any given "ammonia slip" and assist in devising any ammonia treatment for the ash pond in future. The phosphorus in the coal is also carried by the fly ash to the ash pond. This phosphorus in presence of NH_4^+/NO_3^- forms algae, which will also be predicted by the model based on kinetic parameters published in literature. The nitrate forms during the nitrification process in the ash pond.

1.3.2 Mercury

The mercury in the coal passes through various equipments under varying temperature from about 1900^0F in the boiler to 650^0F in the SCR to about 330^0F in the ESP and to about 150^0F in the Flue Gas Desulphurization (FGD) if FGD is present. This

temperature drop in the flue gas causes the mercury to oxidize by the oxygen and the chlorine in the flue gas. The SCR catalyst also assists in mercury oxidation. In FGD it reduces partly in presence of appreciable amount of SO_2/SO_3 (discussed later). The mercury oxidation/ reduction also depends on chlorine, sulfur in the coal. Part of the elemental / oxidized mercury is adsorbed on fly ash surface and separated from the flue gas in the ESP. Mercury is also trapped in the FGD in the oxidized form. The fly ash and bottom ash is collected by sluice water and brought to the ash pond, transferring the mercury from the initial vapor phase to the liquid phase. The recent installation of SCR and specially FGD units in fossil fuel based power plants is largely responsible for the mercury transfer from the vapor to the liquid phase. A continuous stream of FGD blow down may be fed to the ash pond in future in Kingston power plant. This transfer of majority of the mercury from the flue gas to the ash pond is a cause for concern. Mercury from the ash interacts with ammonia in ash pond. The kinetics of mercury desorption in presence of ammonia is studied experimentally as part of this work and incorporated in the model, so that the mercury content at the outfall can be accurately predicted.The envisaged generic model in this work predict the mercury in the flue gas based on minimization of Gibb's energy and in the ash pond based on experimentally determined kinetics. The generic model also includes the FGD unit considered as a future process modification in Kingston in the form of routing of mercury laden FGD blow down to the ash pond.

1.3.3 Water usage management

The water flow inside Kingston power plant is simulated in ChemCAD. The water cycle inside the plant is broadly depicted in Figure 1.3. Water pinch analysis is performed based on ammonia and mercury in ash pond water. The model is simulated for total recycle of the ash pond water with the given composition of ammonia and mercury. The Kingston plant model is validated by actual pollutant (ammonia and mercury) concentration at inlet and outlet of ash pond. The generic ChemCAD model, in addition to the sluice water flows as in Kingston model, also includes FGD blowdown water flow to ash pond. The FGD blow down causes the pH of the water to rise and hence affects nitrification. This modification is analyzed in ChemCAD simulation of the complete water cycle to predict the ammonia and mercury in the effluent. The water cycle simulation will similarly assist any future modification in the water cycle of a power plant. The whole process may also assist in overall water usage reduction in a power plant by predicting effluent composition (ammonia and mercury) at any reduced water flow.

1.3.4 Arsenic and selenium

Besides mercury, arsenic and selenium are the other two trace metals of concern as far as fossil fuel based power plant is concerned. The kinetics of desorption from ash surface and study of interaction with ammonia for these trace metals will be performed as future work. The result of these studies can then be incorporated into the generic model developed in this activity and canl then predict the outlet composition of the pollutants based on total recycle.

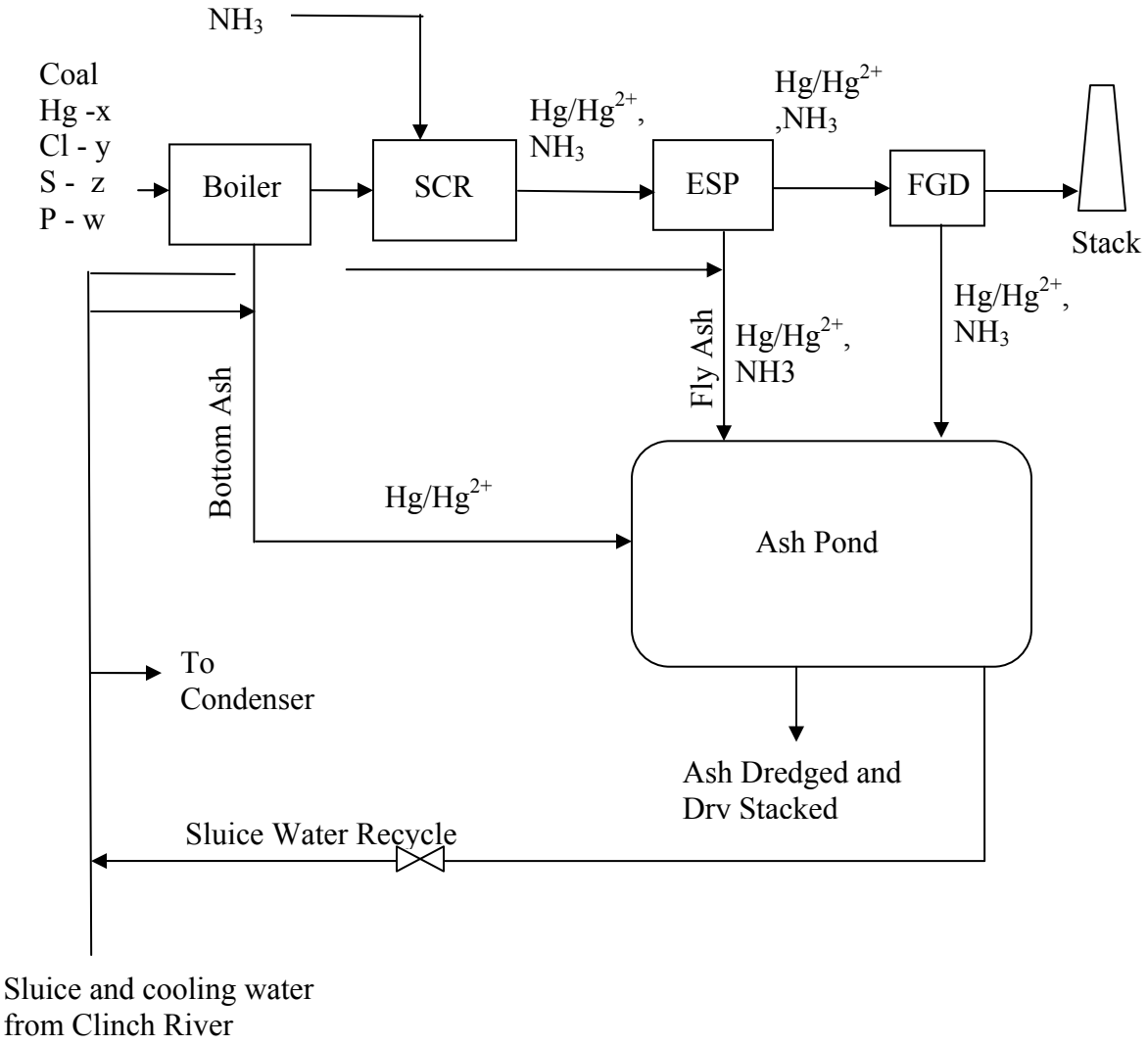

Figure 1.3: Block diagram of water flow inside Kingston power plant

CHAPTER 2.0

LITERATURE REVIEW

2.0 Background for water reduction in power plants

Most power stations world wide recycles waste water or cooling water after treatment. This approach is followed to avoid the need to discharge water into the river. Webb[58] et al suggested that establishing true zero discharge is difficult but achievable. Webb et al achieved zero discharge from the 440-MW Stanton Energy Center (SEC) in Florida by meeting the plant requirement from rainfall, well water and municipal sewage treatment plant effluent. The SEC plant has cooling tower for the condenser cooling water requirement. The cooling tower is the largest consumer of water amounting to 88.4%. Rest is used by pond evaporation, miscellaneous plant equipment evaporation and water entrained in combustion products stored onsite. Total water required by the plant is 5.8 MGD. Water reuse is maximized inside the plant and the unreusable cooling tower blowdown is treated in a brine concentrator and crystallizer and reused. Compare that with the plant in Kingston; Kingston has a total installed capacity of 1400 – MW and uses 1336 MGD of fresh water (1296 MGD for condenser cooling and 40 MGD for ash sluicing and miscellaneous activities) and recycle the entire 40 MGD of contaminated water to the plant and discharges 1296 MGD clean condenser cooling water, as against 5.8 MGD used by SEC and discharging nothing. Frank [31] et al suggests raw water treatment mechanism to provide make up water for cooling tower and demineralized water plant for the 1710- MW Laramie River power station. The raw water consists of

mainly the rainfall water collected on site. The water then goes through a pre treatment plant removing silica, hardness, turbidity and alkalinity. The pre treatment plant provides makeup to the cooling tower, reverse osmosis and demineralizer units in the boiler water system. It also serves as backup to the potable water system. The water pre treatment plant increases the permissible cycles of salt concentration in the cooling system from less than 5 (without treatment) to 15 or more (with treatment). This substantially reduces the amount of blowdown required for the cooling tower. The cooling tower blowdown flows to the FGD absorber. Thus, through internal circulation and efficient reuse of the water, zero discharge is achieved in the Laramie River power station. Sharma[46] suggests air-cooled condensers to reduce water consumption in waste-to-energy plants with zero water discharge. A 500 TPD waste to energy facility in Pennsauken, NJ, designed as a zero discharge facilty using an air-cooled condenser. The author performed a waste water mass balance for a 500 TPD facilty burning garbage with a heating value of 4500 Btu/lb, producing 100% electricity and utilizing a cooling tower and a water balance for a similar facilty using air cooled condensers. The author found that the total waste volume is reduced by more than 50% when using an air-cooled condenser.

2.0.1 Discussion of water usage at Kingston

All the power plant processes mentioned above uses either the cooling tower technique for cooling water or air cooled condensers. Here zero discharge is achievable by directing the blow down to waste water treatment plant and re circulating treated water back to the plant to supplement blow down and evaporation losses as suggested by various authors. The cooling water requirement for condensers in Kingston is met by

directly pumping the required water from the river into the plant and then discharging the hot water from the condenser back to the river. This scheme is entirely different from the other methods of cooling water circulation mentioned above by different authors. The sluicing water is discharged to the plant intake where it is mixed with the river water and circulated back to condenser and sluice water intake. Thus, the contaminant laden sluice water from the ash pond is not allowed to flow into the river directly. Hence, this needs a separate study and separate treatment. First, the contaminants behavior and reactions in the ash pond are studied and modeled and then through water pinch analysis water usage is reduced. Also, the mixing and reintroducing of the sluice water maintains a particular level of contaminants at steady state, which is predicted in this work. The literature study of nitrogen, phosphorus and mercury will be useful before any experimental study and modeling work can be taken up.

2.1 Nitrogen

2.1.1 Nitrogen Source

There are three sources of nitrogen in the system. First, the nitrogen present in the coal. Typically, coal contains 1.16% by weight of nitrogen as per TVA[5]. Second source of nitrogen is the nitrogen in the air. Part of the nitrogen in the coal and air is released as NOx (mainly nitrogen oxide) during coal combustion. The NOx is an air pollutant that cannot be released to the air without treating it. Selective Catalytic Reduction units (SCR) are installed in modern coal based plants and also as retrofits in older plants to mitigate NOx. SCR units consist of a bed of vanadium – titanium catalyst. The SCR reduces NOx to N_2. Ammonia is used in the SCR as a reducing agent. The third source of nitrogen is

the unreacted ammonia called ammonia slip from the SCR unit. A proper system design and engineering can achieve up to 90% NOx removal and <2-ppm ammonia slip. Refer to figure-2.1 for understanding a typical SCR unit. The reaction taking place in the SCR is as follows;

$$4NO + 4NH_3 + O_2 \longrightarrow 4N_2 + 6H_2O \quad \text{.....2.1}$$

Equation 2.1 indicates that, theoretically 1 mole of ammonia is required to reduce 1 mole of Nitrogen Oxide (NO). Process conditions within a reactor vary, thus leaving some NO and ammonia unreacted. The unreacted ammonia, "ammonia slip" is transported by the flue gas and reacts downstream of the SCR with SO_3. By maintaining close to the theoretical stoichiometry, the ammonia slip can be kept at acceptable levels in properly designed modern SCR systems, while NOx reductions in excess of 90 percent can be achieved[15].

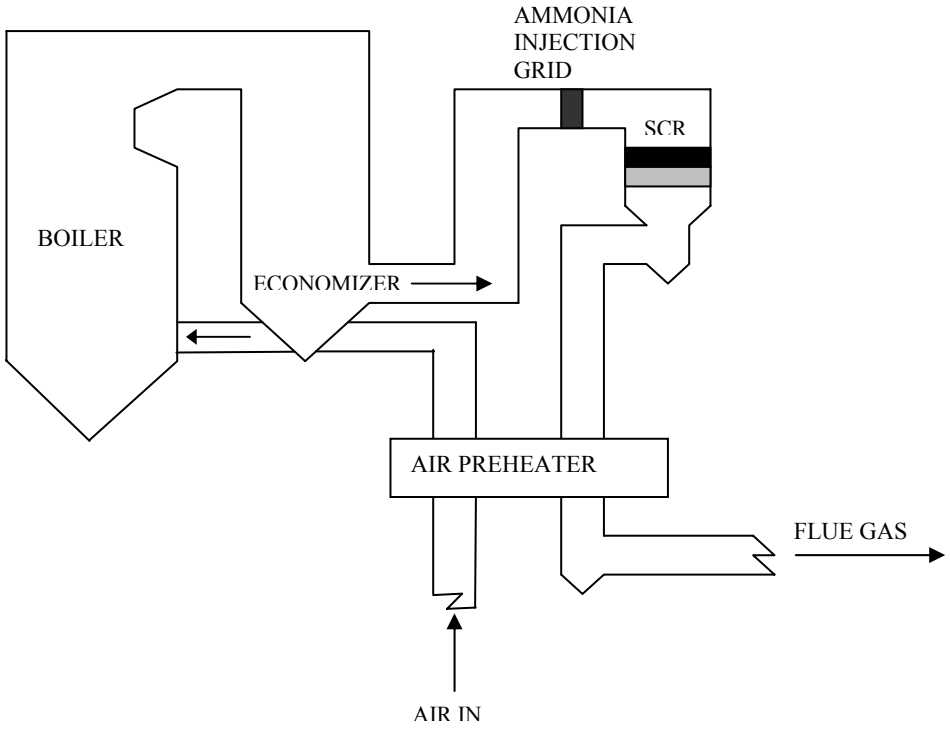

Figure 2.1: Process flow schematic for an SCR Unit (Source: EPA report[15])

In U.S. applications, the ammonia slip is typically limited to 2 $mg.m^{-3}$ (gas concentration stated is concentration at standard temperature and pressure)[49]. Various factors like ammonia/nitrogen oxide molar ratio distribution, flue gas velocity distribution and flue gas temperature distribution are instrumental for high DeNOx and low slip. Sigling[47] et al pointed out that the trend of the ammonia slip versus velocity (or residence time); a range of +/- 10% deviation in velocity results in an average ammonia slip of greater than 2 ppm. Also, the catalyst activity is more or less stable between 650 –750^0F and as such in this temperature range the slip is minimal. Sigling[47] et al concluded that higher the NH_3:NO ratio for a given SCR system, the better the NOx reduction efficiency, however, the corresponding ammonia slip increases exponentially. The ammonia slip reaches extremes when the NH_3: NO ratio exceeds 1. The 2-ppm design ammonia slip occurs when the NH_3: NO ratio is 0.9. The design detail of a SCR unit is beyond the scope of this work. The above details of the SCR are to give a feeling of the SCR unit process variables to the reader. The model developed in this work predicts the amount of ammonia flow to the ash pond.

2.1.2 Fate of Nitrogen

In a typical application of SCR as shown in figure-2.1, the ammonia laden flue gas that exits the SCR reactor will first pass through a air preheater, then a electrostatic precipitator (ESP), a flue gas desulphurization unit (FGD) and finally through the stack to the atmosphere. All of the mentioned systems and units contribute to the ammonia removal in some way or the other. Sulfur in the coal burned by Kingston power plant is a low sulfur variety and amounts to about 0.46%. However, sulfur in some other variety of

coal can be as high as 3%. This implies that a considerable amount of SO_2 forms in the boiler and is transformed into SO_3 in the SCR in the presence of catalyst. As the flue gas is cooled to below the acid dew point (300^0F) in air pre heater, some of the SO_3 present will hydrolyze and condense onto the air heater metal surface as sulfuric acid. Most often the ammonia comes in contact with SO_3 and sulfuric acid to form scales of ammonia bisulfate on the internal metal surface of the preheater. According to Richard[49] et al, it involves a two step process that first converts SO_3 to sulfuric acid and then, depending upon the ratio of the reactants, will form either ammonium sulfate or ammonium bisulfate. In most cases the limiting reactant is ammonia and thus the predominant species of ammonia compound is ammonium bisulfate (ABS). It is shown by Richard[49] et al and will be shown later in this work that ABS is the most thermodynamically stable compound with the given reactants, ammonia, SO_3, SO_2 and water. In other words, the total Gibb's energy of formation of ABS is the minimum. Richard[49] et al mentions that the other factor governing the ABS formation is that the maximum concentration of the ammonia slip in most domestic SCR applications is relatively low at 2 mg/m^3. So, the molar ratio of SO_3 to NH_3 is quite large, and thus does not allow for the necessary stoichiometric amounts of NH_3 to produce ammonium sulfate. The controlling factor in ABS formation then becomes the concentration of SO_3. On a molar basis, ammonium bisulfate is formed with 1 mg/m^3 NH_3 to every 4.7 mg/m^3 SO_3. This according to Richard[49] et al what is important in determining where the ammonia will deposit. For example, if there is little to no SO_3 present in the flue gas because of low sulfur coal or SO_3 removal, the majority of ammonia will not be deposited in the air heater, but will be adsorbed on the fly ash or absorbed in the FGD liquor. The work of Richard[49] et al thus

forms the basis of modeling the flue gas path for nitrogen from the SCR to the ESP and FGD (if it exists) including the percentage of nitrogen adsorbed on the fly ash in ESP and the nitrogen converted to ABS. The initial temperature is itself a function of ammonia and SO_3 concentration. There are several references to the formation temperature of ABS, such as 1994 Electric Power Research Institute (EPRI) report TR-102414. The generally accepted ABS formation temperature is in the range of 392 – 428 ^{0}F for typical medium to low sulfur coals. Richard [49] et al predicted the ammonia removal rates in the air heater are considered 10 to 20%. However, as much as one third of the ammonia deposits are recycled back to the boiler with combustion air as NOx. Ammonia deposits can be revolatilized as the air heater passes back to the hot zone and oxidizes in the presence of oxygen at 600^{0}F via the following reactions[49]:

1%: $4NH_3 + 4O_2 \longrightarrow 4N_2O + 6H_2O$ ……..2.2

4%: $4NH_3 + 7O_2 \longrightarrow 4NO_2 + 6H_2O$ ……..2.3

95%: $3NH_3 + 2O_2 \longrightarrow 3NO + 6H_2O$ ……..2.4

Eventually, air heaters are washed to remove ABS deposits in addition to normal fly ash fouling. Richard[49] et al determined the average concentration of ammonia in wash water to be approximately 3000 mg/l, at the worst case scenario of 2mg/m^3 ammonia slip deposited in the air heater over an entire year of operation between washings and 0.23 m^3/h per MW of wash water flow rate. This sudden high volume discharge of ammonia into the ash pond during cleaning of the air heater causes ammonia spikes in the ash pond.

The largest sink for ammonia removal in the flue gas cleaning system is typically in the ESP fly ash. Ammonia deposits in the ESP fly ash are generally assumed to be

70% of the total ammonia slip[49]. This however is also related on the amount of SO_3 in flue gas. The possibility of ABS capture in fly ash increases as the SO_3 to NH_3 molar ratio increases above one, whereas molar ratios less than one will shift the distribution of ammonia removal to the Flue Gas Desulphurization (FGD)[49]. For wet sluicing of fly ash, like it is being done in Kingston, the ammonia or ABS is carried by the water, also called sluicing, to the ash pond. Richard[49] et al predicted that the ammonia concentration in the ash pond effluent would be approximately 1.8 mg/kg (~1.8 ppm) in the worst case scenario when 75% of the ash is as fly ash and 100% of the 2mg/m^3 ammonia slip is adsorbed on the fly ash with 1% solids in the sluice water. However, the ammonia concentration may increase at times due to SCR malfunctioning and/or preheater washing, the effect of which on the outlet ammonia concentration is simulated and studied in this work. Finally, the Flue Gas Desulphurization (FGD) process removes the remaining 10% of the ammonia[49]. The ammonia sluiced from the air preheater and ESP as ammonium ion and ammonia depending on the pH of the water. Generally, the pH of the scrubbing liquor in FGD is maintained at 8.0 to prevent precipitation of lime at higher pH. At a pH of 8.0, 90% of the ammonia is present as ammonium (NH_4^+) ion.

Aqueous ammonia speciation is pH-dependant equilibrium between ammonia molecules and ammonium ion. Under normal conditions of liquid effluent from a typical coal-based power plant, ammonium ion is likely to predominate because the pH is close to neutral. Ammonia dissolves readily in water where it ionizes to form the ammonium ion as follows;

$$NH_3(g) \rightleftharpoons NH_3(l)$$

$$NH_3(l) + H_2O \rightleftharpoons NH_4^+ + OH^- \quad \text{.....2.5}$$

The total ammonia content of water is the sum of non-ionized (NH_3) and ionized (NH_4^+) species. At the pH of most effluent systems are between 7 and 8, ammonia exists predominantly in the ionized form. At low concentrations, the molarity of total dissolved ammonia is given by International Programme on Chemical Safety Environmental Health Criteria[2]:

$$[NH_3] + [NH_4^+] = H\,[NH_{3\,(gas)}] + K_b H\,[NH_{3\,(gas)}] \quad \text{.....2.6}$$

Where $[NH_{3\,(gas)}]$ is the molar concentration of gas-phase ammonia, K_b is the dissociation constant given by:

$$K_b = \frac{[NH_4^+]\,[OH^-]}{[NH_3]} \quad \text{.....2.7}$$

H is Henry's law constant given by (NRC, 1979):

$$\text{Log}_{10}\,[H] = (1477.8/\,T) - 1.6937 \quad \text{.....2.8}$$

The pK_a for the ammonia/ammonium equilibrium can be calculated at all temperatures between 0 and 50 ^{0}C by the equation (Emerson[27] et al):

$$K_a = [NH_3]\,[H^+] / [NH_4^+] \quad \text{.....2.9}$$

$$pK_a = 0.09018 + (2729.92/T) \quad \text{.....2.10}$$

The fraction (f) of total ammonia that is non-ionized depends on both water temperature and pH, according to the preceding and the following equations:

$$f = 1/\,[10^{(pKa - pH)} + 1] \quad \text{.....2.11}$$

Thus, at 0^0C and a pH of 6, less than 0.01% of the total ammonia present is in the non-ionized form, whereas at 30^0C and a pH of 10 almost 89% of total ammonia is non-ionized.

So, aqueous ammonia is "pH-dependant" equilibrium, between gaseous ammonia molecule and ammonium ion. Under normal operating conditions power plant wastewater streams with a pH range of 7 to 8, ammonium ion is likely to dominate. Therefore, the ammonia that reports to the ash pond continuously through ESP, FGD or through yearly washing of air pre heater will be mainly in ionized form (NH_4^+). The possible removal mechanisms of ammonium ion and ammonia from ash pond are (EPRI[39]):

- Volatilization - only if pH>9, i.e. gaseous ammonia is predominant in water
- Uptake by algae when adequate phosphate is present
- Uptake by autotrophic bacteria such as *Nitrosomonas*
- Uptake by emergent wetland plants
- Reactions with other negative ions and separation from the liquid phase by precipitation and settling on ash pond bottoms: Redox reactions

EPRI[39]and Richard[49] predicted the biological removal of the ammonia in the ash pond. Yantarasri[59] et al tested ammonia oxidation rate of Nitrosomonas spp. at various nitrite concentrations from 14 to 296 mg-N/L in fresh water. Also, the nitrite oxidation rate of Nitrobacter spp was tested at various nitrate concentrations ranging from 11-250 mg-N/L. The nitrification stoichiometry is explained in section 2.1.2.1. The oxidation rates of both bacteria were found to be linearly correlated to free-energy changes (ΔG) i.e., the free energy decreased linearly with ammonia/nitrite removal. Yantarasri[59] et al modeled the bacterial degradation of ammonia and nitrite as Monod Kinetic equation with mixed inhibition model as shown below;

$$\frac{dS}{dt} = \frac{\mu'_{max}}{[\frac{K_s}{S}(1 + \frac{P}{K_i}) + (1 + \frac{P}{K_i})]} \qquad \text{.....2.12}$$

Where,

S – substrate, NH_4^+ / NO_2^- , P – Product , NO_2^- / NO_3^-

K_i – Inhibition constant μ_{max} – max specific growth rate, day^{-1}

The above model equation proposed by Yantarasri basically includes the inhibition effect of substrate on both Nitrosomonas and Nitrobacter bacteria. Both bacteria exhibited substrate inhibition at an ammonia level greater than 1.8 mg-N/L for Nitrosomonas and at a nitrite level greater than 0.5 mg-N/L.

2.1.2.1 Nitrification Process

The nitrification reaction stoichiometry is from *Fundamentals of Chemistry for Environmental Engineering and Science* which is as follows;

$$NH_4^+ + 2O_2 \longrightarrow NO_3^- + 2H^+ + H_2O \quad \text{.....2.13}$$

$$NH_4^+ + 4CO_2 + HCO_3^- + H_2O \longrightarrow C_5H_7NO_2 + 5O_2 \quad \text{.....2.14}$$

Combining equation 1 and 2 and balancing, we get,

$$22\ NH_4^+ + 37O_2 + 4CO_2 + HCO_3^- \longrightarrow C_5H_7NO_2 + 21NO_3^- + 20H_2O + 42H^+ \quad \text{.....2.15}$$

The above reaction is exothermic but the heat release is ignored because of the relatively small quantity of ammonia (few ppm) reacting in the huge ash pond. The ammonia oxidizing bacteria, the Nitrosomonas and Nitrobacter, accomplishes nitrification. The pH of the water is expected to be near neutral (~7), so most of ammonia is in the ionic (NH_4^+) state. The rate equation for the ammonium substrate utilization is from Metcalf[36] and Eddy, which is,

$$r_{su} = \frac{\mu_m X S}{Y (K_s + S)} \quad \text{.....2.16}$$

The reactor is modeled for biomass growth rate and the substrate utilization occurs as per the reaction stoichiometry of reaction 2.15. So, the biomass growth rate is (*Metcalf [36] and Eddy)*,

$$r_g = \frac{\mu_m X S}{(K_s + S)} \quad \text{.....2.17}$$

where,

r_g = rate of bacterial growth

The difference between equations 2.16 and 2.17 is the maximum yield coefficient term(Y) in the denominator of equation 2.16. In activated sludge process and other biological reaction processes the Y term is determined experimentally. The present mathematical model will be based on the reaction 2.15. The biomass growth depends on various environmental factors like temperature, dissolved oxygen concentration (DOC) and pH. *Metcalf [36] and Eddy* suggests the correction terms to be used in conjunction with equation 2.17 to account for the environmental factors. The rate equation with the temperature, DO and pH correction is as follows,

$$r_g = \mu_m * e^{0.098*(T-15)} * \left(\frac{DO}{K_{DO} + DO}\right) * [1 - 0.833(7.2 - pH)] * \frac{X * S}{K_s + S} - k_d * X \quad \text{... 2.18}$$

temperature factor | DO factor | pH factor | endogenous decay factor

Typical kinetic coefficients that are used for the nitrification process is published in *Metcalf [36] and Eddy,* which are as follows;

μ_m = 1 day^{-1}, K_s = 1.4 mg/l, k_d = 0.05 day^{-1}. However, these typical coefficients are specified for sewage and municipal water, which has higher BOD and VSS than can be

expected in an ash pond of a coal plant. Hence, in the current work these coefficients are calibrated experimentally to suit the conditions of an ash pond. The experimental setup and conclusions of this calibration are elaborated in later part of this work.

Sara[19] et al mentioned that nitrogen removal is not accurately predicted with design guidelines that utilize a ‘‘black box’’ approach in which nitrogen loss is predicted from an overall N removal term (k_N) and total nitrogen (TN) in the influent. Published k_N values for surface flow wetlands vary greatly (from <1 to >60 meter/year), making predictions of nitrogen removal inexact. Because of this, treatment wetlands are often designed conservatively, which means that they may be larger than necessary to achieve treatment objectives. Aside from the additional cost in over designing wetland treatment systems, high evaporation rates in the arid west dictate that treatment wetlands as small as possible to meet treatment objectives while minimizing evaporation. Consequently, Sara[19] et al attempted to develop a more accurate design model for nitrogen removal in wetland treatment systems, and use the model to develop approaches to improve nitrogen removal. This was part of their effort to explore low-tech systems to treat and reuse wastewater in arid region. The model was developed from field data and calibrates a simple sequential model of Nitrogen transformation. Three processes were represented: ammonification (ammonia formation from biological organisms), nitrification and denitrification. Each process was represented as a first order process. The model worked well in predicting all three nitrogen species (Particulate Organic Nitrogen, NH_4^+, nitrate) during summer months. Calibration for the ammonification and nitrification steps was also successful during the winter, but denitrification model did not work during winter months even after modifying the model with Monod kinetic equation. An overall net

nitrogen removal rate constant (k_N) was also computed for each month by Sara et al. Calibrated monthly k_N values were different from each other; with winter k_N values significantly lower than summer values. These observations of seasonal variation in nitrogen reaction kinetics of Sara et al further emphasize the necessity of calibrating any nitrification equation for TVA ash pond condition before using them in the ash pond model.

2.1.2.2 Denitrification Process

The denitrification process is the breakdown of the nitrates by heterotrophic bacteria in anoxic condition into nitrogen and other harmless products. The most common denitrifying bacteria are *Bacillus denitrificans*, *Micrococcus denitrificans*, *Pseudomonas stutzeri*, and *Achromobacter sp*[13]. In the absence of oxygen, these organisms use nitrate as terminal electron acceptors, while oxidizing organic matter for energy. The organic matter generally consumed is present in the waste water during activated sludge process. In the present case, some organic matter will have to be added to the pond continuously since the BOD of the pond is quite low (~ 2 ppm). Hanaki et al. [29] found that for a CSTR containing a nitrifier enrichment, influent ammonia was oxidized to nitrite when the DO concentration (0.5 mg/L) and SRT (4 days) were low. Interestingly, these researchers found that the addition of glucose to the influent, and presumably heterotrophic competition for oxygen, reduced the ammonia oxidation efficiency even if the bulk DO concentration was maintained at 0.5 mg/L. The denitrification stoichiometry is as follows (Cheremisinoff [13], © 1996);

$$58NO_3^- + 80\,CH_3OH + 98\,H^+ \longrightarrow 30\,CO_2 + 24N_2 + 10\,C_5H_7NO_2 + 174H_2O \ldots 2.19$$

The rate of denitrification is described by *Metcalf[36] and Eddy,* as follows;

$$U`_{DN} = U_{DN}*1.09^{(T-20)}*(1-DO) \quad \text{.....2.20}$$

Typical values of U_{DN} are given in *Metcalf[36] and Eddy.*

Shawn[23] inferred that following researchers have concluded that low DO concentration was an important factor in nitrite buildup within a variety of reactor types. Shawn inferred "Garrido[18]et al. found that stable nitrite buildup (50%) occurred in a biofilm airlift suspension reactor when the DO was gradually reduced to 1 - 2 mg/L. Bernet[37] et al. obtained stable nitrite accumulation (≈ 90% of influent ammonia) in a stirred biofilm reactor (nitrifier enrichment) if the DO was held at 0.5 mg/L. Bae[55] et al. found that low DO favored nitrite accumulation in batch experiments. Pollice[4] et al. (2002) found that lowering the SRT to 10 days in a batch reactor containing a nitrifier enrichment completely inhibited NOB when the DO was 2.0 mg/L. These researchers also demonstrated that intermittent aeration (aeration 10 minutes every 20 minutes, DO 2.0 - 0.0 mg/L) led to sustained nitrite buildup at SRTs between 3 and 24 days". So, it is inferred here that adding a separate organic carbon source to the pond will lead nitrite build-up. Free Nitrous acid (HNO_2) is suggested by Shawn[23], as inhibiting nitrification. Shawn[23] discussed in his study about the inhibitory effect of free nitrous acid. According to Shawn "Anthonisen[7] et al. investigated free nitrous acid inhibition of nitrification and proposed that concentrations between 0.06 and 0.8 mg HNO_2-N/L inhibited ammonia oxidation. Much higher concentrations are required to completely inhibit nitrite oxidation (Wong-Chong and Loehr, 1978: 2.65 mg HNO_2 -N/L). Abeling[54] and Seyfield indicated that 0.04 mg HNO_2-N/L inhibited denitrification. Fux[9]et al. observed 20 to 25% reductions in AOB activity at 0.16 mg HNO_2-N/L (pH 7, 30°C), while Hellinga[10] et al.

observed 50% inhibition at 0.2 mg HNO_2-N/L at pH 7 (total nitrite concentrations of several hundred mg-N/L at pH 6 - 8). Others have indicated that the total nitrite concentration must be exceedingly high before inhibition occurs. For example, Prakasam[45]and Loehr (1972) observed threshold levels of nitrite inhibition for ammonia oxidation exceeding 1,000 mg NO_2 -N/L. Chandran[26] observed no effect on either the maximum specific substrate utilization rate or substrate affinity constant of AOB at nitrite-N levels up to 100 mg/L. Turk[38] and Mavinic did not observe ammonia oxidation inhibition at 115 mg NO_2--N/L." The above points were put forward to point to the fact that there is a possibility of nitrite build up in the ash pond and the DO is the key factor controlling it. The volume of literature overwhelmingly point towards inhibition of AOB due to nitrite build-up. The ways and means to promote denitrification is being considered as future study of ash pond.

Philips[42] et al analyses the oxygen limited condition from another angle; that is in case of oxygen limitation, nitrifiers switch from nitrification to oxygen-limited autotrophic nitrification-denitrification (OLAND) in order to survive and maintain activity. According to Philips et al, during OLAND, ammonium is oxidized using nitrite as electron-acceptor to form dinitrogen and nitrogen gas. The additional advantage of the OLAND process is that the autotrophic ammonia oxidizer does not need a carbon source for denitrification. Philips et al thus challenges the conventional process for ammonia removal via nitrification and denitrification. This process is different from Anammox process due to the fact that OLAND process does not require anoxic conditions, but can proceed under microaerophilic conditions. Also, the OLAND process is considered to be carried out by ammonia oxidizers with CO_2 as the carbon source. According to Diab[44] et

al. and as mentioned by Philips[42] et al, exposure of nitrifying bacteria to oxygen limitation leads to a physiological modification. These authors suggested that nitrifiers survive these anaerobic conditions by switching their metabolism to a very low rate, a state of resting cells. Alternatively, nitrifiers can switch from a nitrifying activity to a denitrifying activity under conditions of oxygen stress. Philips et al mentions about a good amount of references to support the fact that under oxygen limited conditions, ammonium can be oxidized with nitrite replacing oxygen as an e-acceptor.

2.1.2.2.1 Discussion of Denitrification

As the Equation 2.20 suggests, as the dissolved oxygen (DO) increases, the denitrification rate keeps going down and ultimately becomes 0 at DO concentration of 1 ppm. So, the denitrification reaction will occur at the bottom of the pond (hypolimnion level) near the ash/sediment level where the DO concentration is supposed to be low. As is evident from the reaction stoichiometry, an organic carbon source is required to sustain denitrification reaction, presence of which is currently negligible in the ash pond. The BOD in the ash pond water is about 2 mg/l. Addition of an organic substrate like methanol can have an adverse effect on the nitrification reaction as heterotrophs growth will tend to increase the competition for dissolved oxygen.

2.2 Fate of Phosphorus and Eutrophication

TVA data indicates that the phosphorus present in the bottom ash and the fly ash is about 0.35% to 0.48%. The phosphorus present in the organic form in the coal is converted to oxides of phosphorus and present in the bottom ash and fly ash as P_2O_5 as indicated by ash composition furnished by TVA. When the ash is washed away with

water it comes to the pond as phosphoric acid. Phosphorus is the primary, controllable limiting nutrient in a lake eutrophication. The possibility of eutrophication in the ash pond may be checked by Vollenweider loading plots shown in *Steven C.Chapra*[8]. Since the 1960s, researchers have created plots that classify lakes into trophic states based on lake depth and annual phosphorus loads. Figure 2.2 adapted from Evan[22]et al illustrates one of these original loading plots. The two lines show the thresholds between oligotrophic and mesotrophic, and between mesotrophic and eutrophic. However, these thresholds are based on professional judgment and observation. According to Evan[22] et al, Vollenweider and others suggest that they correspond to phosphorus concentrations of 10 μg/L and 20 μg/L, respectively. Chapra[8] suggests thresholds for several nutrient related parameters regarding trophic state; these thresholds are reproduced in Table 2.1. As far as dependence on DO is concerned, Chapra proposes thresholds based on the percent oxygen saturation of the hypolimnion, the deep portion of stratified lakes. Low oxygen in the hypolimnion can cause the release of heavy metals from sediments due to biogeochemical reactions (Brick [34]and Moore). Chapra suggested that it was recognized by Vollenweider that not only depth but also residence time had an impact on eutrophication. In other words, faster flushing lakes are less susceptible to eutrophication than lakes with long residence times. The effect of this residence time is incorporated into the phosphorus loading plot by adding the inverse residence time to the abscissa as shown in Figure 2.3. These phosphorus loading plots can be used for both simulation and wasteload allocation predictions. Several investigators have applied Vollenweider's plots to larger data bases and have extended it to predict trophic status. As depicted in

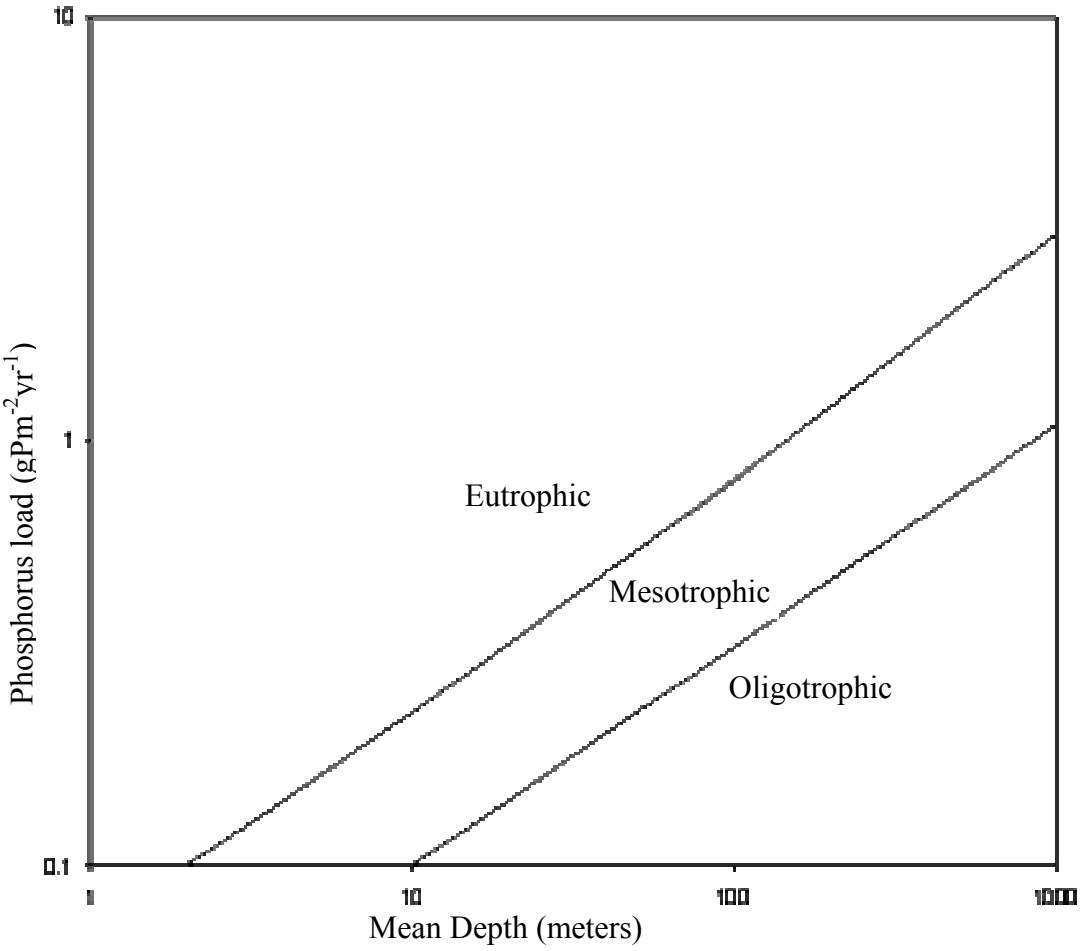

Figure 2.2: Phosphorus loading plot

Note: Adapted from Chapra[8], which references Vollenweider,1968 and copied from Evan[22] et al.

Table 2.1: Trophic state thresholds suggested by Chapra for several parameters

Notes: Copied from Chapra [8].

Parameter	**Oligotrophic**	**Mesotrophic**	**Eutrophic**
Total phosphorus (µg/L)	< 10	10 – 20	> 20
Chlorophyll *a* (µg/L)	< 4	4 – 10	> 10
Secchi depth (m)	> 4	2 – 4	< 2
Hypolimnion oxygen (% saturation)	> 80	10 – 80	< 10

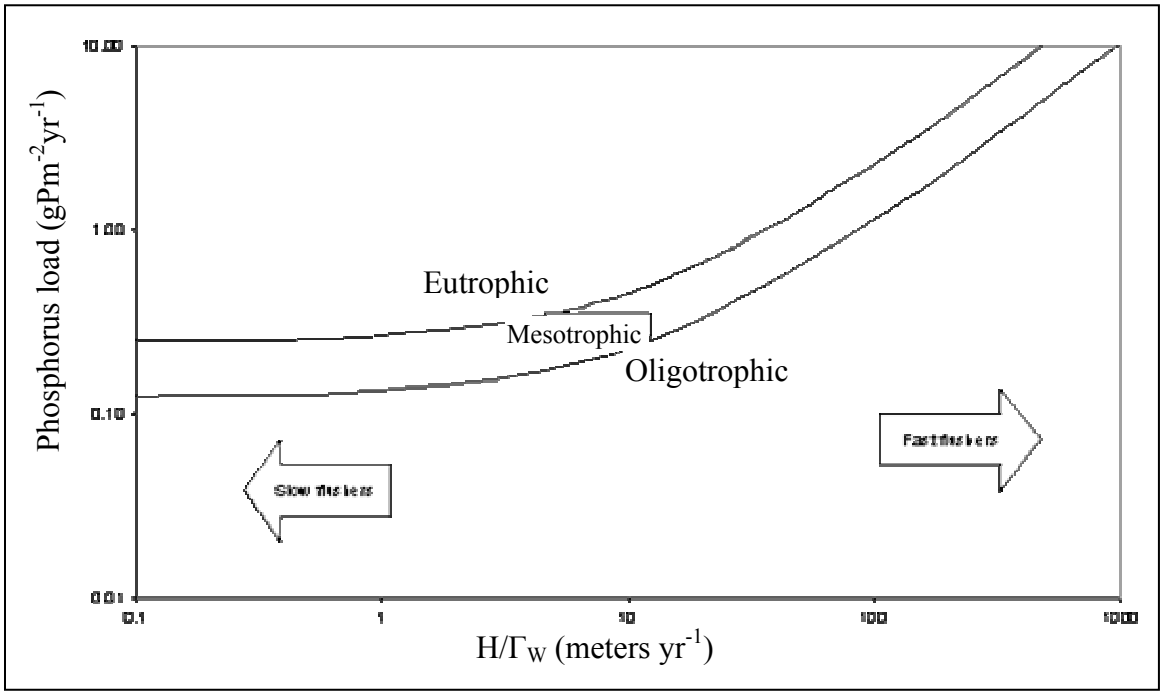

Figure 2.3: Phosphorus loading plot based on mass balance equations

Note: Adapted from Chapra[8].

Figure 2.4 (adapted from Chapra[8]), algae is the first product in the food chain of nitrate, ammonium and phosphorus.

The phosphorus destruction will be modeled as algae growth. The algal formation is expressed by Chapra with the following reaction;

$$106CO_2 + 16NH_4^+ + HPO4_2^- + 108H_2O \rightleftharpoons C_{106}H_{263}O_{110}N_{16}P + 107O_2$$

"algae" $+14H^+$ …….. 2.21

The above formula holds when ammonium is the source of inorganic nitrogen. For the case when nitrate is the source of inorganic nitrogen, the reaction is represented as follows,

$$106CO_2 + 16NO_3^- + HPO_4^{2-} + 122H_2O + 18H^+ \rightleftharpoons C_{106}H_{263}O_{110}N_{16}P + 138O_2$$

"algae"……2.22

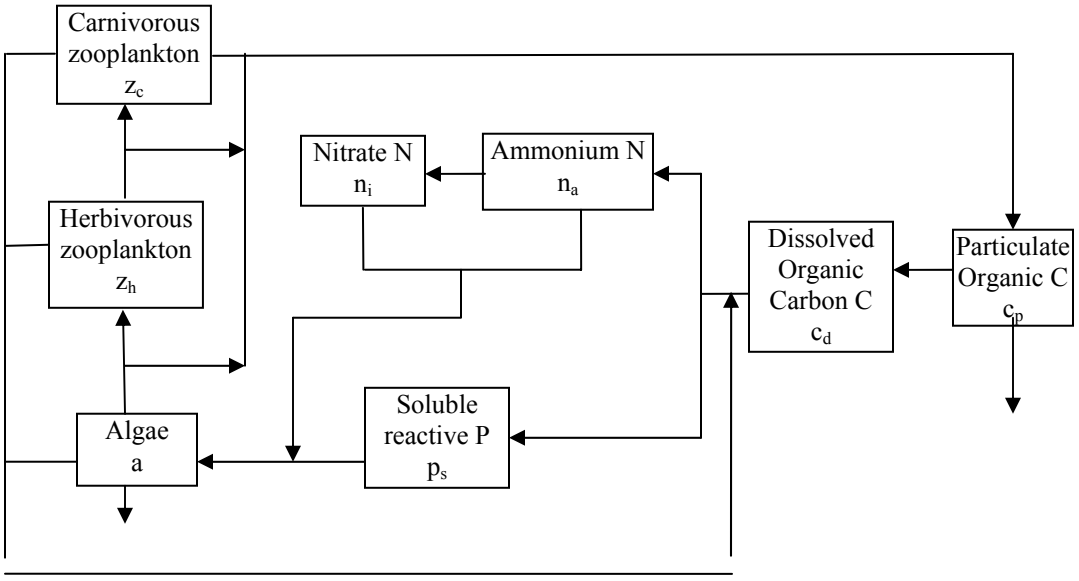

Figure 2.4: Kinetic segmentation

Note: Adapted from Chapra[8], Figure 35.2.

Algae grow as a function of temperature, nutrients, and solar radiation and is predicted by Chapra[8] as follows;

$$V\frac{da}{dt} = k_g(T, n_t, p_s, I)Va - k_{ra}(T)Va - C_{gh}(T, a, z_h)Va + v_a A_t a_u - v_a A_t a \quad \text{.....2.23}$$

where, V = volume of ash pond (m^3)

a = algal concentration (µg/ m^3)

$k_g(T, n_t, p_s, I)$ = algal growth rate (d^{-1}) = Equation 35.4[8]

$$= k_{g,20}\,1.066^{T-20}\left[\frac{2.718f}{k_e H}(e^{-\alpha_1} - e^{-\alpha_0})\right]\min\left(\frac{n_t}{k_{sn}+n_t}, \frac{p_s}{k_{sp}+p_s}\right) \quad \text{.....2.24}$$

Temperature Light Nutrients

$k_{g,20}$ = 2 d^{-1}

f = 0.5, considering half a day of available sunlight

α_1 & α_0 = light extinction coefficient = 0.158 and 1.667 respectively

$\min\left(\frac{n_t}{k_{sn}+n_t}, \frac{p_s}{k_{sp}+p_s}\right)$ =nitrogen(n_t) or phosphorus(p_s) concentration (µg/L), whichever is lower

k_{sn} = 15 µg/L ; k_{sp} = 2 µg/L

T = temperature of pond (^{0}C)

H = depth of pond

$k_{ra}(T)$ = losses due to respiration and excretion (d^{-1}) = 0.025 (d^{-1})

$C_{gh}(T, a, z_h)$ = grazing losses (d^{-1}) = 5

v_a = phytoplankton settling velocity (md^{-1}) = 0.2

2.2.1 Discussion of eutrophication

In the Vollenweider plot shown in Figure 2.2 & 2.3, Vollenweider compiled areal loadings of total phosphorus L_p ($mgPm^{-2}yr^{-1}$) and mean depth of lake H (m). Each lake is then labeled depending on its tropic status (*oligotrophic, mesotrophic, eutrophic).* Eutrophication of the ash pond is possible in the dangerous "eutrophic" zone. In the permissible "oligotrophic" zone, the phosphorus is tolerable. As it was presented by Tim Lohner, American Electric Power, supplemental phosphate in the form of phosphoric acid was added in their test pond to encourage algal growth. This indicates that the amount of phosphate released from a coal based power plant is not enough for eutrophication.

2.3 Fate of Mercury

The exact behavior of mercury in presence or absence of SCR units is unknown at this stage, however several DOE/NETL funded studies are going on to establish it. The amount of mercury present in coal varies between 0.07 – 0.19 ppm[5]. Majority of this mercury, in the absence of SCR unit (as per TVA data[5]), is emitted in the vapor form as elemental mercury along with the flue gas. However, in plants where SCR units are installed, the ash pond shows higher concentration of mercury along with other trace elements. According to Richardson[43] et al, recent tests performed for EPRI by different groups have shown a wide range of observed results ranging from 0 to over 70% mercury oxidation across SCR units. This is possible because the SCR units catalyses the reaction of mercury with chloride, sulfate or nitrate ion to form water soluble salts which is separated out in the ESP along with fly ash. The SCR units convert elemental mercury to

$HgSO_4$ and other mercury oxidation products which will be removed in the future by scrubbers and sent to the ash ponds[6]. Another hypothesis that can be given is in the presence of ammonia, the mercury and other trace elements are separated out in the ESP. Jianmin[56] et al inferred that in a system containing fly ash, ammonia, and heavy metals, the metals forms metal hydroxides, metal-ammonia complexes and adsorbed free metal, adsorbed metal hydroxides and adsorbed metal ammonia complexes. In other words, in the presence of ammonia, the metal ions have higher propensity to form complex ions and metal complexes and is adsorbed on the fly ash surface. Richardson[43] et al, however, observed that the addition of ammonia to the flue gas before it is introduced into the SCR resulted in decrease Hg oxidation. Handagama[21] et al thermodynamically analyzed the mercury speciation and mercury reemission across FGD and inferred that the mercury oxidation besides depending on the temperature drop also depends on the chlorine and sulfur in the coal. The ChemCAD simulation model for mercury speciation will be based mainly on the concept of minimization of total Gibb's Energy concept highlighted in the paper by Handagama et al and will be dealt with again later. Licata[33] et al suggested that the mercury vapor forms mercury (II) chloride when it comes in contact with gaseous hydrochloric acid at reduced temperature in the boiler (convection section) as follows;

$$Hg^0 + 2HCl \rightleftharpoons HgCl_2 + H_2O \quad \text{……..2.25}$$

As the temperature decreases, the equilibrium of the reaction shifts more and more to the right side. The complete transformation of Hg^0 into $HgCl_2$ cannot be expected as the thermodynamic balance of the above mentioned reaction appears to be blocked thermodynamically[33]. Licata[33] et al further states that a higher amount of mercury (I) chloride (Hg_2Cl_2) could be formed out of $HgCl_2$ in the presence of reducing

effects, for example by fly ash or SO_2. At the boiler's outlet temperature, the Hg_2Cl_2 is solid, and will be removed with the fly ash (sublimation temperature 383^0C). Up to 10% of the total mercury amount can be removed in this way. Handagama[21] et al further stressed the fact that the oxidation of mercury is inhibited in the presence of substantial amount (more than minute concentrations) of SO_2 in the flow gas. The portion of elemental mercury in the flue gas originating from a coal-fired power station is usually about 30 to 50%[33], which depends on the type of coal, UBC, surface area of ash, percent iron, calcium, availability of catalytic material, moisture, nitrogen, sulfur and chlorine in the coal[28]. Also, the type of Air Pollution Control Device (APCD) used determines the amount of mercury captured. Hot-side electrostatic precipitators (ESPs) do not allow as much capture of mercury on the fly ash as cold-side ESPs and fabric filters due to the operation of hot side ESPs at high temperature. Canadian Electricity Association[3] (CEA) data indicates mercury concentrates ranging from <0.002 to 1.221 ppm in fly ash and from 0.001 to 0.342 ppm in bottom ash. However, the vapor pressure of both Hg^0 and $HgCl_2$ are high, which are 14000 $\mu g/m^3$ and 800 $\mu g/m^3$ at 1 atm, 20^0C respectively (Table 1[33]). Hence, the downstream fly ash removal equipment (the cold ESP in Kingston) is not effective mercury removal equipment. The typical mercury removal efficiency is given in Table 2 of Licata[33] et al which is reproduced in Table 2.2. As may be seen from Table 2.2, about 81% of the mercury is captured in case of a plant equipped with cold ESP and wet FGD. Licata [33] et al further infers that test data from the US indicates that the oxidation shift of mercury takes place in boilers that are burning "high" chlorine coals, and does not occur when burning low chlorine coals such as PRB coal. Gale[28] et al focused on the effects of un burnt carbon (UBC) and iron in ash and the importance of

Table 2.2: Mercury capture as a function of coal type and APC equipment

Note: Adapted from Licata[33], Table 2

	% Mercury Capture		
	Bituminous	**Sub-bituminous**	**Lignite**
W/ Particulate Matter Controls			
Cold ESP	46	16	0
Hot ESP	12	13	?
Fabric Filter (FF)	83	72	?
Wet Scrubber	14	0	33
W/ FGD Controls			
Spray Dryer/FF	98	3	17
Hot ESP & Wet FGD	55	33	?
Cold ESP & Wet FGD	81	35	44
FF & Wet FGD	96	?	?

chlorine and other acid gases on mercury speciation. Canadian Electricity Association[3] indicates that carbon sorbents are expected to be used in many systems as part of the mercury control technologies and it is important to note that normal activated carbon sorbents are not expected to perform differently than unburned carbon associated with fly ash, and samples of fly ash with unburned carbon have shown similar performance in evaluations of mercury stability.

Turner[53] et al studied the sediment-water partitioning and speciation of inorganic mercury under simulated estuarine conditions by monitoring the hydrophobicity and uptake of dissolved ^{203}Hg(II) in samples from a variety of estuarine environments. In this study, Turner et al review K_Ds and sorption data for Hg (II) which are relevant to estuaries and present partition and speciation results derived under simulated estuarine conditions using natural samples from contrasting estuarine environments. Figure 2.5 is a compilation of sorption constants and field measurements for Hg(II) which are pertinent to estuaries, including results derived by radiotracer experiments in Turner [53]et al study. Although this review by Turner et al encompasses experiments undertaken using a variety of synthetic and natural sorbents under different conditions (duration, pH, particle-water ratio, particle size, degree of agitation), some general observations has been made by Turner et al.

First, in the absence of organic matter, K_Ds (mL g-1) defining Hg(II) sorption to synthetic inorganic phases (clays, oxides, silica) are on the order of 10^2-10^4 mL g-1 and exhibit a decrease with increasing salinity. This behavior according to the author is consistent with that of most other trace metals, including the other Group IIb metals, Cd and Zn, and is attributed to the tendency of Hg(II) to form soluble and stable complexes

TABLE 2. Distribution Coefficients Defining Hg(II) Sorption to Natural and Synthetic Particles (as log K_D) or Solvent (as log K_{ow}) in Fresh Water (Salinity < 1) and Seawater (Salinity > 30)

sorbent	water	POC[a], %	log K_D, mL g^{-1} (or log K_{ow}) freshwater	seawater	ref
Synthetic Particles					
illite	artificial river water and seawater		3.72	3.41	*21*
kaolinite	artificial river water and seawater		4.28	3.95	*21*
silica	natural seawater			2.36	*22*
montmorillonite	natural seawater			3.30	*22*
fulvic acid-coated montmorillonite	natural seawater			4.83	*22*
calcite	natural estuarine water and seawater		4.38[b]	3.83	*23*
	natural estuarine water and seawater, UV-photolyzed		2.69[b]	3.19	*23*
Solvents					
octanol (Hg as $HgCl_2^0$)	pure water		0.52		*15*
octanol (Hg as $Hg(OH)_2^0$)	pure water		−1.30		*15*
Natural Particles					
Hudson estuary suspended sediment	natural river water and seawater	10[c]	4.76	5.08	*5*
Narragansett Bay sediment	natural seawater	2.0		5.23	*24*
Carbonate ooze	natural seawater	0.5		4.40	*25*
silicious clay	natural seawater	1.3		3.47	*25*
deep-sea sediment	natural seawater	2.5		4.85	*25*
Long Island sediment	natural seawater	~5		5.23	*22*
Trinity River particles	natural river water and seawater		5.40	5.50[d]	*6*
Beaulieu estuarine sediment	natural river water and seawater	6.9	4.56	5.42	this study
Plym estuarine sediment	natural river water and seawater	2.1	4.73	5.42	this study
Mersey estuarine sediment	natural river water and seawater	7.5	4.74	5.74	this study
Mersey estuarine sediment, organic matter removed	natural river water and seawater	<0.1	3.70	3.40	this study
Field Studies					
Gironde estuarine end-member particles	natural river water and seawater		5.35	5.08	*26*
Lena estuarine end-member particles	natural river water and seawater		5.20	5.40	*27*
Loire estuarine end-member particles	natural river water and seawater		5.30	5.60	*28*
Ob estuarine end-member particles	natural river water and seawater		4.90	5.20	*27*
Rhône estuarine end-member particles	natural river water and seawater		5.75	5.65	*29*
Scheldt estuarine end-member particles	natural river water and seawater		5.70	5.70	*10*
Seine estuarine end-member particles	natural river water and seawater		6.00	5.90	*28*
Yenisei estuarine end-member particles	natural river water and seawater		5.30	5.20	*27*

[a] POC values are usually reported but cannot always be linked to corresponding sorption data. [b] Salinity = 3. [c] As loss on ignition. [d] Salinity = 24.

Figure 2.5 Distribution coefficients of Hg (II) with various sorbents

Note: Copied from Turner[53], Table 2

with Cl^- (principally as $HgCl_4^{2-}$) in the presence of seawater ions. Second, the presence of organic matter in the aqueous phase enhances the sorption of Hg(II) to mineral surfaces. For example, sorption of Hg(II) to calcite is reduced by factors of about 50 and 4 when organic matter is removed from river water and seawater, respectively. Sorption enhancement in the presence of dissolved organic matter is due to the greater affinity of organic-complexes of Hg(II) (compared with inorganic species) for mineral surfaces and enhancement of the general sorptive properties of the particle surface by adsorbed organic matter. Third, sorption of Hg(II) is significantly enhanced by the presence of preexisting particulate organic matter. For example, experiments conducted as part of Turner et al study showed that sorption of Hg(II) to Mersey estuarine sediment was reduced by 1-2 orders of magnitude once particulate organic matter had been digested in H_2O_2. According to Turner et al, the association of Hg(II) with sediment organic matter is exemplified by the relationship between the distribution coefficient defining Hg(II) sorption to natural particles in seawater and particulate organic carbon (POC) concentration.

Fourth observation by Turner et al is that the sorption of Hg(II) to natural sediment exhibits a significant increase with increasing salinity or the opposite effect to that predicted from simple inorganic speciation considerations and observed for other Group IIb trace metals. Distribution coefficients (as K_D and organic carbon normalized values, K_{oc}) defining ^{203}Hg(II) sorption to estuarine sediments measured in this study are plotted against salinity. The ash from a coal fired power plant resembles the synthetic inorganic phases (clays, oxides, silica) in characteristics, which according to Turner et al has a K_Ds in the range of 10^2-10^4 mL g^{-1}. However, the desorption kinetics and K_Ds will

be evaluated for the model, to arrive at a near accurate mercury concentration under various process condition of the power plant. As per Allison[14] et al, mercury is among the metals having higher K_d (partition coefficient) than most. In other words, mercury have higher propensity to remain in the solid media (soil, sediment, etc) than other metals. To put things in perspective, Allison et al arranged the metals in the order of decreasing K_d;

Soils: Pb > Cr^{III} > Hg > As > Zn = Ni > Cd > Cu > Ag > Co

Sediment: Pb > Hg > Cr^{III} > Cu > Ni > Zn > Cd > Ag > Co > As

SPM: Pb > Hg > Cr^{III} = Zn > Ag > Cu = Cd = Co > Ni> As

As is evident from above, K_d of mercury is higher than most other metals in all the three media. The suggested mean values of K_d by Allison et al are;

Soil/Soil water	:	3.6	L/Kg
Sediment/porewater	:	4.9	L/Kg
Suspended matter/water	:	5.3	L/Kg

The partition coefficient suggested by Turner[53] et al for sediment/fresh water ranges from 3.7 to 5.4. A preliminary calculation done as part of this work suggests a value of 3.93 L/Kg for ash/ash pond water, which is within the range suggested by Allison et al and Turner et al. In order to get a more credible steady state concentration of mercury in ash pond water, the kinetics of mercury desorption from ash is studied and presented later.

2.3.1 Discussion on fate of Mercury

TVA data furnished by Handagama[20] suggests 70% of the total mercury capture with the fly ash in the ESP and about 4.5% with the bottom ash in case of Kingston plant.

This will form the basis of our model for mercury separation with bottom/fly ash. The suggested high percentage of capture with fly ash is due to the installation of SCR units, which oxidizes substantial amount of elemental mercury. The mercury laden fly ash and bottom ash is wet sluiced and carried to the ash pond in Kingston power plant. Very little information is available about the desorption kinetics of the mercury into ash pond water.

2.3.2 Mercury leaching from ammoniated fly ash

Preliminary leaching results by Murarka [40] et al confirms that ammonia is easily leached from fly ash. Moreover, the increased levels of ammonia did not increase the mercury in the leachate, which means ammonia has no effect on mercury leaching from fly ash. This fact is also confirmed by Cardone [12] et al. Theis[51] et al studied Mercury leaching with changing pH and concluded that mercury leaching has no correlation with ash properties such as pH(pH and ammonia concentration has a direct relation). However, Handagama [20] suggested no recent studies confirms the claim and hence a thorough study of the ammonia mercury interaction will be helpful.

2.4 Water Pinch Analysis

Fresh water usage reduction is one of the many problems power plants world wide faces currently. High costs for freshwater, effluent treatment, and disposal are the reasons for attempting to reduce fresh water intake. This will dictate process debottlenecks caused by water-system limitations. In order to solve the problems associated with water usage reduction, several new tools for industrial water-system optimization (WSO) have emerged since the mid-1990s. Mann[17] and Liu helps in understanding some of the new WSO tools, including water-pinch technology and

mathematical optimization, and demonstrates how to apply a stepwise procedure that can serve as a proven method for implementing water-saving projects, and generating significant economic and environmental benefits. Wang [41, 57] et al of the University of Manchester Institute of Science and Technology published two articles on water-pinch technology, demonstrating how to integrate the use of water resources to maximize water reuse, minimize wastewater generation, and reduce effluent treatment. To put it in simple form, this technology treats a water-using operation as a problem of mass transfer from a *contaminant-rich* process stream to a *contaminant-lean* water stream. "Contaminants" may include suspended solids, chemical oxygen demand, a pollutant like mercury or other water-quality factors that limit water reuse. The process identifies a pinch point, called *the freshwater pinch* that is based on the concentration of a key contaminant. Streams with contaminant levels above that concentration do not require freshwater, but can reuse water streams from elsewhere in the process having out let concentration of the contaminant lower than the pinch point. Using this information, we can then maximize water reuse and minimize wastewater generation.

There are software tools available to implement water – pinch technology. The following methods are mainly used for designing the various available software for water pinch analysis;

- Concentration-composite curve
- Water Source and demand plot
- Source-sink mapping diagram

The software *Water Design* can be freely downloaded from the website, www.che.vt.edu/Liu/liu.htm is based on *concentration composite curve*.

2.4.1 Water Target

The *Water Target* is commercially available software from Linnhoff March Energy Services (www.linnhoffmarch.com), an affiliate of KBC Technologies. WaterTarget is a software suite enabling the efficient use and re-use of water to minimize the cost of consuming, treating and discharging water and to minimize capital expenditure on treatment facilities. The suite comprises two parts - WaterTracker for generating reconciled water balances with a minimum of flow and contaminant measurements and WaterPinch for the design of optimum water networks and wastewater treatment strategies. WaterPinch implements Linnhoff March's patented systematic technology for analyzing water networks and reducing water costs for processes. It uses advanced algorithms to identify and optimize the best water re-use, recycling, re-generation and effluent treatment opportunities. The software implements what is potentially a very complex technology in an intuitive, user friendly manner, enabling engineers to analyze even the most complex problems at the touch of a button. By analyzing complete or partial water systems, WaterPinch highlights those processes where money saving potential is greatest. Figure 2.6 gives an indication of the user interface of the WaterTarget and the input required from the user to analyse a particular network.

The software then helps to:

- Identify where water can be simply re-used or recycled and how this is best achieved
- Find the best intermediate treatment options that will allow water to be re-used or recycled

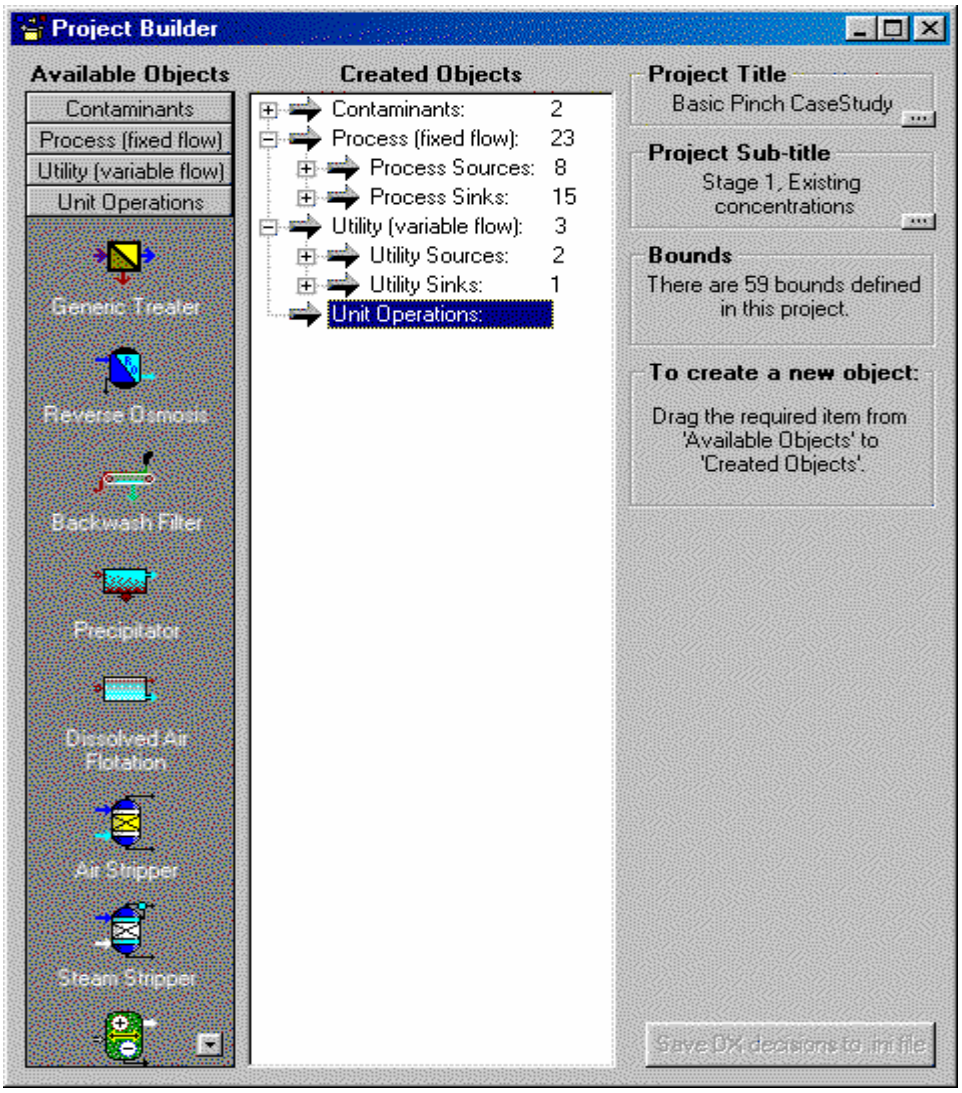

Figure 2.6 User interface of WaterTarget (adapted from Linnhoff March Energy Services website, www.linnhoffmarch.com)

- Investigate the potential benefits of relaxing the current operating practices of the water-using processes
- Determine which streams to include in a distributed effluent treatment scheme to reduce overall wastewater treatment cost

2.4.2 Cascade Analysis

Manan[35] et al describes the cascade analysis technique as a new method to establish the utility targets for water networks. Cascade analysis is a numerical alternative to the graphical targeting technique known as the surplus diagram. The cascade analysis can quickly yield accurate utility targets and pinch point locations for water or hydrogen network, thereby offering the design and retrofit of a process water network. In water pinch analysis, this numerical tool is known as *water cascade analysis* (WCA). The main objective of the Water Cascade Analysis (WCA) as given in Manan[35] is to establish the minimum water targets, i.e. the overall fresh water requirement and wastewater generation for a process after looking at the possibility of using the available water sources within a process to meet its water demands.

To achieve this objective, one has to establish the net water flow rate as well as the water surplus and deficit at the different water purity levels within the process under study. The detailed method is not discussed here and reader may refer Manan [35]et al for further details. Manan et al concludes that all the key features and the systematic nature of the cascade analysis make it easy for the technique to be automated and translated into any computer language for software development and that the WCA feature has been recently incorporated in *Heat-MATRIX*, a new software for energy and water reduction

developed by the Process Systems Engineering Group, Department of Chemical Engineering, Universiti Teknologi Malaysia. Since, no software has so far been developed to do Cascade analysis, the method could be cumbersome and full of errors.

Hence, the only alternative for the pinch analysis in the present context of power plant water usage reduction pinch analysis is the freely available software *Water Design*. The detailed method used in *concentration-composite curve* used in *Water Design* is discussed later in Chapter 8. However, the basic idea behind which the pinch analysis works for a particular contaminant and operation is as follows;

$$f_i^{lim}\ (te/hr) = \frac{\Delta\ m_{i,tot}\ (kg/hr)}{[C_{i,out}^{\ lim} - C_{i,in}^{\ lim}]\ (ppm)} \times 10^3 \quad \ldots\ldots\ldots\ldots\ldots\ldots 2.26$$

Where,

f_i^{lim} = limiting water flow rate in a particular operation

$\Delta\ m_{i,tot}$ = mass of contaminant picked up in that operation per hour

$C_{i,out}^{\ lim}$ = contaminant level in the outlet stream in ppm

$C_{i,in}^{\ lim}$ = contaminant level in the inlet stream in ppm

The pinch analysis can be done for one contaminant at a time by *Water Design*.

2.5 Discussion on fate of Arsenic and Selenium

Arsenic and Selenium speciation in flue gas is not well understood from the literature. Murarka[40] et al suggests that increased levels of ammonia in fly ash increased leaching of both arsenic and selenium. Theis[51] et al suggested that most of the trace metals displayed slight increases in release at high pH, arsenic desorption rose sharply,

reaching an average of 40% of the total available at pH 12. Arsenic forms precipitates with many trace metals, especially iron and the sudden jump of Arsenic desorption at pH 12 is attributed to the unavailability of free metal ions to cause its precipitation. Dowling[16] et al suggests that there are strong correlations among high levels of dissolved arsenic and iron, ammonia and methane. The correlation for the presence of arsenic and ammonia in groundwater of Bengal Basin is quite high at 0.87, suggesting desorption of arsenic from sediment in presence of ammonia. The interaction of arsenic, selenium and ammonia in ash pond and the arsenic and selenium speciation needs further study and incorporated in the model. Due to the volume of work needed to properly predict arsenic and selenium in the ash pond, the desorption kinetic study and their interaction with ammonia is not considered part of this work and needs separate attention.

CHAPTER 3.0

THEORY

3.1 Nitrification in Ash Pond

Nitrogenous compounds are deleterious to aquatic environment. These compounds can cause a significant depletion of dissolved oxygen in receiving waters, exhibit toxicity towards fish, and present public hazard. Presence of ammonia causes increase in the nitrogenous oxygen demand (NOD) of the water and causes the nitrification to become active and causing acute toxicity. Hence, the release of the nitrogenous compounds is being strictly regulated by environment authorities. Nitrification followed by denitrification processes plays an important role in meeting these regulations in NH_4^+/ammonia release to ponds and rivers. Nitrification, as is well known, is the process by which ammonia is first converted to nitrite and then to nitrate. Denitrification process produces nitrogen from nitrates and nitrites. Nitrogen is unique in the sense that it has the capability to exist in seven oxidation states, ranging from minus 3 to plus 5, and therefore found in many compounds. Generally in wastewater, nitrogen is found as organic nitrogen, ammonia nitrogen, nitrate nitrogen or nitrite nitrogen.

The fate of nitrogen in ash pond and before coming to the ash pond is discussed in detail in chapter 2. Majority of the ammonia comes to the ash pond as ammonium bisulfate (ABS). This is concluded in various literature and is demonstrated by a ChemCAD model. The model flowsheet is shown as figure 3.1.

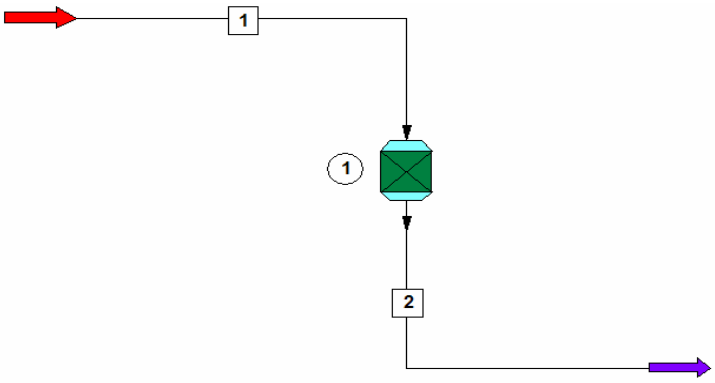

FLOW SUMMARIES		
Stream No.	1	2
Stream Name		
Temp F	68	77.1213
Pres bar	1	1
Enth kJ/h	-7.03E+05	-7.03E+05
Vapor mass fraction	0	0
Ph value	0.2525	0.1744
Ionic strength molal	0.5803	0.6455
Total lb/h	100	100.0022
Flowrates in lb/h		
Ammonia	0	0
NH4 Bisulfite	0	0
Ammonium Sulfite	0	0
Ammonium Sulfate	0	0
NH4 Bisulfate	0	0.0004
Water	94.6983	94.6324
Sulfuric Acid	0	0
H2SO3	0.3	0
H+	0.0534	0.0638
OH-	0	0
NH4+	0.0001	0
HSO4-	4.7578	5.172
SO4--	0.1905	0.1336

Figure 3.1 : ChemCAD simulation flowsheet for ABS formation

The stream 1 in the flowsheet in figure 3.1 is the inlet stream containing some arbitrary amount of ammonium, sulfate, bisulfate besides other things. The purpose of this flowsheet is to show that in presence of ammonium, sulfate and bisulfate ions, the product that will form is ammonium bisulfate. Stream 2 is the product stream and it is shown that all the ammonium ion is converted to ammonium bisulfate (ABS) and not ammonium bisulfite, ammonium sulfite or ammonium sulfate. Equipment 1 is a gibb's reactor, which takes a feed of reactants and produces a combination of products in such a way so that the total Gibb's free energy is minimum or zero. The mercury speciation is also done on the same principle of minimization of Gibb's free energy, as explained later in this chapter.

So, the ammonia will come to the ash pond as ammonium bisulfate. Organic nitrogen may release ammonia during the bacterial decomposition of these compounds. Ammonia nitrogen, as described in chapter 2.0, may exist in aqueous solution as either ammonium ion or unionized ammonia or both depending on the pH of the system. Unionized or free ammonia greater than 0.2 ppm is fatal to several species of fish[11]. Nitrite nitrogen is unstable and easily converted to nitrate. It is the intermediate compound in the process of nitrification of ammonia to nitrates. Some industrial wastes due to oxygen depletion may have higher amounts of nitrites. Nitrite build up in waste water inhibits ammonia oxidizers. Nitrate nitrogen is the most stable oxidized form of nitrogen. Nitrate nitrogen release to rivers and streams do not cause any oxygen demand and hence not considered toxic. However, excess nitrate release may result in eutrophication (algae growth), which prevents oxygen diffusion deep into the water.

As shown in equation 2.7 in chapter 2, the nitrification reaction is indicated as follows;

$$22\ NH_4^+ + 37O_2 + 4CO_2 + HCO_3^- \longrightarrow C_5H_7NO_2 + 21NO_3^- + 20H_2O + 42H^+$$

The above equation indicates the destruction of alkalinity. One mole of calcium bicarbonate is required to neutralize every two moles of nitric acid produced by the above reaction,

$$2H^+ + 2NO_3^- + Ca(HCO_3)_2 \longrightarrow Ca(NO_3)_2 + 2CO_2 + 2H_2O \quad \text{…….3.1}$$

In other words, alkalinity destruction is expressed as 7.14 mg/l[13] of alkalinity as $CaCO_3$ destroyed per mg NH_3-N oxidized.

3.1.1 Nitrification Process Variables and Kinetics in Ash Pond

Nitrifying bacteria needs specific environmental conditions unlike most heterotrophic bacteria. The most important process conditions which affect nitrifying bacteria growth are temperature, pH, dissolved oxygen, solids retention time (SRT), ammonia concentration, organic concentration, and inhibitory compounds. It has been reported by Cheremisinoff[13] and Sawyer[11] et al that ammonium oxidation to nitrite and nitrate is a zero-order reaction with respect to ammonium concentration for concentrations down to about 1 to 5 mg/l. However, things are much more different in an ash pond, where maximum ammonia-nitrogen concentration is expected to be 2 ppm. Hence, the ammonia oxidation by nitrifying bacteria is not likely to follow Monod kinetic equation as given by equation 2.18 in chapter 2.

$$r_g = \mu_m * e^{0.098*(T-15)} * \left(\frac{DO}{K_{DO} + DO}\right) * [1 - 0.833(7.2 - pH)] * \frac{X * S}{K_s + S} - k_d * X$$

Also, if the nitrification process is modeled as equation 2.18, the various constants in the equation e.g, half saturation constant (K_s), maximum specific growth rate (μ_m), etc, needs to be calibrated for the specific case of a ash pond. These constants as given in Table 11-16 of Metcalf [36] and Eddy are for the specific case of activated sludge process where the NH_4^+- N concentration will be much higher (50 ppm or higher). Another factor to be considered in a sewage treatment plant is that there will be continuous aeration in the pond which will prevent oxygen depletion. The biomass concentration is also important in judging the Monod kinetic equation constants. The VSS concentration in the ash pond is 2.5 mg/l, whereas in a sewage water it will typically be approximately 1500 mg/l. The more the amount of biomass the faster and easier it is to oxidize ammonia. Moreover, the solid retention time (SRT) will not play any role in the ash pond as no biomass recycle mechanism is involved here. Considering the difference in biomass concentration and various mode of operation of an ash pond from a sewage treatment unit, it will be necessary to calibrate the Monod kinetic constants.

3.2 Denitrification in an Ash Pond

The process of reduction of nitrate nitrogen by certain species of bacteria under anoxic conditions is called denitrification. The denitrification process produces nitrogen, nitrogen oxide or dinitrogen oxide which then escapes from solution to the atmosphere. The nitrate from nitrification increases the TDS of the water. There is an upper limit stipulated as 750 mg/l[39] of TDS regulated in some states in the US. A few ppm of nitrate addition do not pose a serious problem to the TDS in water. However, the study of denitrification in a separate pond, with external addition of an organic source is possible

and can be studied further. The process of denitrification in the ash pond needs to be separated from nitrification, as external organic source will cause oxygen depletion leading to nitrite build-up. The denitrification stoichiometric equation is typically represented as equation 2.19 in chapter 2 and shown below;

$$58NO_3^- + 80\,CH_3OH + 98\,H^+ \longrightarrow 30\,CO_2 + 24N_2 + 10\,C_5H_7NO_2 + 174H_2O$$

As shown above, denitrification bacteria need a carbon source for nitrate reduction. Methanol is shown here as a typical carbon source. Hence, unlike the nitrifying bacteria which are autotrophic in nature, denitrifying bacteria consists of heterotrophic organisms. These organisms use nitrate or nitrite as terminal electron acceptors, while oxidizing organic matter for energy. This process called nitrate dissimilation results in the eventual reduction of nitrate to nitrogen gas. Presence of oxygen actually inhibits denitrification. Consequently, at DO concentrations greater than approximately 0.5 mg/l, oxygen will be more readily utilized as the final electron acceptor than nitrates by the heterotrophic organisms[13]. In addition to a organic source, certain species of autotrophic bacteria has been found that are capable of oxidizing sulfur and sulfur compounds while reducing nitrate to free nitrogen gas. Lab-scale studies by Biscogni[24] et al indicated that reliable autotrophic denitrification could be obtained using thiosulfate and/or sulfide as electron donors for T.denitrificans, a species of bacteria capable of autotrophic denitrification. The low sulfur variety of coal, the PRB coal, has 2.5 -3.5% of sulfur present in it. Much of this sulfur converts to SO_2 and to SO_3 and finds its way into the ash pond as ammonium bisulfate/sulfate (if SCR and ammonia is present) or as adsorbed sulfuric acid. The presence of sulfur in ash pond is well documented in TVA. This sulfur can be

beneficially used in the denitrification process. This will serve the dual purpose of denitrification as well as eliminating the requirement of a organic source for denitrification.

3.2.1 Denitrification Kinetics

As in the nitrification process, denitrification process also needs specific environmental conditions to be able to sustain and proceed. Factors important for denitrification are nitrate nitrogen concentration, pH, temperature, and carbon concentration.

The denitrification equation is expressed by equation 2.20 in chapter 2, which is;

$$U`_{DN} = U_{DN} * 1.09^{(T-20)} * (1-DO)$$

Where,

$U`_{DN}$ = overall denitrification rate

U_{DN} = specific denitrification rate, lb NO_3 – N/lb MLVSS . d

DO = dissolved oxygen in the wastewater, mg/l

The DO term in the above equation indicates that as the DO increases to 1, the denitrification rate keeps on decreasing and ultimately becomes zero when the DO is 1. Table 11-19 gives the denitrification rate for various carbon sources like, methanol, wastewater, endogenous metabolism. The overall denitrification rate in the above

equation is given by;

$$U'_{DN} = \frac{S_0 - S}{\theta X}$$

where, S_0 = Initial concentration of nitrate, mg/l

S = Final concentration of nitrate, mg/l

Θ = residence time, hr or day

X = biomass or MLVSS, mg/l

So, given the inlet, outlet concentration of nitrate and biomass concentration in the wastewater, the residence time required to reduce a given amount of nitrate can be calculated. The denitrification rates are expected to be lower when oxidizable organic substances in water (BOD) are substituted for methanol. As per TVA indication, the BOD of the ash pond water is as low as 2 ppm. There is also the absence of methanol in the ash pond water. This suggests that denitrification by traditional methods is not probable. Denitrification by other means such as reduction of sulfur compounds may be studied. Addition of methanol into the ash pond is also likely to inhibit the denitrification process.

3.3 Mercury Speciation in a Fossil Fuel based Power Plant

Fossil Fuel based power plants concern with mercury centers around the nature of mercury that is emitted and that goes to the water. Combustion of coal produces hot gases

and particles that are typically contained in a radiant furnace operating at temperatures exceeding 2000 °F (1093 °C). Most of the mercury in coal entering the furnace is rapidly volatilized and moves through the convective section and economizer (colder convective section) of the boiler before exchanging heat in the air preheater. The extent to which mercury is removed from the flue gas is severely limited because of the extreme temperatures associated with this portion of the power plant. Mercury emissions from coal- fired boilers can be empirically classified, based on the capabilities of currently available analytical methods, into three main forms: elemental mercury (Hg^0), oxidized mercury (Hg^{2+}), and particle-bound mercury (Hg_p). The concentration of Hg^0, Hg^{2+}, and Hg_p primarily depends on coal composition and combustion conditions. Depending on the coal type, a significant fraction of the mercury can be oxidized, as well as become associated with the fly ash particles in the colder zone of boiler, and in the colder parts of the plant. Relative to Hg^0, Hg^{2+}, and Hg_p are more effectively captured in conventional pollution control systems, such as flue gas desulfurization (FGD) systems, fabric filters, and electrostatic precipitators (ESPs). The identification of a process for converting Hg^0 to Hg^{2+} and/or Hg_p forms could potentially improve the mercury removal efficiencies of existing pollution control systems.

The thrust is on to establish a link between concentrations of mercury in the ambient air, soil, water, and sediments to evaluate the benefits of various control strategies. The term “Speciation” is a very commonly used word for mercury identification as various oxidation types, particulate bound and elemental form in coal based power plant. Various theories and suggestions have been put forward by various literature based on various theoretical and experimental analyses. This work considers the

mercury oxidation under different process conditions based on the concept of "minimization of total Gibb's free energy of the system". That is, mercury and its oxides reach equilibrium at all conditions while traveling from high temperature zones, to ammonia injected SCR zone to low temperature zone after air preheater (APH). As the mercury in the flue gas travels through different temperature zones in the plant, the equilibrium of equation 2.25 keeps shifting towards left or right;

$$Hg^0 + 2HCl \rightleftharpoons HgCl_2 + H_2O$$

The equilibrium shift takes place by minimization of "Gibb's free energy". Equation 14.3 in Smith and Van Ness[25] is,

$$(dG^t)_{T,P} \leq 0 \quad \text{.....3.2}$$

Smith et al indicates by the above equation that all irreversible processes occurring at constant T and P proceed in such a direction as to cause a decrease in the Gibb's energy of the system. Therefore, the equilibrium state of a closed system is that state for which the total Gibb's energy is a minimum with respect to all possible changes at the given T and P. This criterion of equilibrium provides a general method for determination of equilibrium states. One writes an expression for G^t as a function of the numbers of moles of the species in the several phases, and then finds the set of values for the mole numbers that minimizes G^t, subject to the constraints of mass conservation. This procedure is applied to the ammonium bisulfate problem in figure 3.1. As illustrated there, ABS formation minimizes the G^t of the system at that condition of temperature and pressure. This is the principle applied in a Gibb's reactor in ChemCAD and ASPEN process simulation packages. To apply equation 3.2, one develops an expression for G^t as a function of the mole numbers of the species in the various phases, and sets it equal to

zero. The resulting equation along with those representing conservation of mass provide working equations for the solution of equilibrium problems. However, this convergence of equations and minimization of Gibb's energy for the purpose of calculating equilibrium mole fractions will be done in this work by Gibb's reactor in ChemCAD. The author will be providing the input details to the reactor and the possible product components. The product calculates the amount of various components formed.

By the time the flue gas reaches the Flue Gas Desulphurization (FGD), the temperature drops appreciably to alter the equilibrium. The equilibrium of elemental mercury to oxidized mercury keeps shifting back and forth depending on the temperature fall in the system, addition of ammonia. The chlorine to sulfur ratio in the coal also determines the reemission of elemental mercury after FGD. As the chlorine (ppm) to sulfur (percentage) ratio in coal falls below 300, part of oxidized mercury starts getting reduced in the FGD and is emitted as elemental mercury. This fact reemission of mercury was noticed by various researchers and it was first analyzed by "minimization of total Gibb's energy" concept by Handagama[21] et al. Similarly, a number of concepts taking place in the power plant in general and with respect to mercury speciation in particular can be explained by the "Gibb's free energy" concept.

The particulate bound mercury does not follow any definite mathematical model or explained in literature. The amount of mercury (both Hg^0 and Hg^{2+}) captured by the fly ash and then ultimately captured in the ESP is specified based on experience of TVA and as specified in other publications. The captured mercury then comes to the ash pond with fly ash sluice water. The mercury in the ash pond partly desorbs from the ash surface and goes into the aqueous phase and then to the river. The rate of desorption is determined

experimentally, as described in chapter 4, and incorporated in the model.

3.4 Sluice water pinch analysis and sluice water recirculation

Water reuse: Wastewater can be reused directly in other water-using operations when the level of previous contamination does not interfere with the water – using operation. The reuse amount can be regulated by water pinch analysis, so that the previous contamination does not affect the process. This reduces both freshwater and wastewater volumes but leaves the mass load of contaminant essentially unchanged. Many water-using operations involve multiple contaminants and physical limitations. In such cases, mathematical optimization techniques can be used, which effectively minimize an objective function subject to constraint relationships among the independent variables—for example, the total cost of freshwater consumption and wastewater treatment involving multiple contaminants. The mathematical optimization can be achieved either by *linear programming*, used for linear objective functions subject to linear constraints, and *nonlinear programming* (NLP), used when nonlinearities appear in either the objective functions or constraints. Mann[17] and Liu provide detailed examples applying both approaches to water-using operations and effluent-treatment systems using inexpensive software tools such as the MINOS solver for NLP problems, available from the GAMS Development Corporation (www.gams.com). However, multiple contaminants and physical limitations are not considered in this present work.

The water pinch analysis is done with nitrates (NO_3^-) first and then with mercury, using *Water Design*. The pinch analysis will be done on the sluice water used for ash

sluicing and collected in ash pond. From the ash pond it will be proposed to recycle part of this water for sluicing. In Kingston power plant, the condenser cooling water has a separate source and sink in the plant and this is the case in general. The cooling water does not get contaminated generally. The cooling water usage reduction will not be suggested by pinch analysis.

The present work implements water-pinch analysis based on *concentration-composite curve* by using *Water Design* (which can be downloaded from the website, www.che.vt.edu/Liu/liu.htm). The reason for choosing this method is because it is easy to understand, simple and the freely available software can be used to make a foundation on which the ash pond water pinch analysis can be done and built upon further for future use.

We discuss the concentration-composite curve below to highlight the concepts of water-pinch technology. A typical water pinch analysis done on the ash pond is shown here to explain the concept for pinch analysis (concept source: Mann[17] and Liu). A pinch analysis on similar lines will be performed based on ammonia/ammonium, mercury and nitrate. Each one will be analyzed and waste water reuse will be suggested based on the optimum condition. The pinch analysis and suggestion for water reuse is done in chapter 8. Table 3.1 shows an example with three water-using operations: a fly ash sluicing (operation 1), a bottom ash sluicing (operation 2), and a washing and maintenance step (operation 3). The primary contaminant in the example that limits water reuse is nitrate ion. We require that the water stream enters the water-using operation i at a contaminant concentration less than a specified limiting inlet concentration ($C^{lim}_{i,in}$ in ppm). Likewise, the water stream leaves the water-using operation i at a contaminant concentration less

Table 3.1 Limiting process condition for pinch analysis

Operation	Description	Limiting Flowrate (te/hr)	Limiting Inlet Conc.(ppm)	Limiting Outlet Conc.(ppm)	Mass Load (kg/hr),Δm_i
1	Fly ash sluice water	4000	0	0.36	1.44
2	Bottom ash sluice water	1000	0.3	0.4	0.1
3	Washing & Maintenance	1000	0.3	0.5	0.2

than a limiting outlet concentration ($C^{lim}_{i,out}$ in ppm). The limiting water flow rate for operation i (f^{lim}_i in te/hr) [1 metric ton or tonne (te) = 1 m^3 = 1000 liter; 1 te/hr = 4.4029 gpm] is the water flow rate needed to achieve the transfer of the mass load of contaminant, $\Delta m_{i,tot}$ (kg/hr). We relate these quantities by:

$$f_i^{lim}\left(\text{te/hr}\right) = \frac{\Delta m_{i,tot}\left(\text{kg/hr}\right)}{\left[C_{i,out}^{lim} - C_{i,in}^{lim}\right]\left(\text{ppm}\right)} \times 10^3 \qquad \text{.....3.3}$$

The concentration-composite curve and the water-supply line for the above example is plotted as follows.

Step 1. Each water-using operation is on a plot of concentration versus mass load of contaminant transferred within the operation (Figure 3.2).

Step 2. Sum the mass load within each concentration interval, created from the set of inlet and outlet concentrations to give the composite curve (dashed red lines in Figure 3.2)

Step3. Remove the original lines representing each operation to yield the concentration-

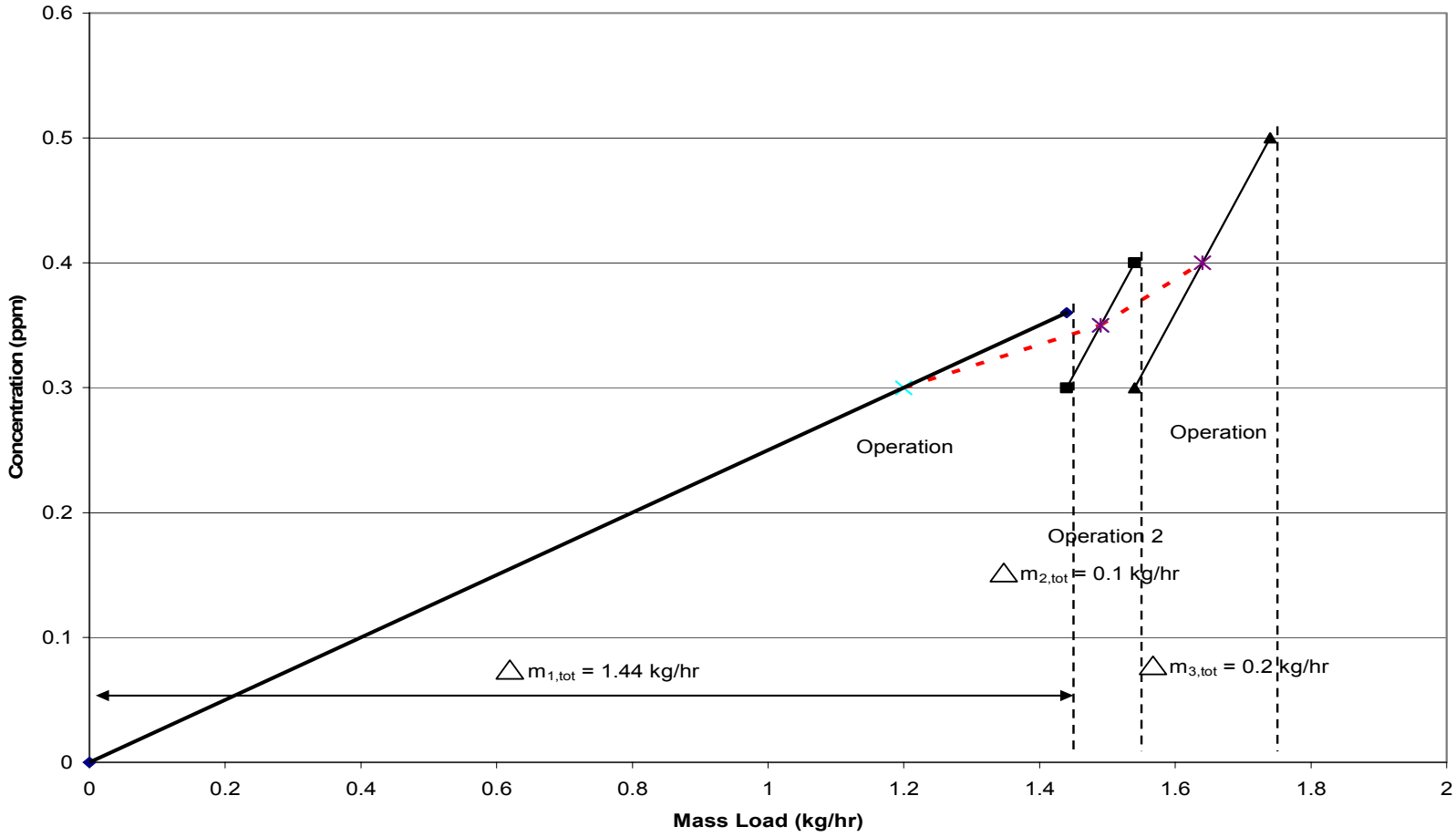

Figure 3.2 : Concentration – composite curve

composite curve shown in Figure 3.3.

Step 3. Plot a water-supply line (solid blue line) that begins at the origin and rotate the line counterclockwise about the origin until it becomes tangent to the composite curve, intersecting at a contaminant concentration of 0.36 ppm. This intersection point is **the freshwater pinch.** In other words, water-using operations do not require freshwater above the freshwater-pinch concentration of 100 ppm. Applying Eq. 3.3 to the water stream between the origin and the pinch gives a minimum freshwater flow rate of 50 te/hr:

$$f_{min}(te/hr) = \frac{\Delta m_{pinch}}{C_{pinch}} \times 1000 = \frac{1.56}{0.36} \times 1000 = 4333.33(te/hr)$$

The minimum freshwater flow rate then corresponds to the inverse of the slope of the tangent water-supply line between the origin and the freshwater pinch. *Water Design* yields the concentration-composite curve and calculates f_{min} and the freshwater-pinch concentration as seen in Figure 3.3. The pinch point not only determines the minimum fresh water requirement suggesting reuse option but it can also be used to identify water-cycle bottlenecks by identifying more concentrated water source than the pinch point and mixing with less concentrated ones can reduce the freshwater consumption further. composite curve shown in Figure 3.3.

Step 3. Plot a water-supply line (solid blue line) that begins at the origin and rotate the line counterclockwise about the origin until it becomes tangent to the composite curve, intersecting at a contaminant concentration of 0.36 ppm. This intersection point is **the freshwater pinch.** In other words, water-using operations do not require freshwater above the freshwater-pinch concentration of 100 ppm. Applying Eq. 3.3 to the water

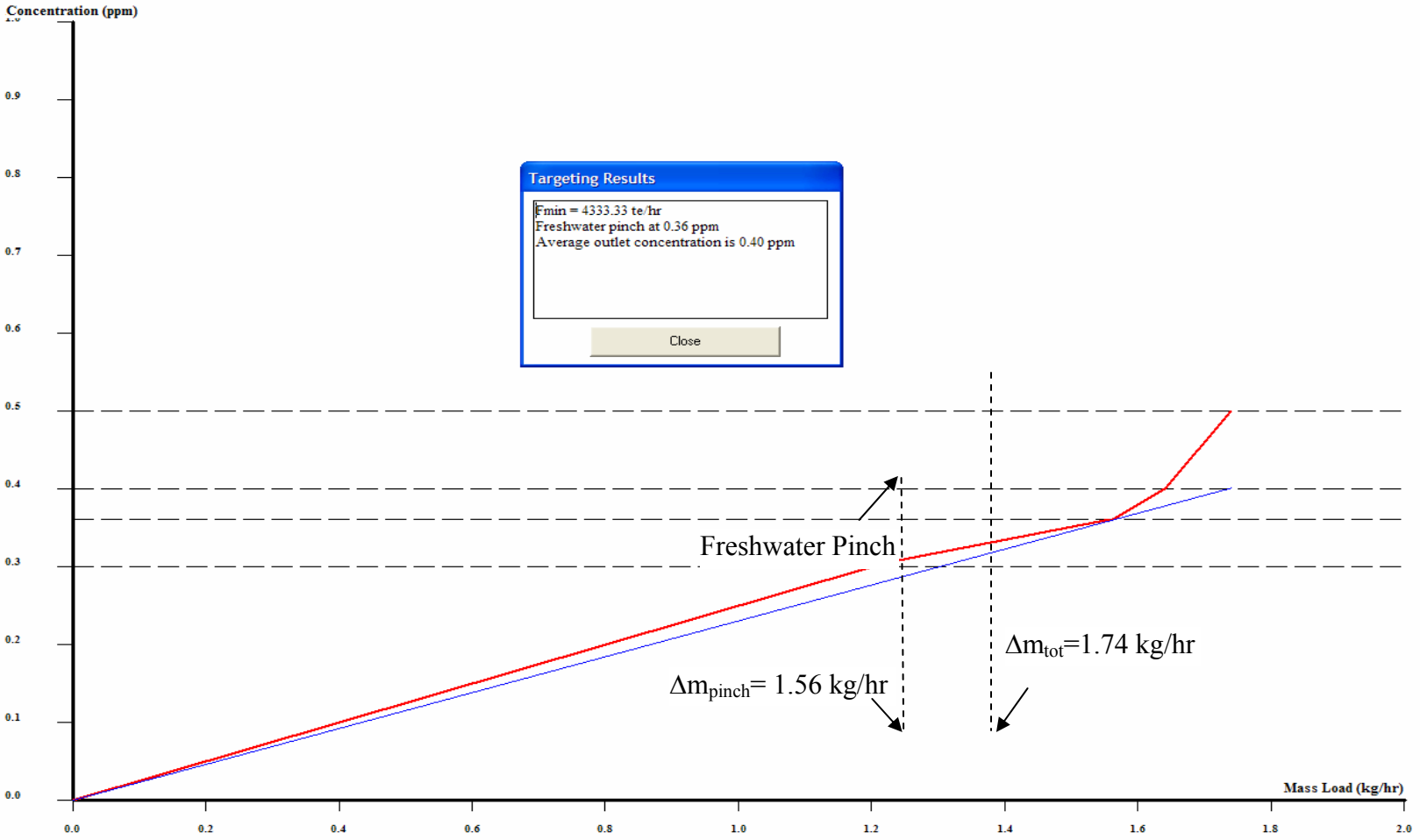

Figure 3.3 : Concentration – composite curve showing pinch point

stream between the origin and the pinch gives a minimum freshwater flow rate of 50 te/hr:

$$f_{min}(te/hr) = \frac{\Delta m_{pinch}}{C_{pinch}} \times 1000 = \frac{1.56}{0.36} \times 1000 = 4333.33(te/hr)$$

The minimum freshwater flow rate then corresponds to the inverse of the slope of the tangent water-supply line between the origin and the freshwater pinch. *Water Design* yields the concentration-composite curve and calculates f_{min} and the freshwater-pinch concentration as seen in Figure 3.3. The pinch point not only determines the minimum fresh water requirement suggesting reuse option but it can also be used to identify water-cycle bottlenecks by identifying more concentrated water source than the pinch point and mixing with less concentrated ones can reduce the freshwater consumption further.

Figure 3.4 indicates the optimum water – usage network for the above example problem. The net fresh water intake is reduced by 1666.67 te/hr (6000-4333.33), which is about 27% reduction.

The pinch analysis will be performed on the Kingston power plant of TVA after the plant is modeled in ChemCAD and the predictive concentration of ammonia, mercury and nitrates in the ash pond are known. Subsequently, water usage and recycle will be suggested based on the pinch analysis. Refer Chapter 8 for details.

3.5 Model Development in ChemCAD

The basis of the model in ChemCAD will be the Kingston power plant, about 60 miles from Knoxville, Tennessee. The model will be further developed into a generic model by including flue gas desulphurization unit. ChemCAD is a process simulator for users

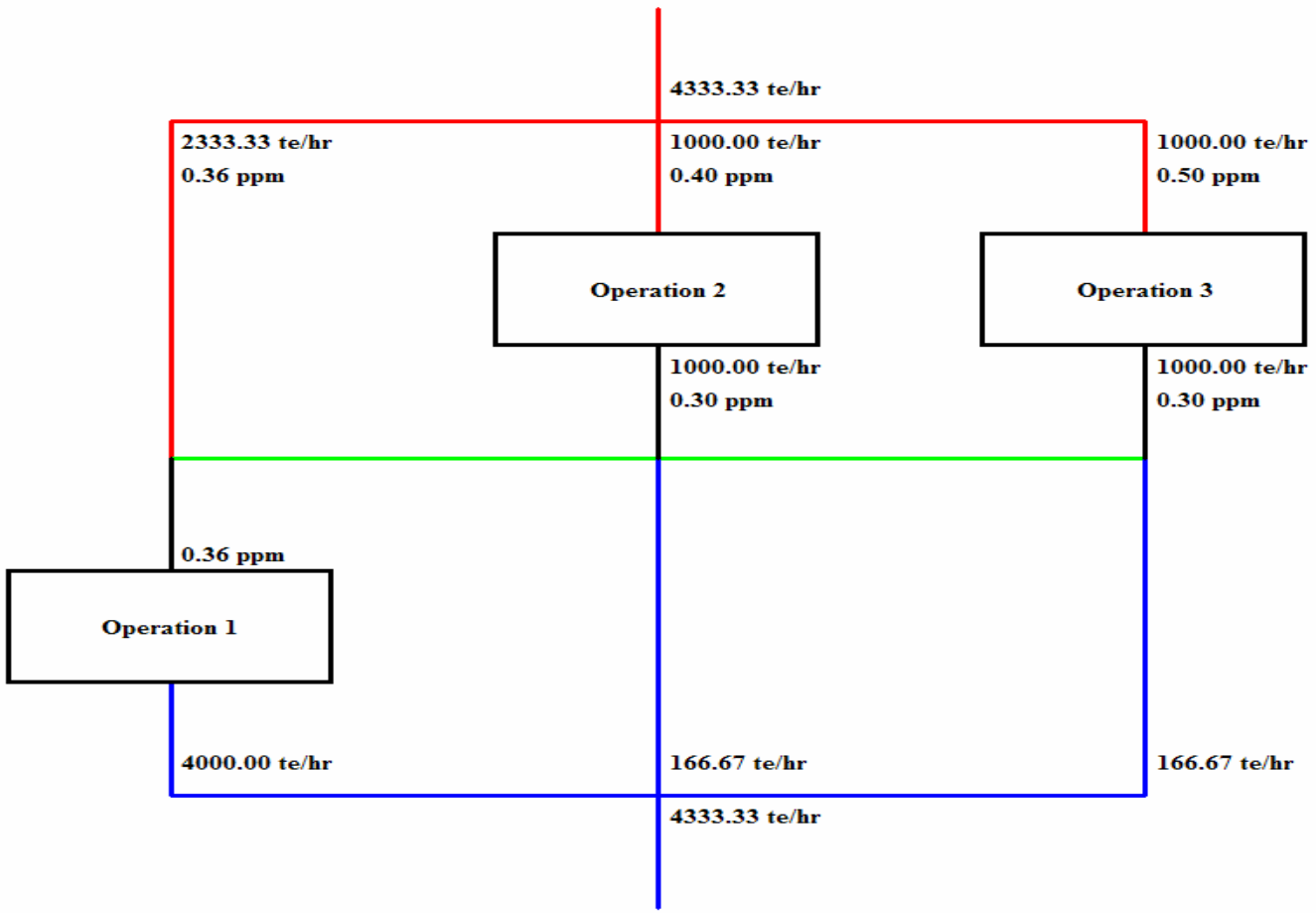

Figure 3.4 : Optimum water-using network

working for a chemical manufacturing company, refinery, engineering firm, pharmaceutical company, etc. It allows the user to simulate the complete chemical plant / refinery, etc by incorporating each equipment of the plant and then joining each of them by lines for fluid flow. Once the inlet flow and equipment is specified in flowsheet and the program ran, the other joining stream and outlet stream is calculated by the program. In general, the best uses of a simulator like ChemCAD are as follows:

(1) Investigating a new process by simulating various alternatives to determine the feasibility of each.

(2) Simulating an existing process to determine optimal conditions, bottlenecks, or sensitivity to process changes. (3) Simulating an existing process to determine control schemes, dynamic behavior, etc.

(4) Day to day engineering work (e.g. bubble/dew points, fluid properties, equipment sizing) Kingston power plant does not have a FGD unit.

The simulation of the power plant is discussed in detail in the following sections and the flowsheet itself is shown in Chapter 7 with results. This model can be applied to any coal power plant having similar unit operations as that in Kingston power plant and a FGD unit. The inlet flow rates, temperature and pressure of the flue gas stream are taken from ALSTOM drawing (87W800-2, 6, and 7) and reproduced in Table 1.1. The sluice water flow rates are taken from "Kingston Steam Plant WasteWater Flow Schematic – NPDES Permit # TN0005452", which is shown in Figure 1.2.

3.5.1 Boiler

The boiler is modeled as an isothermal Gibb's reactor, as the reactions in the boiler are spontaneous reaching equilibrium in no time. The user interface of the boiler is shown as Figure 3.5. The boiler is modeled as an isothermal reactor because the heat generated is readily absorbed by the boiler feed water generating steam in the process. The temperature is set at 1900^0F, which is the average operating temperature of the boilers in Kingston. However, the temperature varies within the boiler from 1700^0F in the convection zone to 2000^0F in the firing zone. The boiler minimizes the total Gibb's free energy and gives the output mass fraction of components accordingly. The heat duty is calculated based on the heat of reactions minus the enthalpy change of all the components from standard state (68^0F, 1 bar) to the boiler temperature. The low tolerance is selected to take care of the ppm level mass changes. The smaller the tolerance, the more accurate the output stream composition would be. However, the program takes more time to converge at a very low tolerance. If any of the components in the inlet stream is considered to be inert or solids, then it would be selected under the inert or solid list.

3.5.2 Economizer and Air Preheater

The economizer and the air preheater are modeled as simple heat exchanger. The economizer is an integral part of the boiler, considerable heat exchange takes place by convection in this zone by superheating steam with the hot flue gas. The flue gas comes out of this zone at 650 – 750^0F. The flue gas from the SCR unit (if SCR is present) enters the air preheater, where it preheats the air feed to the boiler to about 450^0F. The ChemCAD user interface for the economizer and the air preheater is shown as Figure 3.6.

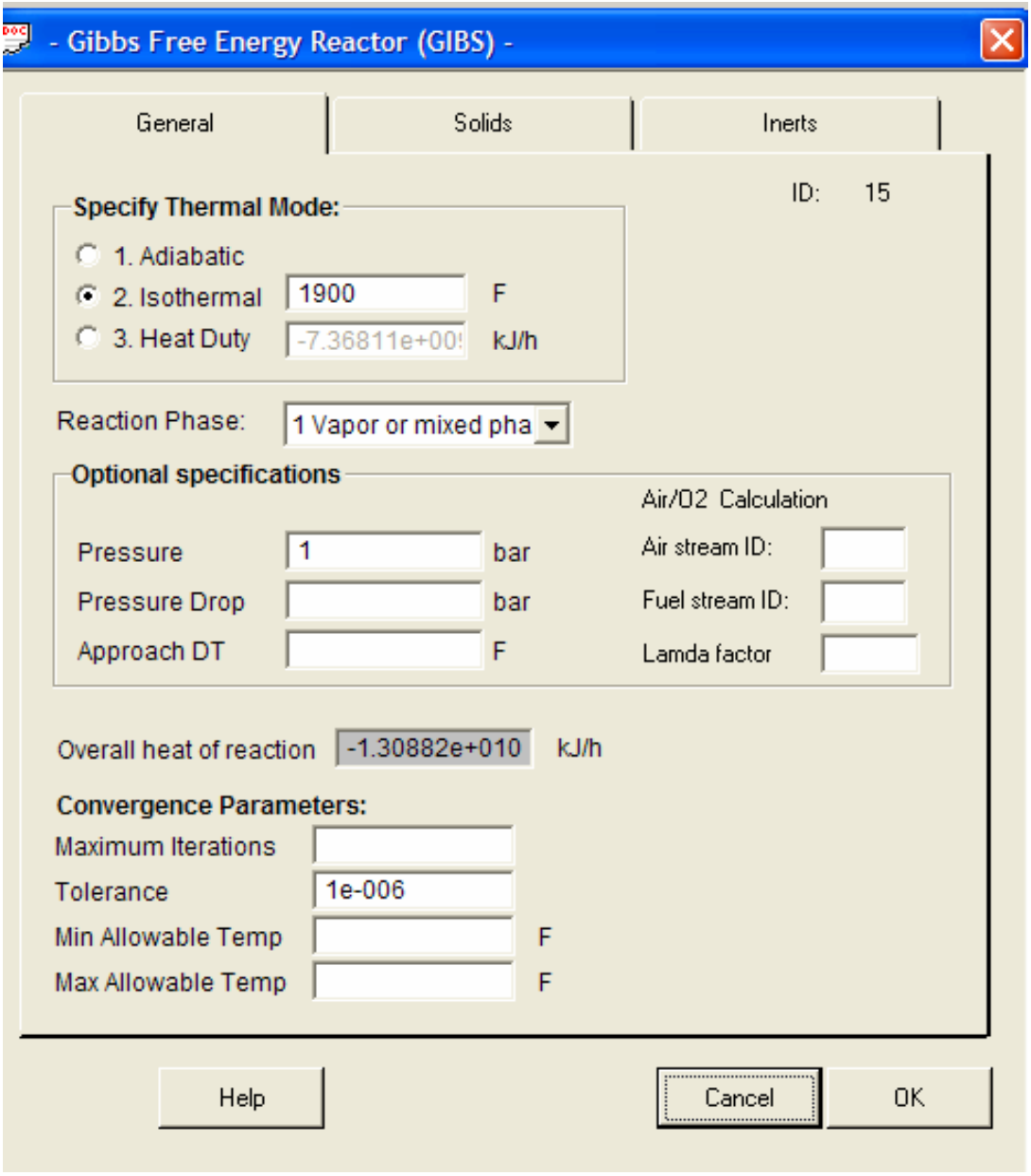

Figure 3.5 : User interface for boiler

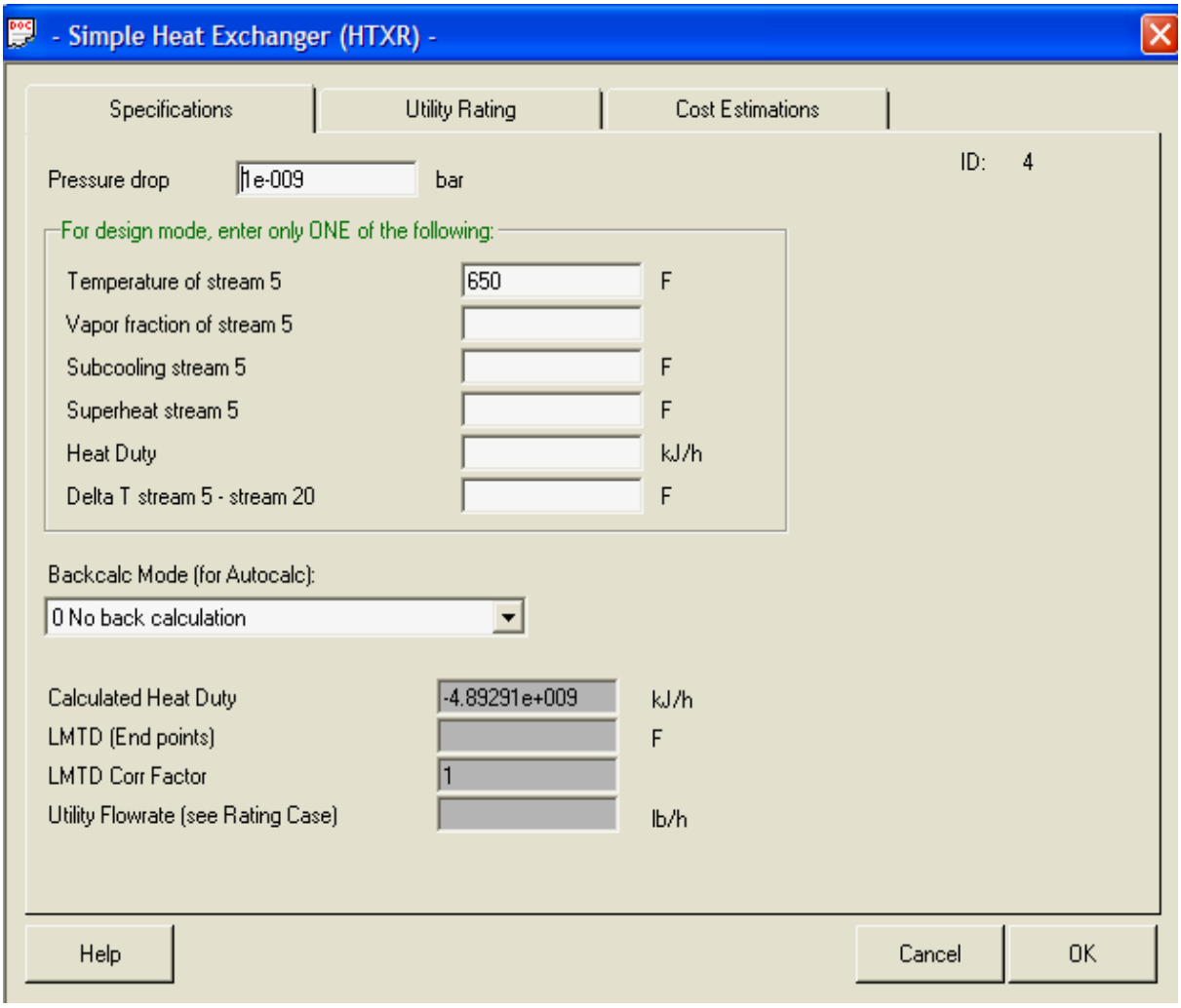

Figure 3.6 : User interface for economizer/air preheater

As shown, only one of the six parameters needs to be entered. The outlet temperature (stream 5) is entered in this case, which is known. The outlet temperature of the economizer is entered as 650^0F (inlet/operating temperature of SCR) and that of the air preheater is entered as 329^0F (operating temperature of electrostatic precipitator).

3.5.3 Selective Catalytic Reduction Unit (SCR) and Flue Gas Desulphurization unit (FGD)

The SCR is meant for NOx reduction as earlier explained. The reactions are occurring spontaneously due to the presence of catalyst. Similarly, the reactions in FGD are also occurring spontaneously. The reactions in the FGD have not been discussed before as FGD unit is not installed in Kingston. The FGD is added into the model to make it a generic model. Chapter 7 shows two models, one of Kingston plant for model validation and the other with FGD, the generic model. Figure 3.7 shows the schematic of a typical FGD unit and figure 3.8 , the generic model with FGD.

The FGD is fed with lime slurry where the SO2 from the flue gas is absorbed in the lime slurry and reacts with dissolved limestone (CaCO3) in the slurry to form calcium sulfite hemihydrate (CaSO3 · ½H2O) according to the following reaction:

$$SO_2 + CaCO_3 + \tfrac{1}{2} H_2O \longrightarrow CaSO_3 \cdot \tfrac{1}{2}H_2O + CO_2$$

Carbon dioxide formed from reaction of limestone with SO_2 is released into the flue gas. Air is bubbled constantly through the slurry to convert $CaSO_3 \cdot \tfrac{1}{2}H_2O$ to gypsum ($CaSO_4 \cdot 2H_2O$) according to the following reaction:

$$CaSO_3 \cdot \tfrac{1}{2}H_2O + \tfrac{1}{2}O_2 + 1.5\ H_2O \longrightarrow CaSO4 \cdot 2H2O$$

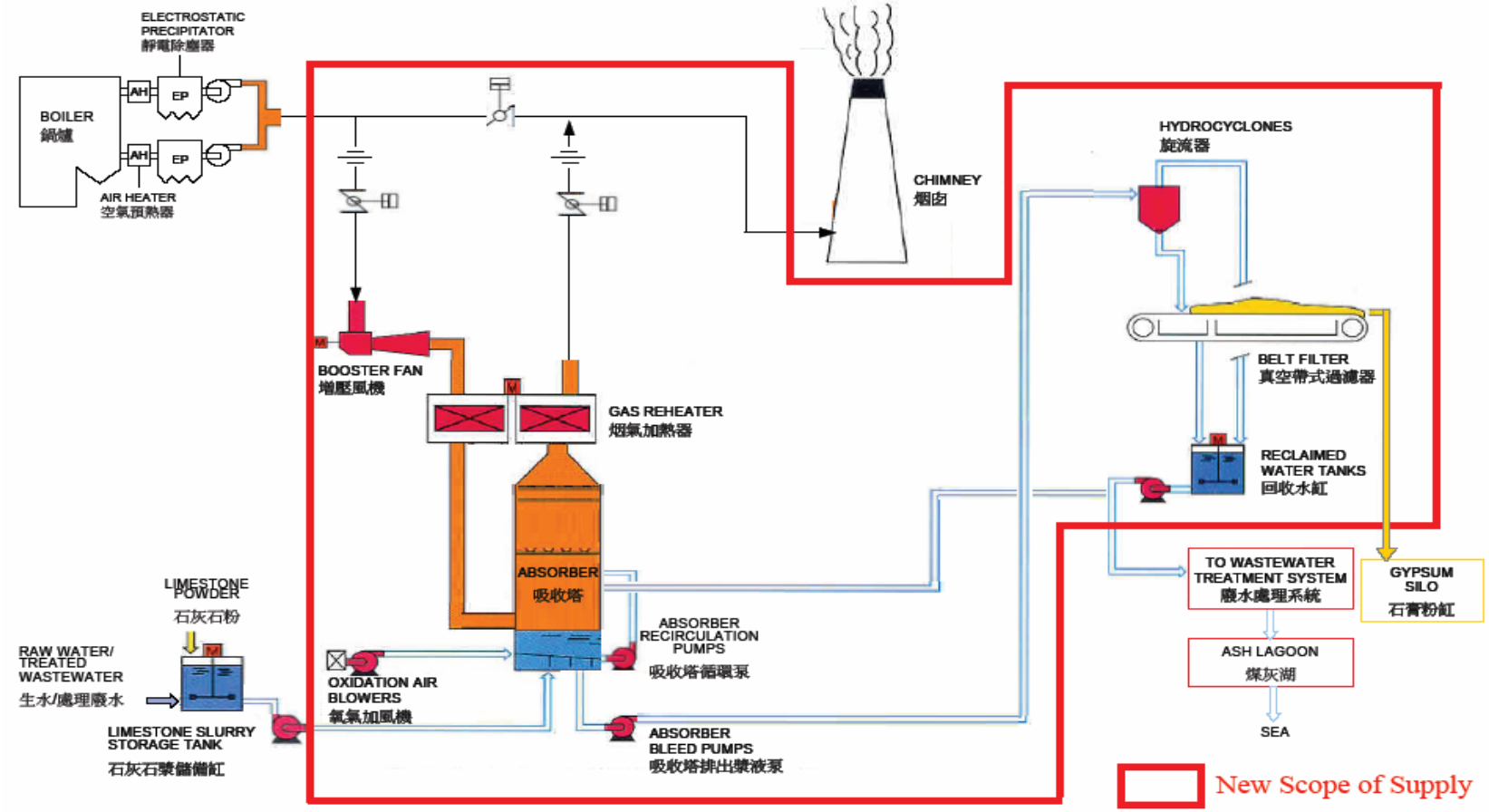

Figure 3.7: Schematic diagram of a typical FGD unit (Source: Hong Kong Electric Company[50])

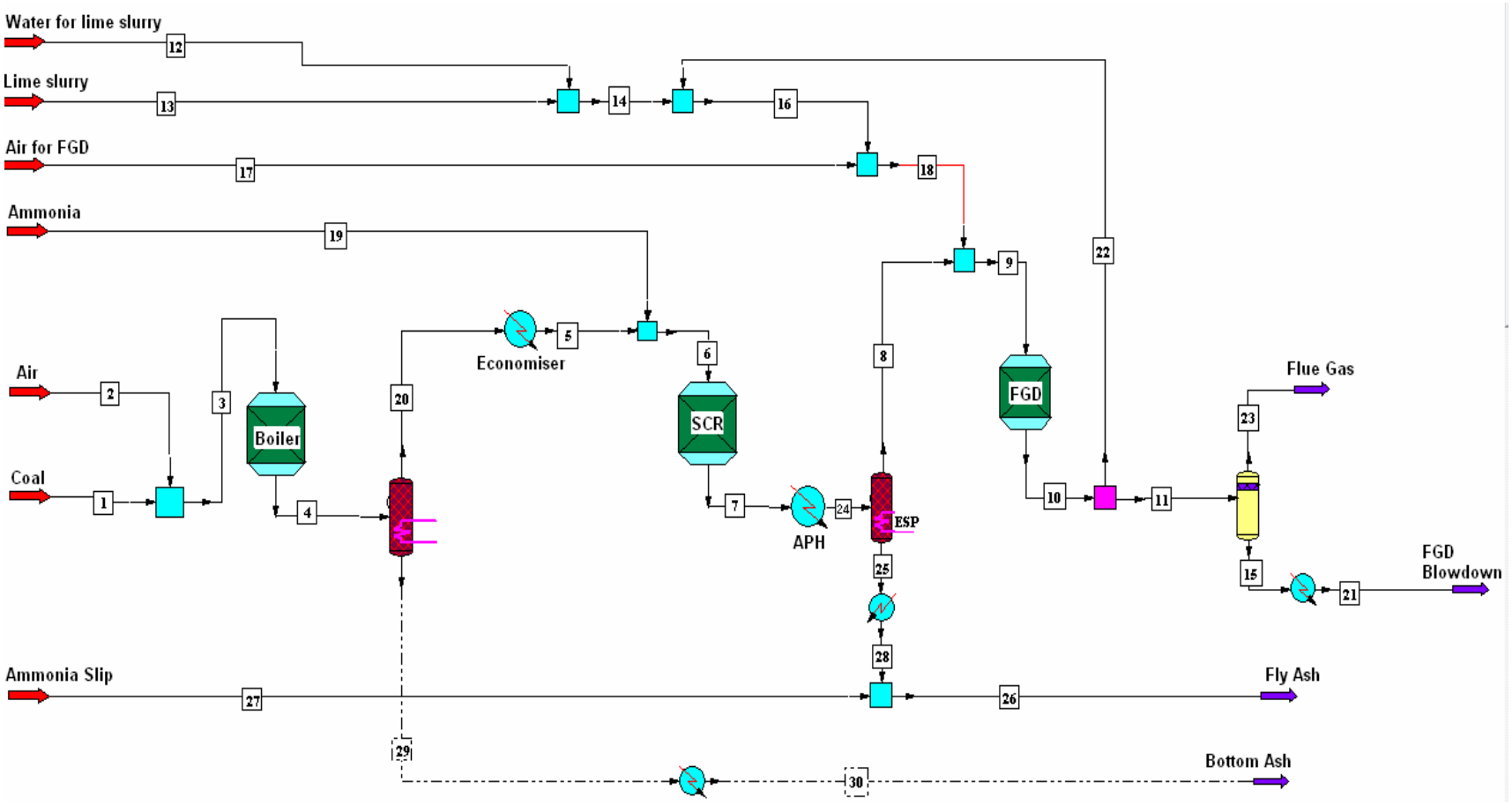

Figure 3.8: The generic model of flue gas side of a power plant with FGD unit

Aeration oxidizes all the calcium sulfite to calcium sulfate, which precipitates as gypsum crystals in the reaction tank.

As the reactions in the SCR and the FGD are spontaneous, both the reactors are modeled as gibb's reactor. The user interface will be same as that of boiler (figure 3.5), except that the SCR and FGD are modeled as adiabatic reactors. In other words, the equilibrium reactants and products consume the heat of reaction in the SCR and FGD unlike the boiler where heat of reaction is used for generating steam. The generic model shows a recycle stream at the FGD outlet, recycling part of the outlet stream to the inlet and the rest flowing as blowdown to the ash pond. This is same as the recycled stream from the reclaimed water tanks in the schematic to the FGD inlet, with the rest flowing into the wastewater treatment systems and ash lagoon.

3.5.4 Electrostatic Precipitator (ESP)

The electrostatic separator is modeled as a component separator. The bottom ash separation in the boiler is also separated in a component separator. The component separator serves as a black-box separator that splits an input stream into two output streams of different compositions and thermal conditions. By specifying split fraction or split flow rate component by component, almost any kind of separation can be performed. Various output temperature specifications are provided for the product streams including bubble point, dew point, subcooled, and superheated conditions. The default for the outlet temperature is the inlet temperature. This module can be used to model an "abstract" separator, such as isolating a pure component from a mixture or separating the solid components from a process stream before a rigorous VLE calculation

is performed. This module is used in our application, as the various components like mercury and its compounds and fly ash/bottom ash separates in different ratio in the ESP and in the boiler. The ratio of separation of bottom ash/ fly ash and mercury is obtained from literature, discussed in chapter2. The electrostatic precipitator module in ChemCAD is not used instead because it separates purely on the basis of particle size distribution and so separating fly ash and mercury in different ratios suggested by literature is not possible. The user interface of the component separator is shown as figure 3.9. The ash separation in the ESP is typically 99% and the mercury and its various compounds are 70% (source: TVA). However, the mercury separation achieved in Kingston based on ash mercury analysis is 0.009% with bottom ash and 0.5% with fly ash.

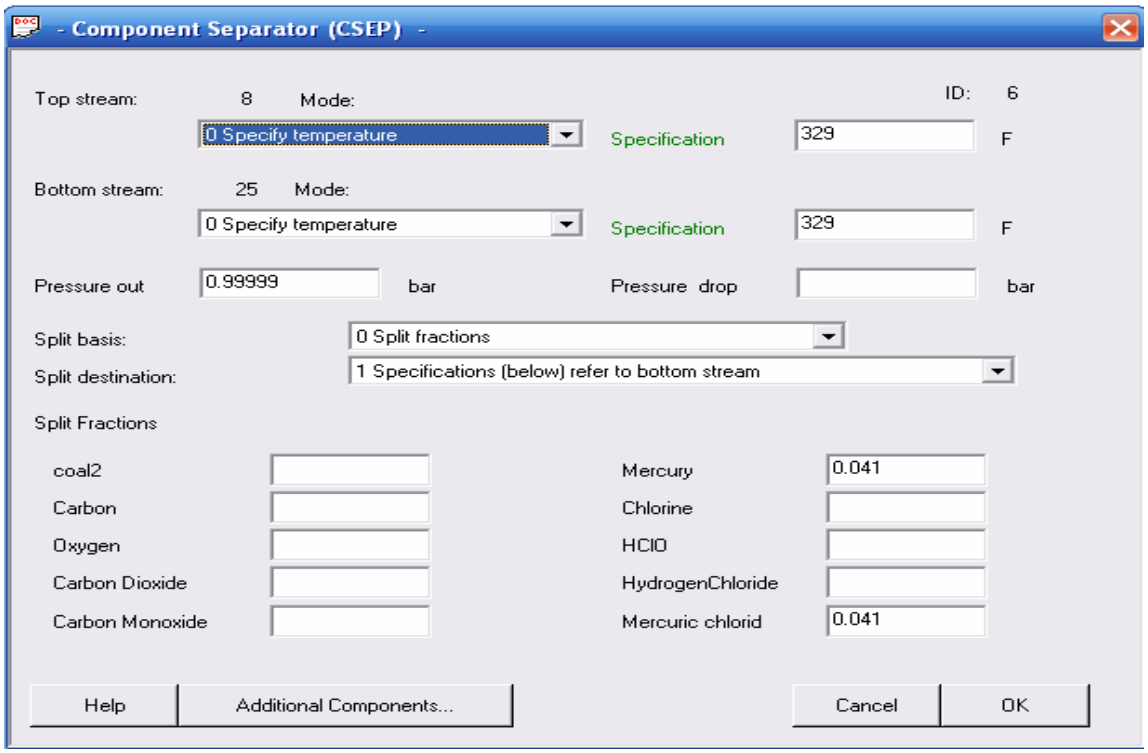

Figure 3.9: User interface of a component separator (ESP)

3.5.5 Ash Pond

The ash pond is modeled as shown in Figure 3.10. The stream 4 fed to the mixer is the combined stream of bottom ash sluice water and fly ash sluice water. In the case of the generic model, the FGD blow down will be introduced at a different point shown in Figure 3.11 to prevent upsetting the pH. The mixer, as the name suggests, is used to mix the various streams. The nitrifier is for the biological oxidation of ammonia / ammonium ion. The mercury comes to the pond adsorbed on the ash surface. The mercury interacts with ammonia and desorbs from the ash surface in the mercury desorber.

The nitrifier, eutrophication and the mercury desorber are modeled as kinetic reactors. The user interface of a general specifications page of a kinetic reactor is shown as Figure 3.12, the kinetic data page (which includes stoichiometric coefficient) as Figure 3.13 and the user rate expressions as Figure 3.14. The kinetic rate expression can be user specified or standard based on activation energy. The user expression in our case both for nitrifier and mercury desorber is experimentally found rate equation discussed in chapter 6 and 7. The user expression for eutrophication is from Chapra[8].

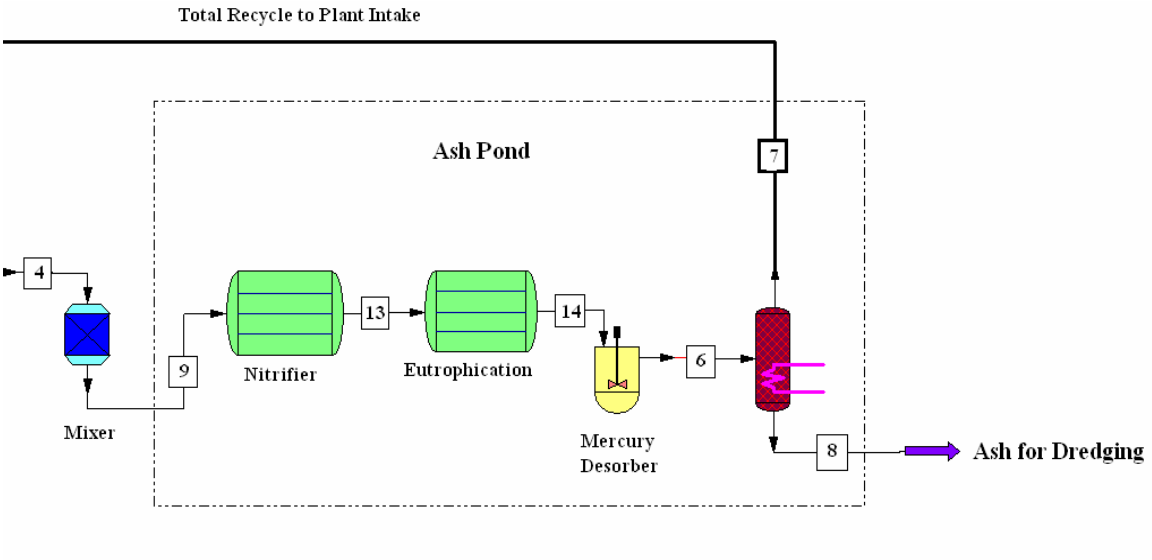

Figure 3.10: Ash pond setup in Kingston plant model

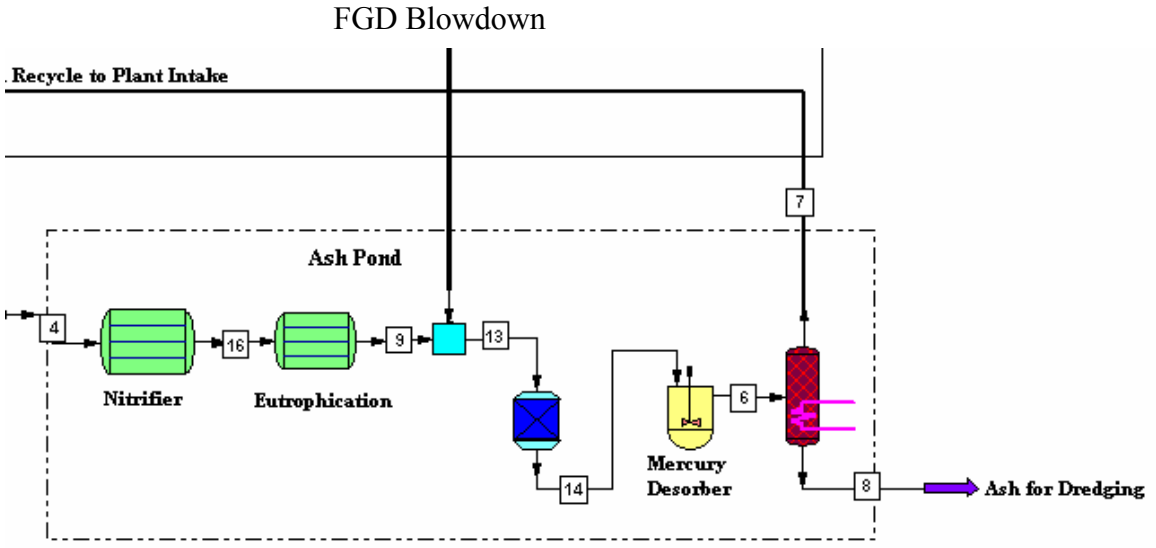

Figure 3.11: Ash pond setup in generic model

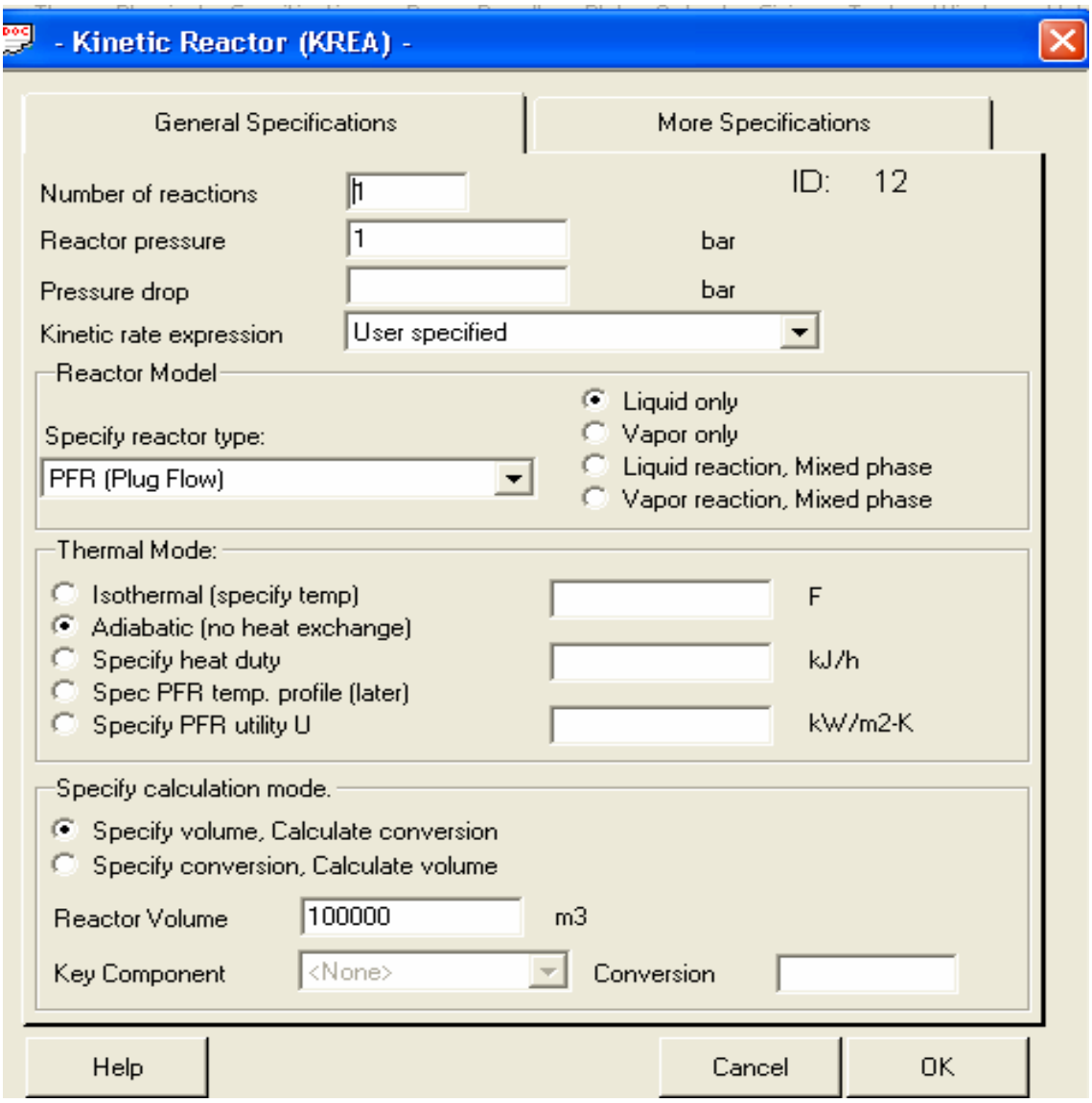

Figure 3.12: User interface of a general specifications page of a Kinetic Reactor

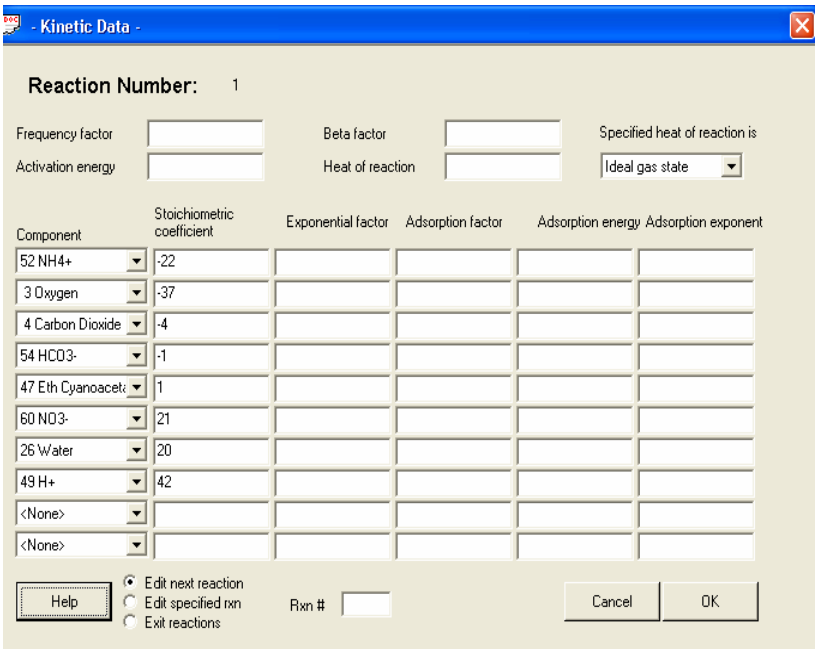

Figure 3.13: User interface of a kinetic data specifications page of a Kinetic Reactor

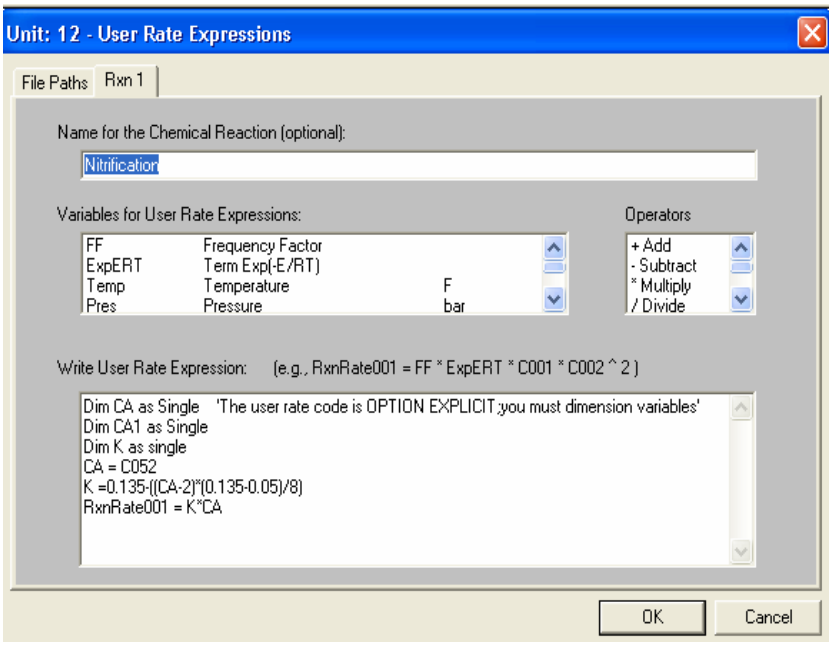

Figure 3.14: User interface of a user rate expressions page of a Kinetic Reactor

CHAPTER 4.0

MATERIALS AND METHODS FOR MODEL DEVELOPMENT

4.1 Overview of Experimental Approach

The generic power plant model developed in ChemCAD is based on TVA plant data on coal composition, coal flow rate, flue gas temperature and pressure at various points, ammonia flow rate in SCR, and amount of ammonia and mercury separation from flue gas. The lime slurry composition and flow rate is from plant of TVA where FGD is present. For detailed process conditions and assumptions in ChemCAD model, refer to chapter 7. The mercury and ammonia / ammonium bisulfate separation from flue gas is also evaluated from the various literature values obtained from literature review. But, in order to model the ash pond, very little or no information is available on the ammonia breakdown in the ash pond. The nitrification in a sewage treatment plant or municipal waste water treatment plant is quite different from an ash pond. A municipal waste water treatment plant typically has a VSS of 5000 ppm or higher and BOD of 15000 ppm or more. The Kingston ash pond has a BOD of 2 ppm and VSS of 4 ppm. Hence, it will not be prudent to consider the Monod kinetic equation with its constants published in Metcalf[36] and Eddy for the nitrification reaction in the ash pond. Also, the fate of the bulk of the mercury and oxides of mercury captured from the flue gas and coming with the ash into the ash pond is not well known. Hence, during the course of this work, it was felt that without experimenting with the ammonia kinetics in the ash pond and mercury desorption from the ash into the aqueous phase, the model development will not be

accurate. This is especially so because nitrification reactions are generally very slow and with the Volatile Suspended Solid (VSS) of 4-5 ppm in the ash pond, the nitrification is expected to be even slower. Also, due to the high adsorbing capacity of the fly ash, majority of the mercury is expected to be adsorbed on the fly ash surface and very little should go into the aqueous phase during the residence time of the fly ash in the ash pond. The following sections describe how the experimental approach is made to describe the nitrification kinetics and mercury adsorption/desorption kinetics in the ash pond in presence of ammonia. These kinetic equations are then incorporated in the computer model to describe the power plant.

4.2 Lab Scale Nitrification Reactor

Before carrying out any experiment to determine the coefficients in Monod kinetic equation (equation 4.1 below), the Volatile Suspended Solid (VSS) of the ash pond water was determined. It was found to be 2.5 mg/l. Although it is very low, still biological breakdown of ammonia was observed during the course of the experiment as shown in chapter 6. The result of the experiments follows in chapter 6.0.

The Monod kinetic equation for nitrification is (source: Metcalf[36]),

$$r_g = \mu_m e^{0.098(T-15)}\left(\frac{DO}{K_{DO}+DO}\right)[1-0.833(7.2-pH)]\frac{XS}{K_s+S} - k_d X \quad \text{..... .....4.1}$$

temperature correction factor	dissolved oxygen factor	pH correction factor	endogenous decay factor

Where,

r_g – specific rate of biomass growth, day^{-1} = $- Yr_{su} - k_dX$ [source: Metcalf [36]] …..4.2

r_{su} – Rate of substrate consumption

Y – 0.28 mg VSS/mg of NH_4^+-N (= 113/396, derived from the nitrification stoichimetric equation shown below)

K_S – half Saturation constant of ammonium ion, mg/l

S – substrate concentration (ammonium conc.), mg/l

X – biomass conc., mg/l

DO – dissolved Oxygen concentration, mg/l

μ_m – maximum sp growth rate of bacteria, day^{-1}

K_{DO} – coefficient of oxygen consumption, mg/l

T – temperature, ^0C

k_d – endogenous decay coefficient, day^{-1}

The nitrification reaction is given by[Cheremisinoff[13]];

$$22\ NH_4^+ + 37O_2 + 4CO_2 + HCO_3^- \longrightarrow C_5H_7NO_2 + 21NO_3^- + 20H_2O + 42H^+$$

In order to determine the rate of ammonium oxidation in the ash pond, the constants which can vary considerably with the environmental condition are half saturation constant (K_s) and maximum specific growth rate of bacteria (μ_m). The other constants of equation 4.1 mentioned above will be considered from Metcalf[36] and Eddy. For determining half Saturation constant (K_s) experimentally, following assumptions are made;

1. The maximum specific growth rate of bacteria, temperature correction, dissolved oxygen, yield coefficient and pH correction factors are assumed to remain

constant during the course of the different experiments listed as Table 4.1. So, they are all put together as one constant k.

2. The biomass concentration change (ΔX) is negligible compared to nitrogen breakdown. So, X will be treated as a constant in the experiments.

3. Empirical formula of Biomass – $C_5H_7NO_2$ (Mol wt. – 113)

So, from equation 4.1 and 4.2 the governing equation for rate of substrate utilization becomes,

$$r_{su} = -k\frac{XS}{K_s + S} \quad \text{.....4.3}$$

The experiments were carried out in 500 ml flasks, as batch reactors. Samples were taken at regular intervals, as mentioned in Table 4.1. As per the batch reactor model,

$$\int_{S_0}^{S} \frac{dS}{r_{su}} = t \quad \text{.....4.4}$$

So from equation 4.2 and 4.3 for a batch reactor model, we get,

$$\int_{S_0}^{S} \frac{dS}{\frac{S}{K_S + S}} = -tkX$$

Where

S_0 = initial concentration of substrate (ammonium)

S = concentration of substrate at time t

Solving the above integral, we get

$$kXt = [(S_0 - S) + K_S(\ln\frac{S_0}{S})] \quad \text{.....4.5}$$

Table 4.1: List of experiments performed for nitrification equation calibration

Serial no. of Sample	Sample Description	Day 0			Day 2						Day 4						Day 10						Day 17						Day 23	Volatile Suspended Solid (VSS) after 17th day
		NO_2^-	NO_3^-	NH_4-N	NO_2^-	NO_3^-	NH_4-N	OD 600	pH	DO	NO_2^-	NO_3^-	NH4-N	OD 600	pH	DO	NO_2-	NO_3-	NH_4-N	OD 600	pH	DO	NO_2-	NO_3-	NH_4-N	OD 600	pH	DO	DO	
1	500 ml of pond water in a 500 ml flask and injected 2 ppm of Ammonium-N	0.023	0.203	0	0.015	0.363	0	0.0047	8.13		0.0253	1.8571	0	0.0025	8.45	-	0.0113	2.2321	0	0.0016	7.68	-	0.08294	2.436	0	0.0015	7.3	6.75	7.66	7.442
2	500 ml of pond water in a 500 ml flask and injected 10 ppm of Ammonium-N	0.023	0.203	10.46	0.415	0.39	8.743207	0.0016	8.05		2.2488	2.1564	7.1614	0.0015	8.85	-	11.246	1.5159	6.079	0.0007	8.14	-	13.2253	0.98	5.042	0.0021	6.73	7.33	6.4	9.76
3	500 ml of pond water in a 500 ml flask and injected 100 ppm of Ammonium-N	0.023	0.203	100.5	1.289	1.683	73.98725	0.0008	7.85		1.3061	3.6701	70.015	0.0037	8.75	-	16.042	0.3711	60.31	0.0016	8.23	-	1.64515	0.126	55.2	0.0029	7.98	7.3	6	8.7
4	500 ml of pond water in a 500 ml flask with no external addition of ammonia	0.023	0.203	0.455	0.113	0.422	0.405368	0.003	8.5		0.159	1.7262	0.3447	0.0008	8.89	-	0.1509	0.3925	0.348	0.003	10.32	-	0.15901	0.14	0.278	-	9.5	6.18	7.5	5.532
5	Autoclaved 500 ml of pond water in a 1000 ml flask and injected 10 ppm of Ammonium-N	0.023	0.203	0	0.023	0.794	0		8.83	7.5	0.0303	0.5139	0	-	8.6	5.8	-	-	0	-	-	-	0.02532	0.61	0	-	-	-	-	0

4.2.1 Experimental setup of Nitrification reaction

The ash pond water for the experiment were taken in 500 ml flask and covered as shown in figure 4.1 with black cloth/paper to prevent algae growth. The mouth of the flask was kept uncovered to simulate the ash pond condition. Algae growth is not desirable in these experiments because ammonia can react to form algae. Thus it will be difficult to predict the amount of ammonia lost in nitrification reaction. Five cases of the ash pond water with different ammonium concentration were experimented with to get the half saturation constant, K_S. The five cases are as follows and set up as shown in figure 4.2;

- 500 ml of ash pond water taken in a 500 ml flask and inject 2 ppm NH_4OH
- 500 ml of ash pond water taken in a 500 ml flask and inject 10 ppm NH_4OH
- 500 ml of ash pond water taken in a 500 ml flask and inject 100 ppm NH_4OH
- 500 ml of ash pond water taken in a 500 ml flask and inject no NH_4OH – ash pond water contains 0.45 ppm of NH_4^+-N. The idea in this case is to study the kinetics with the intrinsic ammonia present in the water.
- 500 ml of ash pond water taken in a 1000 ml flask and inject 10 ppm NH_4OH and autoclaved

The above flasks mentioned in the above five cases were kept as shown in figure 4.2 for 17 days. Each flask had a magnetic rod to enable it to stir it continuously at a low speed to simulate the condition of the ash pond. Samples were collected at regular intervals of 0 (initial sample), 7, 14 and 17 days as shown in Table 4.1 for each of the 5 different cases. Each sample was measured for ammonium-N, nitrate-N and nitrite-N to analyze the

Figure 4.1: Nitrification experimental set up covered with black cloth

Figure 4.2: Nitrification experimental set up; 5 flasks for 5 cases

ongoing nitrification. The samples were also measured for dissolved oxygen (DO) at random to ensure oxygen supply for nitrification. The samples were also checked for biomass growth in OD600 and pH monitored at regular intervals shown in Table 4.1.

The ammonium concentration at time t will be used as S in equation 4.5. The various constants in the equation such as μ_m, K_{DO} were assumed from the values given in literature (source: Metcalf[36]) and combined in the constant k of equation 4.5. The dissolved oxygen concentration (DO) and the pH in equation 4.1 were measured at various intervals, and the average of these values is considered and integrated in the constant k in equation 4.5.

4.3 Lab scale Mercury Adsorption

The elemental mercury and oxides of mercury is adsorbed on the ash surface and comes to the ash pond via the ESP and/or the FGD. The exact composition of mercury in ash is not known. Hence, the kinetic studies are done on total mercury (elemental and oxidized) adsorbed and desorbed from the ash surface. The mercury content in the ash collected from Kingston was 31.5 ng/g. This amount is too low to perform any meaningful kinetic study on mercury desorption from the ash without first adding mercury externally, thereby increasing the mercury in ash and then performing the desorption experiment. The ultimate goal is to find out the desorption coefficient from the ash and fit into the overall model in ChemCAD.

As suggested by Turner[53] et al and is shown in chapter 6, mercury and its oxides have very high Partition or distribution coefficient between ash phase and water phase. According to the initial calculation done in this work for distribution coefficient (K_D), it

is found to be about 8500 mL/g. This suggests that mercury has a tendency to adsorb on the ash.

4.3.1 Experimental Procedure

A lab scale experiment was designed to study the rate of mercury adsorption on the ash. A batch experiment was set up for the purpose. 1 liter of ash pond water was taken in a 1-liter bottle and 9 gramme of ash was added to it. Then 0.25 µg of mercury was added externally into the solution to make the concentration of mercury as 0.25 ppb. The mercury adsorbed on ash with 0.25 ppb mercury in water will give mercury content in ash close to what we might expect from a typical coal plant burning Powder River Basin (PRB) coal. The bottle was then placed on a magnetic stirrer with a stirring rod moving at a slow speed to simulate the ash pond. Unlike the case of the nitrification experiments, the mercury adsorption experiments were carried out in a closed bottle to minimize mercury vapor escape into the atmosphere. Like the nitrification experiments, the bottle was covered with a black cloth during the course of the experiment to prevent any mercury reaction in the presence of light. Liquid samples were collected at intervals shown in table 4.2 using a syringe and a non-sterile 25 mm Millex syringe filter unit. The filter unit was used to collect samples, so that no suspended ash particles are present in the sample. The whole purpose of this experiment was to determine at what rate mercury adsorbs on the ash surface, by determining the mercury in the aqueous phase at different time t. The mercury concentration keeps on falling from 0.25 ppb till it reaches equilibrium with the concentration in the ash. The difference between the mercury concentration in water at any given time t and the initial concentration indicates the

Table 4.2 Sampling interval of ash water during mercury adsorption experiment

Sample #	Time, hrs
1	3
2	7
3	11
4	27
5	31
6	51
7	78
8	83
9	99
10	103

amount of mercury gone into the ash. Refer to chapter 6, for results. Once the mercury concentration in the water is steady and assumed to be in equilibrium with the ash, the water and the ash suspension is centrifuged to separate the ash and the water. The ash is then taken into a separate 1 liter bottle and dechlorinated tap water is added into the bottle to initiate the desorption experiment.

A second experiment was also performed by adding 10 µg into the ash pond water and making the concentration 10 ppb. The set up and the mode of sample collection were same as above. The results obtained from these experiments are discussed in chapter 6.

4.4 Lab scale Mercury Desorption

The design of the mercury desorption experiment was designed keeping in mind the actual ash pond condition, as depicted in figure 4.3. The experiment was performed as a batch process with 1 liter dechlorinated tap water which has a mercury content of 1.2 ng/l[48]. The water is dechlorinated by keeping it in the bottle overnight, keeping the mouth of the bottle open. It is necessary to dechlorinate because presence of chlorine can hasten the desorption process. The process water used for sluicing is assumed to have the same mercury and chlorine content as the tap water. Water samples were then collected at regular intervals, as in table 4.2. The equation for desorption is arrived as follows (read this in conjunction with figure 4.3);

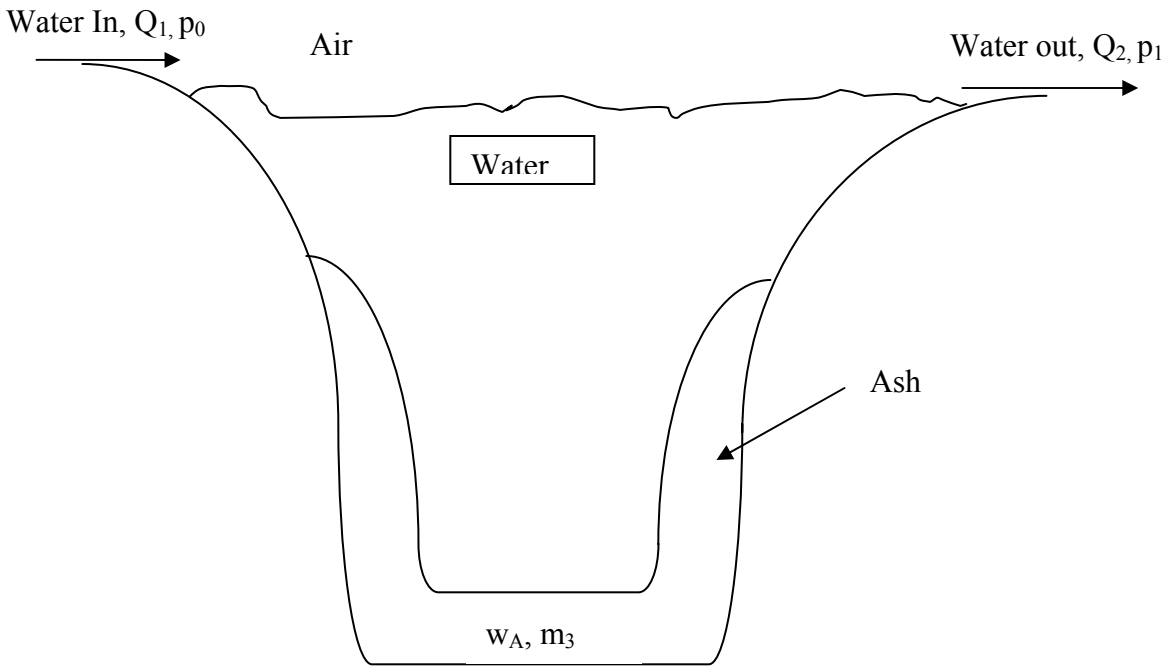

Figure 4.3: Graphical Representation of the ash pond simulated for mercury desorption experiment

4.4.1 Materials and Methods for Desorption of Mercury from ash particles

The residence time of the water in the ash pond is approximately 91 hours (3.8 days). Also, the solid ash is dredged from the ash pond once in 3-4 days (as confirmed by the shift engineer of Kingston plant). So, during these 3.8 days the water and the ash will behave as if in a batch process. So, compare the experiments with the actual ash pond conditions, the sluice water feed to the ash pond can be equated to the condition at time t = 0 and the near water exit condition may be compared with the last time scale in the experiment t = 70 hours. In this manner the experimental setup simulates the ash pond condition in the laboratory and can obtain mercury adsorption / desorption kinetics. The only parameter which appears to be different in batch vs continuous analysis is ρ_{A22} in equation 5.2.71 of Thibodeaux. The ρ_{A22} is neglected in subsequent derivation of equation 5.2-74. This is a valid assumption in our model also for simplification.

A mass balance of Hg^{2+}, yields the following (equation 5.2-74 in Engineering Chemodynamics by Louis J. Thibodeaux [52]),

$$t = \frac{m_3 * K_D}{{}^3K_{A2} * A} ln \frac{w_A^0}{w_A} \quad \text{..... 4.6}$$

Where,

m_3 = total mass of ash, kg (a constant neglecting mass loss due to mercury desorption)

w_A = mass fraction of mercury in ash at time t

w_A^0 = mass fraction of mercury at time, t=0

${}^3K_{A2}$ = overall liquid-phase mass transfer coefficient across a ash-water interface, kg/hr

K_D = Partition or distribution coefficient for mercuric chloride between ash phase and water phase

A = sorption area of fly ash

Cold-Vapor Technique as described in chapter 5 analyzed the water samples for mercury. The result of the analysis will give the mg/l of mercury that escaped into the aqueous phase from ash. That when subtracted from w_A^0, will give w_A at time t. This w_A when plugged into equation 4.6 for known values of K_D, A, m_3 and w_A^0 will give $^3K_{A2}$ (overall liquid-phase mass transfer coefficient across a ash-water interface, kg/hr). The mass of mercury volatilized can be ignored, as the material balance shown in chapter 6 shows that the mercury lost to the environment is negligible. For a continuous process, K_D, the partition coefficient, A, the desorption area of ash, m_3, total mass of ash, and w_A^0 can be treated as constant at all time t. This is because the amount of ash and water was selected in such a way that the amount of ash in water in a continuous flowing ash pond will be same as those in the experiment. This makes equation 4.6 for mercury desorption as a first order reaction equation, which is further discussed in chapter 6.

4.5 Mercury- Ammonia Interaction

To study the effect of ammonia on the mercury desorption, adsorption experiment followed by desorption experiment were set up similar to the adsorption and desorption experiments explained in sections 4.3 and 4.4. The only difference is that autoclaved deionized water was used for both adsorption and desorption experiments to offset the effect of any other substance in the water on mercury desorption. To prevent biological

degradation of ammonia, the water was autoclaved. The adsorption was started with three 1-L water filled flasks injected with 0.25 ppb mercury, three 1-L water filled flasks with 0.5 ppb mercury and three with 1 ppb mercury. All the flasks were sit on magnetic stirrer for 3 days to allow mercury to adsorb on the ash surface. After 3 days, all the water was centrifuged out of all the nine flasks mentioned above. Ammonium in the form of ammonium sulfate was added after the completion of adsorption experiments. Ammonium sulfate in the required proportion mentioned in Table 4.3 was added to each flask on the centrifuged ash. 1-L autoclaved water was then added to each flask. Table 4.3 depicts a full factorial design of ammonia – mercury interaction study.

The concentration of mercury indicated in Table 4.3 as 0.25 ppb, 0.5 ppb and 1 ppb is the concentrations of mercury in water at the start of adsorption and not the concentration of water during desorption. During the adsorption, certain amount of mercury is adsorbed during the various cases of 0.25, 0.5 and 1 ppb solution, which is centrifuged and desorption started. The 0.25, 0.5 and 1 ppb is only indicative of these cases in which adsorption started with 0.25, 0.5 and 1 ppb mercury solution respectively. Mercury and ammonia samples at intervals mentioned in Table 4.3 were collected. Mercury samples were collected to ascertain desorption rate and ammonia samples to ascertain that there is no loss by reaction or volatilization, etc. Mercury samples were analysed by cold vapor atomic absorption spectrometry and ammonia analysed by M/s Galbraith laboratories. The pH was measured for all the samples at the end of the desorption run.

Table 4.3 Full Factorial design of mercury-ammonia interaction experiment

Time, hrs	2ppm Ammonium-N			5 ppm Ammonium-N			14 ppm Ammonium-N		
	0.25 ppb Hg	0.5 ppb Hg	1 ppb Hg	0.25 ppb Hg	0.5 ppb Hg	1ppb Hg	0.25 ppb Hg	0.5 ppb Hg	1ppb Hg
0	X	X	X	X	X	X	X	X	X
5	X	X	X	X	X	X	X	X	X
20	XX	XX	XX	XX	XX	XX	XX(1)	XX(2)	XX(3)
43	X	X	X	X	X	X	X	X	X
70	XXX(4)	XXX(5)	XXX(6)	XXX(7)	XXX(8)	XXX(9)	XXX(10)	XXX(11)	XXX(12)

X- only mercury analysed (mercury analysis result in Table 6.11)

XX- mercury and ammonia analysed

XXX- mercury, ammonia and pH analysed, numbers inside parenthesis are the sample ID used by M/s Galbraith for ammonia analysis (ammonia results in Appendix-2)

CHAPTER 5.0

DETECTION SYSTEM DESIGN AND EVALUATION

5.1 Nitrification experiment

The nitrification in the ash pond was modeled as a Monod kinetic equation, as discussed in chapter 4. In order to calibrate the Monod kinetic equation (equation 4.5), samples were collected at regular interval (table 4.1) to measure ammonia, nitrite and nitrate. The dissolved oxygen (DO), pH and biomass growth by OD 600 were measured intermittently. The Mixed liquor volatile suspended solids (MLVSS) was measured at the beginning and then at the end of the experiment to indicate the biomass growth. The analytical instruments used for the above measurements are described below.

5.1.1 Suspended solids

Mixed liquor volatile suspended solids (MLVSS) were analyzed with method 2540 E: Fixed and Volatile Solids Ignited at 550°C (APHA, 1998). A known volume of water sample (V) was dispensed onto a pre-ignited 47 mm, 1.5 micron glass fiber filter (typically Proweigh®; Environmental Express; Mt. Pleasant, SC) in a vacuum flask assembly. After drying for at least one hour at 103°C, the weight of the filter with dried solids was measured and expressed as W_1. The filter was then placed in a 550°C muffle furnace for at least 15 minutes and then the weight measured. The MLVSS concentration was calculated using the following equation:

mg volatile suspended solids/L = $\frac{W_1 - W_2}{V}$

where,

V = volume of sample (L)

W_1 = weight of filter with dried solids (mg)

W_2 = weight of filter with ash (mg)

5.1.2 Ammonia measurement

The ammonia in the collected samples were measured by Standard Method 4500 D. Ammonia-Selective Electrode Method (APHA, 1998) was used to determine ammonia concentrations in 50 ml samples. An Orion 250A analyzer equipped with a model 95-12 probe (Orion Research, Boston, MA) was utilized in this procedure. The analyzer was first calibrated with standard solutions of 0.1 ppm, 1 ppm, 10 ppm and 100 ppm. The milivolt (mV) reading given by the analyzer was plotted against $\log_{10}C$ (ammonia concentration in standard solution). The trendline equation from the plot will then be used to evaluate any unknown concentration, once the millivolt (mV) is known.

5.1.3 Nitrate/Nitrite measurement

For nitrate/nitrite measurement samples were filtered (typically Millipore 25 mm or 13 mm 0.45 μm) and stored at 4°C until analysis. Analysis was by using standard method 4110 B: Ion Chromatography with Chemical Suppression of Eluent Conductivity (APHA, 1998). A DX-500 Ion Chromatograph (Dionex Corporation, Sunnyvale, CA) equipped with an Ionpac® AS9-HC 4 mm guard (P/N 51786) and anion exchange (P/N51891) column was used for the analysis. The IC was run in auto-suppression

recycle mode with an anion self regenerating suppressor-ultra (ASRS-Ultra, P/N 53946) using 9 mM Na2CO3 eluent at 1 mL/min. An AS-40 auto sampler performed injections through a 25µL sample loop. The analyzer was first fed with calibration samples and then with working samples. The IC then furnished the nitrate / nitrite concentration of the samples once the injection is over.

5.2 Mercury Analysis

The mercury analysis in water samples was done using Leeman PS200 mercury analyzer. Refer figure 5.1 for an overview of the Leeman analyzer system. It is based on EPA Method 1631. Aqueous samples are digested overnight (or longer) at room temperature in acidic bromine monochloride (BrCl) solution. The purpose of preserving with bromine monochloride is to oxidize all mercury and keep it dissolved in water and thereby prevent its loss by volatilization or any other means. Before analyzing, these samples are treated with hydroxylamine hydrochloride to remove the BrCl. The analyzer mixes the sample with a solution of 1 g/L stannous chloride in 0.1N hydrochloric acid, and then sparges the solution with nitrogen. Stannous chloride serves to reduce all the oxidized mercury and present it in the elemental form to the analyzer. The nitrogen/mercury stream then passes through a tube containing anhydrous perchlorate which absorbs any moisture present in the gas. The dry vapor then enters one path of a double path optical cell, which is optimized for fast response time (small diameter) and sensitivity (long length). A mercury source, powered by a constant power supply, delivers a stable source of emission at 254 nm[32]. Absorbance by the mercury cold vapor is measured using a solid state detector with a wide dynamic range. The resulting signal

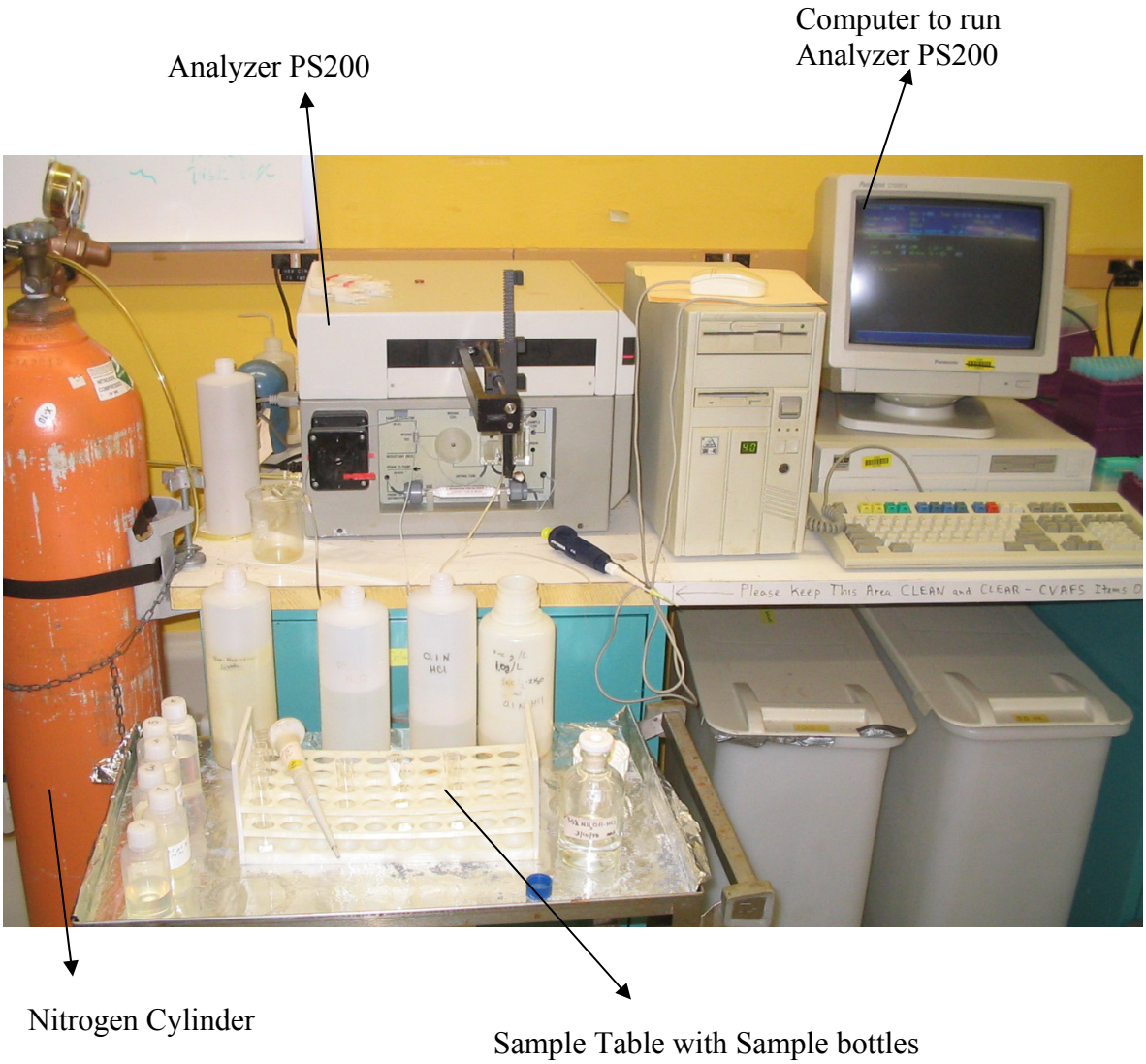

Figure 5.1 Mercury Analyzer PS200 and associated accessories

is referenced to the simultaneous absorbance of the pure carrier gas flowing through the second optical path under identical conditions. The PS200 analyzer is governed by a PS200 software which basically runs the analyzer through the various steps of the analysis.

CHAPTER 6.0

RESULTS AND CONCLUSIONS

6.1 Results from Nitrification experiment

The phenomenon of nitrification in ash pond and biological removal of ammonia from an ash pond is a relatively new concept and gained importance due to the introduction of SCR units in a fossil fuel based power plant. In order to model the nitrification process in the ash pond, laboratory scale experiments were performed as described in chapter 4 and the various parameters were measured by equipments and instruments described in chapter 5. The result of these experiments is discussed in this chapter. The conclusions drawn from these experiments will be used in the ChemCAD model for the rate of ammonia oxidation by nitrification, which is presented in chapter 7. Table 6.1 presents the analysis result of the experiment with ammonia in ash pond water. The fact that biological process of nitrification is the only process involved in the ammonia removal/oxidation in the ash pond water is sought to be proved. In order to prove this, 500 mL of ash pond water with 10.28 ppm was "autoclaved" to kill any microorganisms present in the water and then kept for 17 days on a magnetic stirrer. Table 6.2 shows the sample analysis result. Table 6.2 and figure 6.1 proves conclusively that ammonia oxidizers are solely responsible for ammonia breakdown in the present condition. The ammonia concentration before autoclave was 10.28 ppm and it is 4.35 ppm after autoclaving the sample by the standard autoclave procedure at 121^0C. The difference is due to ammonia loss due to volatilization at that temperature.

Table 6.1: Analysis results of experiments performed with ammonia in ash pond water

500 ml of pond water in a 500 ml flask and injected 2 ppm of Ammonium-N															
T, ^{0}C	DO	K_{DO}	pH	μ_m	k	X	Y	Time,d	S_0	S	kXt	kXt+S	S_0 - S	ln (S_0/S)	K_s
20	7.2	1.3	7.89	0.3	2.33	4.97	0.28	0	2.282	2.282	0	2.2815	0	0	81.021
								2	2.282	1.9772	23.1938	25.17	0.3043	0.1432	
								4	2.282	1.855	46.3876	48.243	0.4265	0.207	
								10	2.282	0.59623	81.178	81.77	1.6853	1.342	
								17	2.282	0.244	197.1473	197.39	2.0371	2.2337	

Table 6.1: Continued

500 ml of pond water in a 500 ml flask and injected 10 ppm of Ammonium-N															
T, ^{0}C	DO	K_{DO}	pH	μ_m	k	X	Y	Time,d	S_0	S	kXt	kXt+S	S_0 - S	ln (S_0/S)	K_s
20	6.8667	1.3	7.94	0.1	0.79	6.13	0.28	0	10.4554	10.455	0	10.45	0	0	87.805
								2	10.4554	8.7432	9.73	18.47	1.7122	0.1788	
								4	10.4554	7.1614	19.45	26.616	3.294	0.3784	
								10	10.4554	6.0789	48.636	54.715	4.3765	0.5423	
								17	10.4554	5.0424	82.68	87.723	5.413	0.7292	

Table 6.1: Continued

500 ml of pond water in a 500 ml flask and injected 100 ppm of Ammonium-N															
T, ^{0}C	DO	K_{DO}	pH	μ_m	k	X	Y	Time, d	S_0	S	kXt	kXt+S	S_0 - S	ln (S_0/S)	K_s
20	6.65	1.3	8.20	0.16	1.432	5.6	0.28	0	100.4554	100.46	0	100.45	0	0	85.852
								2	100.4554	73.987	16.036	90.023	26.468	0.3058	
								4	100.4554	70.015	32.072	102.086	30.441	0.361	
								10	100.4554	60.313	80.18	140.493	40.142	0.5102	
								17	100.4554	55.2	136.3	191.505	45.255	0.5988	

Table 6.1: Continued

500 ml of pond water in a 500 ml flask with no external addition of ammonia															
T, ^{0}C	DO	K_{DO}	pH	μ_m	k	X	Y	Time,d	S_0	S	kXt	kXt+S	S_0 - S	ln (S_0/S)	K_s
20	6.84	1.3	9.30	0.05	0.68	4.02	0.28	0	0.4554	0.4554	0	0.45	0	0	82.76
								2	0.4554	0.4054	5.456	5.86	0.05	0.1164	
								4	0.4554	0.3447	10.91	11.257	0.1107	0.2785	
								10	0.4554	0.3479	27.28	27.63	0.1075	0.2693	
								17	0.4554	0.2776	46.38	46.655	0.1778	0.4951	

Table 6.2: Analysis result of "Autoclaved" ash pond water

500 ml of "Autoclaved"pond water in a 500 ml flask and injected 10 ppm of ammonia-N						
T, ^{0}C	DO	pH	X	Time, days	S_0	S
20	6.05	6.8	0	0	4.346865	4.3469
				2	4.346865	3.8478
				4	4.346865	3.8478
				7	4.346865	3.6951
				17	4.346865	3.6

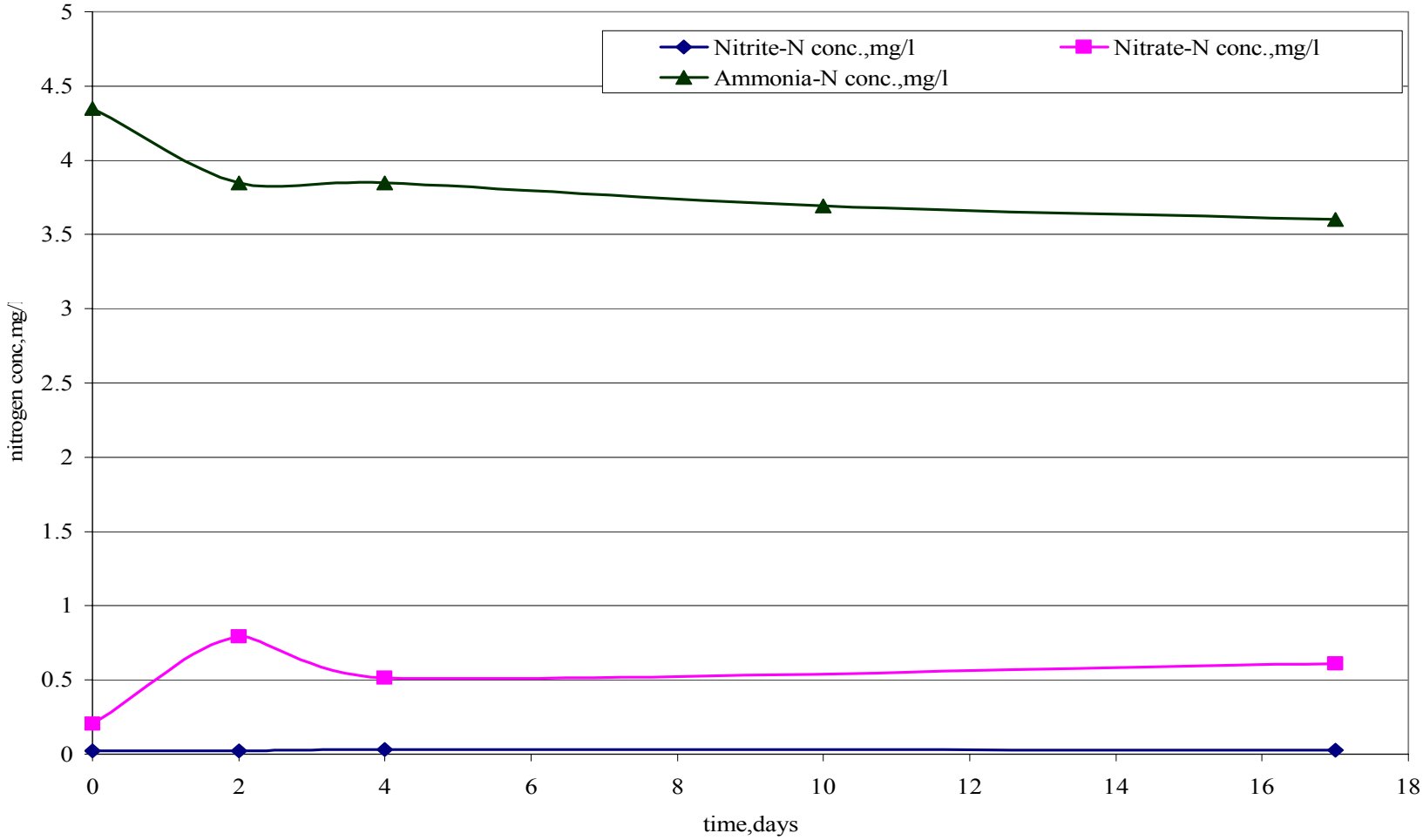

Figure 6.1: Autoclaved ash pond water with 10 ppm Ammonia-N injected

The ammonia concentration in figure 6.1 remains almost constant after the second day. In the first 2 days, it drops a bit due to probable volatilization after when it becomes more or less steady.

6.1.1 Nitrification as first order reaction

When the laboratory scale nitrification reactions in batch process were modeled as first order reaction, the rate constants at different ammonia concentration were different. The rate constant was highest at 2 ppm NH_4^+-N and considerably low at 10 ppm . It remained almost constant between 10 and 100 ppm NH_4^+-N. At concentration of 0.4554 ppm (no external addition of ammonia), the constant was again lower as it is in case of 10 ppm. Yantarasri [59] et al suggested that both ammonia oxidizers and nitrite oxidizing bacteria exhibited substrate inhibition at an ammonia level greater than 1.8 ppm and at a nitrite level greater than 0.5 ppm. This explains why the rate constant starts decreasing above 2 ppm ammonium concentration. The first order rate equation is,

$$C_{NH3} = C_{NH30}e^{-kt} \quad \ldots\ldots\ldots\ldots\ldots\ldots 6.1$$

Where, k = first order rate constant, day^{-1}

t = time, days

Refer figure 6.2 for rate constant at 2ppm NH_4^+-N, at 10 ppm NH_4^+-N, and at no external addition of ammonia. Figure 6.3 shows the first order decay at 100 ppm NH_4^+-N. The equation of the trendline shown in figure 6.2 and 6.3 is for a first order decay of ammonium ion, the rate constant being the constant multiplied by t. The summary of the rate constant at various concentrations is shown in table 6.3. The R^2 in case of 100 ppm ammonium concentration is nearly 0.5, whereas the R^2 in case of 10 ppm ammonium is

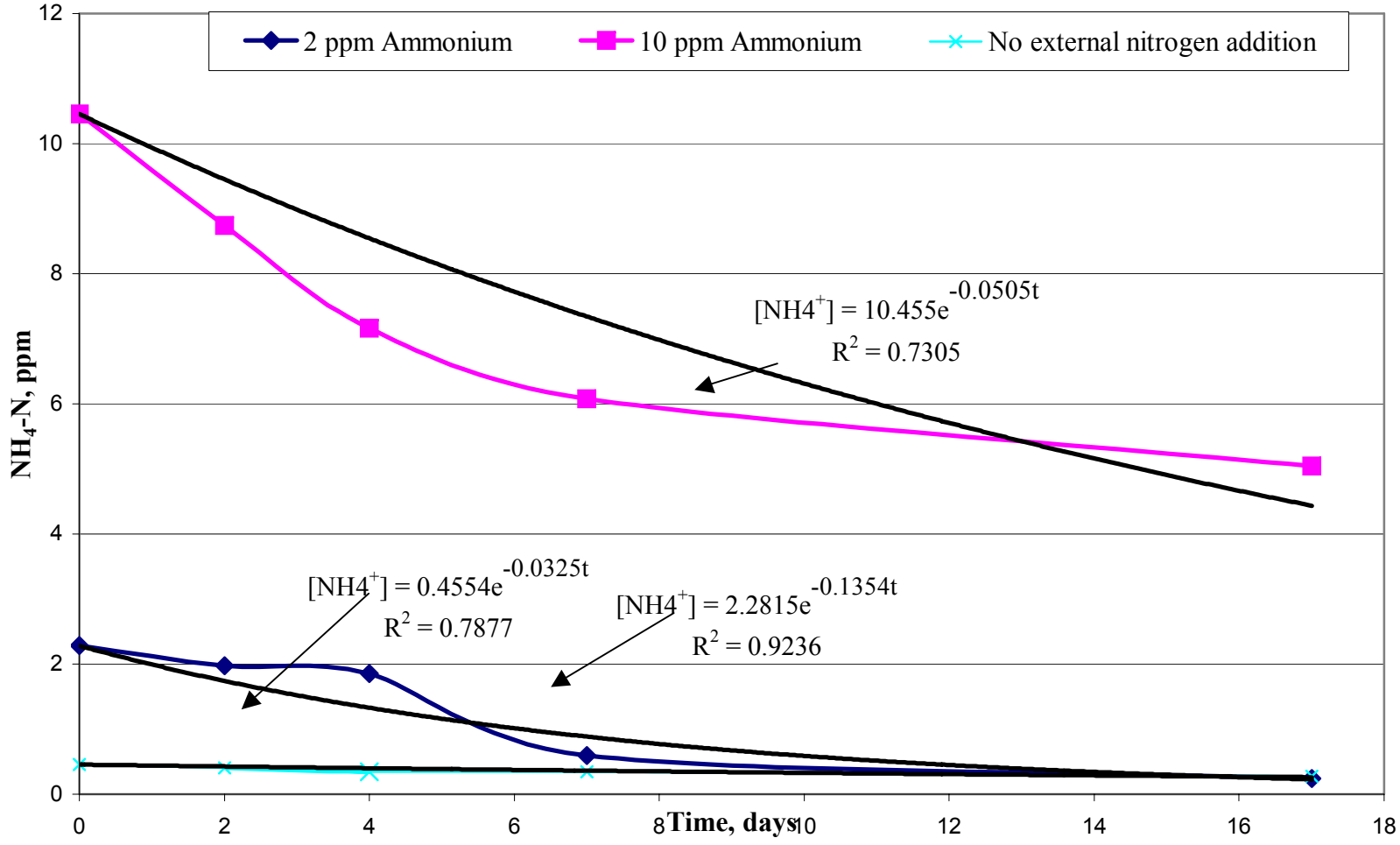

Figure 6.2: Rate of Ammonia Consumption

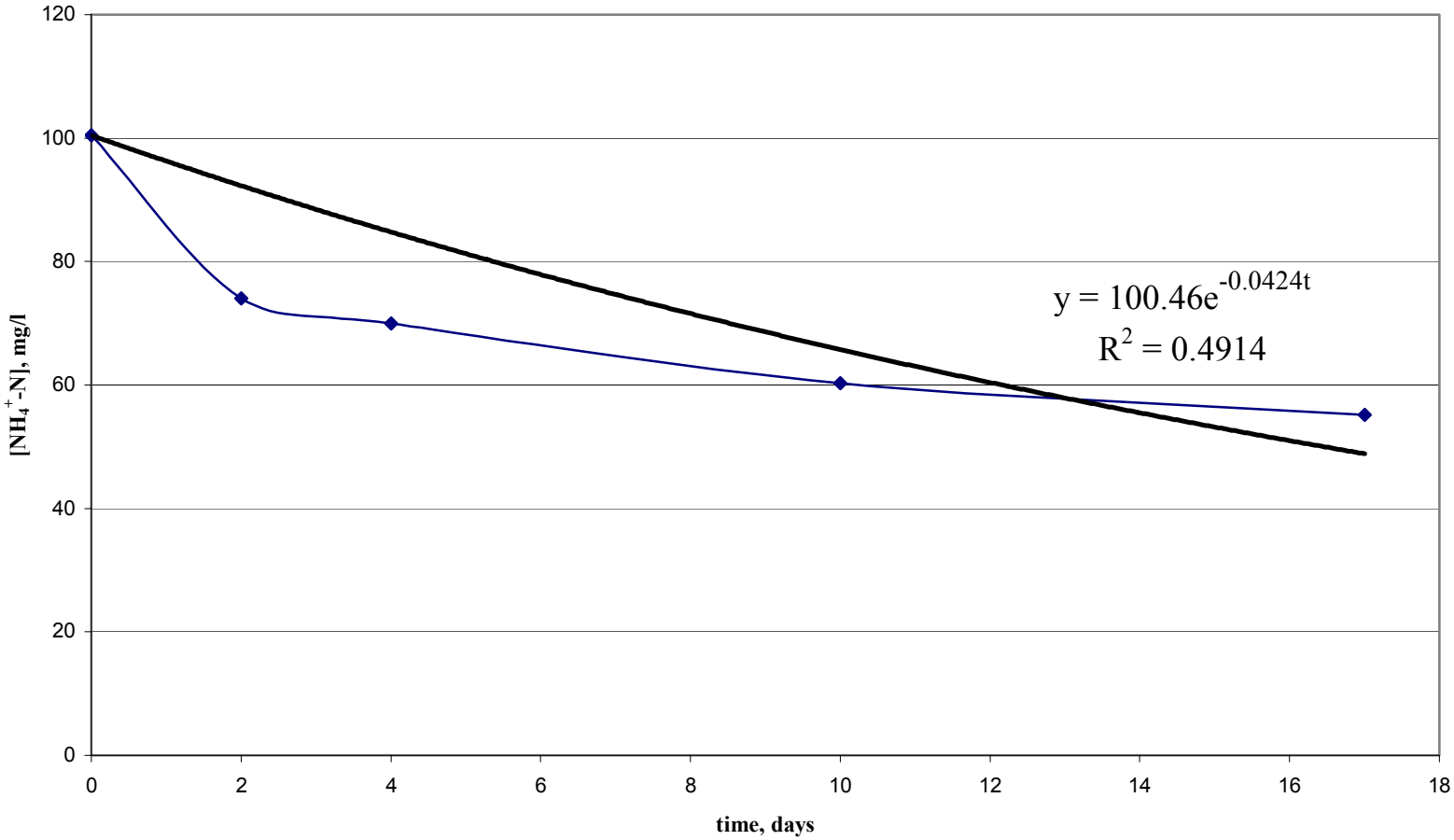

Figure 6.3: Rate of ammonium consumption at 100 ppm initial concentration

Table 6.3: Summary of 1st order rate constant at various NH_4^+-N concentrations

If C_{NH3}	= 2	k =	0.135
If C_{NH3}	< 2	k =	0.135-((2-C_{NH3})*(0.135-0.025)/2)
If C_{NH3}	>2 and <10	k =	0.135-((C_{NH3}-2)*(0.135-0.05)/8)
If C_{NH3}	>10	k =	0.05

0.73, and in case of no external addition of ammonia it is 0.78. The R^2 is best in case of 2 ppm ammonia. The conclusion that can be drawn here the nitrification follows a near first order when the concentration is 2 ppm and it deviates more from first order as the concentration goes up.

6.1.2 Nitrification following Monod kinetic equation

The Monod kinetic equation for nitrification is expressed by equation 4.5 as follows;

$$kXt=[(S_0 - S) + K_S(\ln\frac{S_0}{S})]$$

The values of kXt + S, as tabulated in table 6.1 when plotted against $\ln\frac{S_0}{S}$ (also tabulated in 6.1) gives a straight line for all ammonium concentrations; no external addition, 2 ppm, 10 ppm and 100 ppm and shown in Figure 6.4 for 2 ppm, Figure 6.5 for 10 ppm, Figure 6.6 for 100 ppm and Figure 6.7 for no external addition (0 ppm). The slope of the lines gives the half saturation constant for the Monod kinetic equation for nitrification.

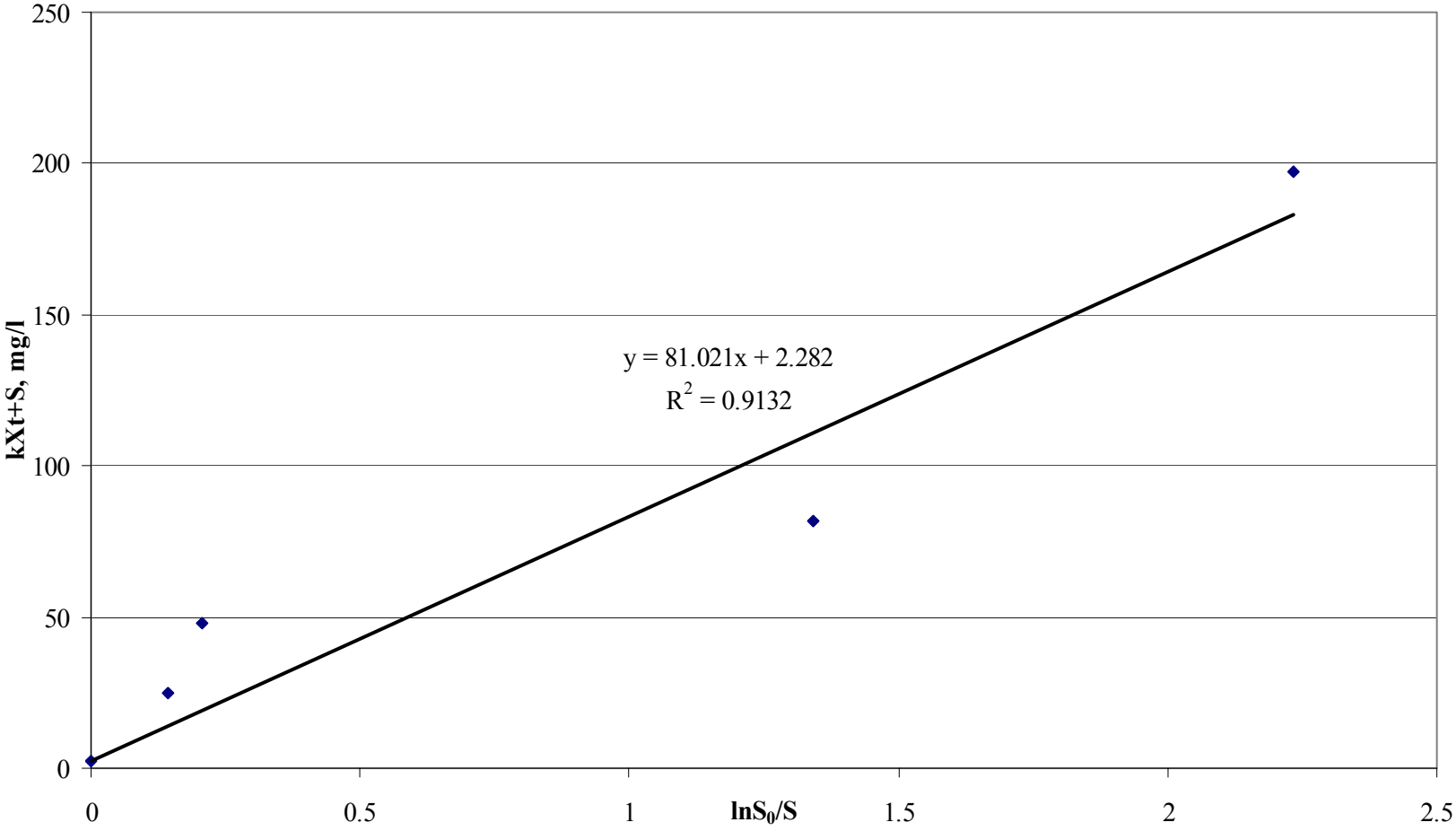

Figure 6.4: Calibration of nitrification equation for 2 ppm ammonia

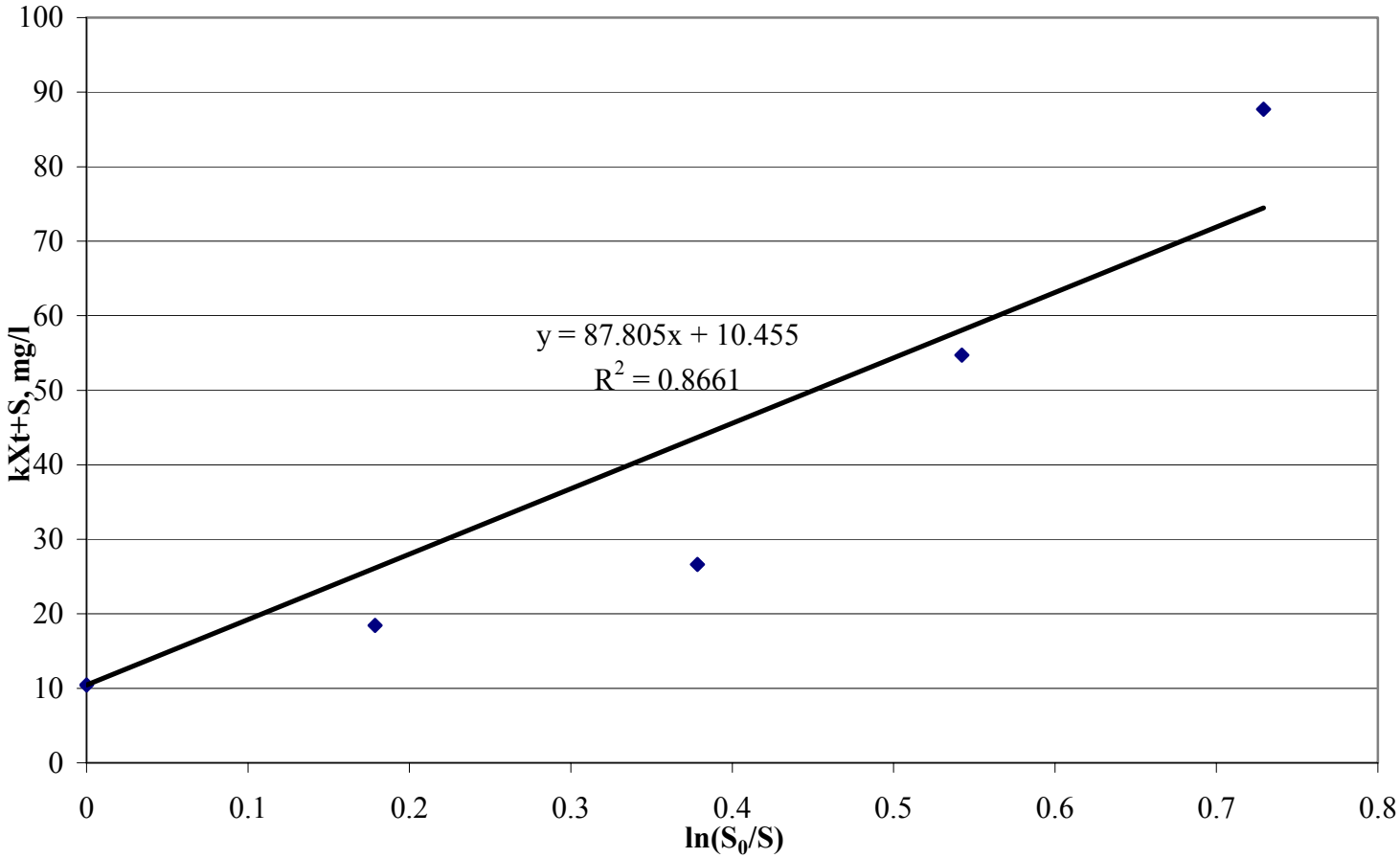

Figure 6.5: Calibration of nitrification equation for 10 ppm ammonia

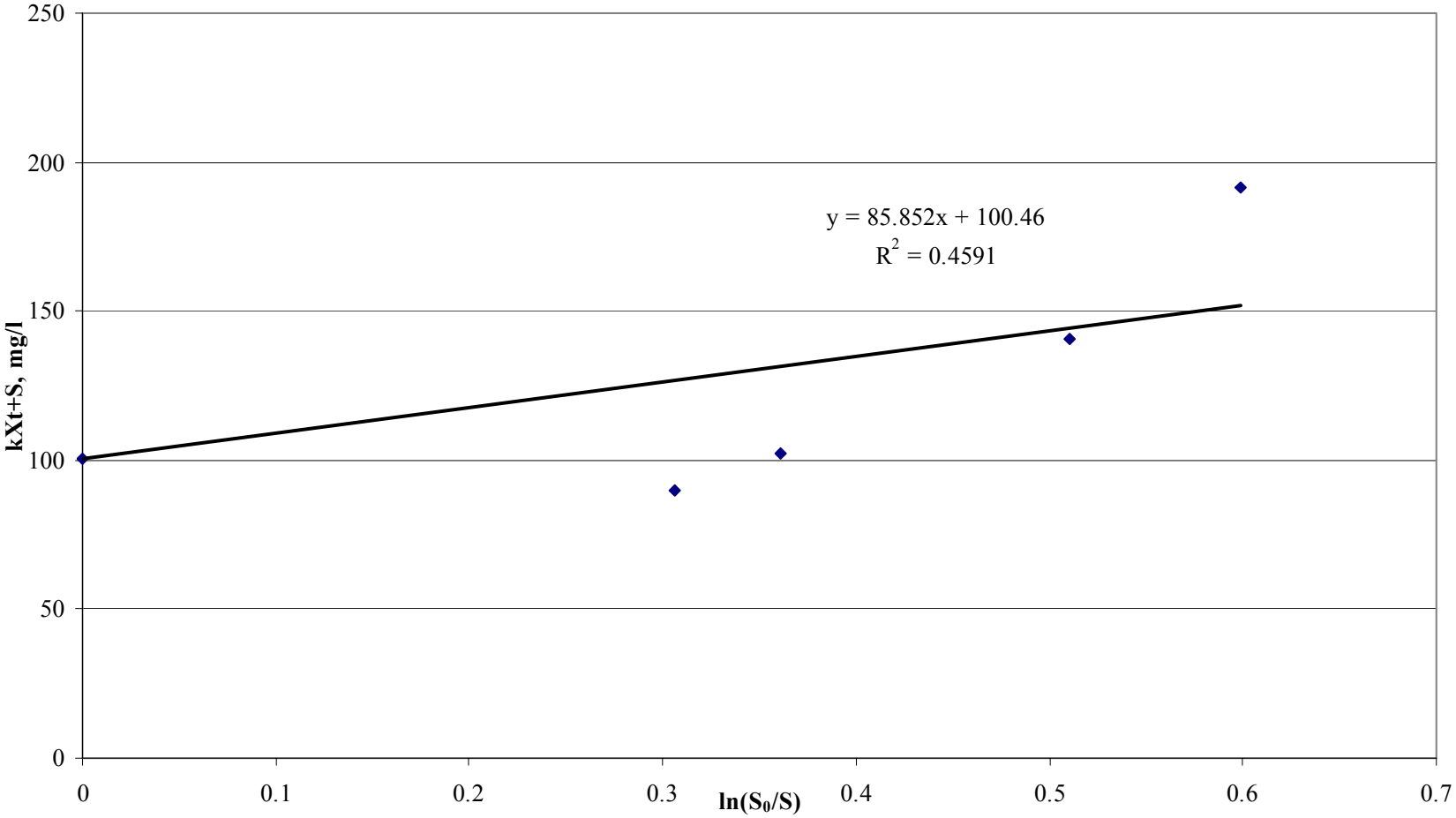

Figure6.6: Calibration of nitrification equation for 100 ppm ammonia

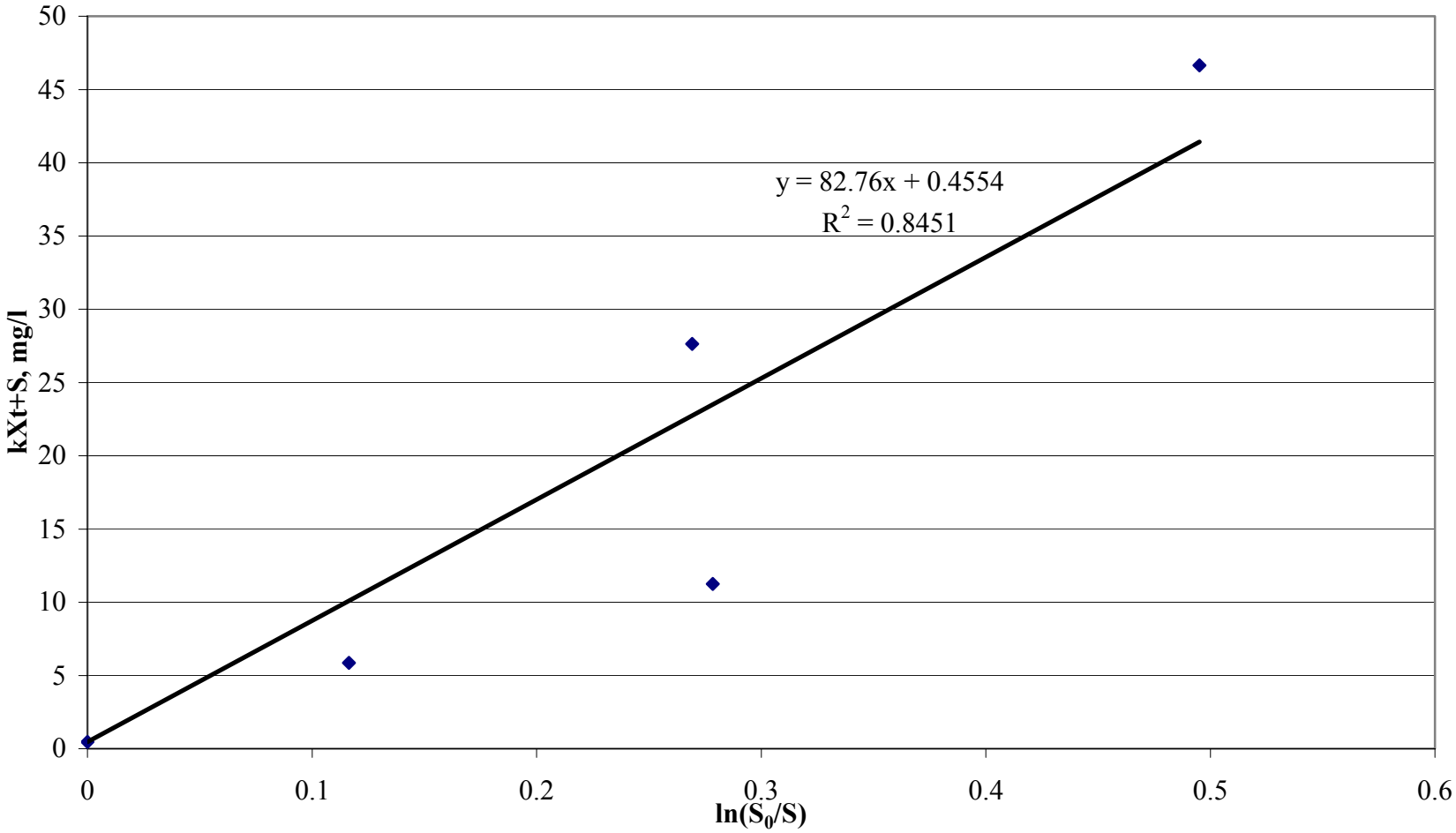

Figure 6.7: Calibration of nitrification equation with no external ammonia

The initial concentration S_0, which is known for all experiments, gives the intercept of the lines. The summary of the experiments to calibrate the Monod kinetic equations is listed in Table 6.4. Figure 6.8 shows the nitrogen balance with time for the case of 2ppm NH_4^+-N in ash pond, Figure 6.9 for the 10 ppm, Figure 6.10 for the 100 ppm and Figure 6.11 ppm for the no external addition case (~0 ppm). The nitrogen balance indicates that the total nitrates and nitrites formed in most of the time does not add up to the ammonium oxidized, indicating denitrification by other means such as reduction by sulfur compounds in the presence of nitrates thereby forming nitrogen. Appreciable amount of sulfur is present in the coal (about 2-3%), which comes to the ash pond via ESP or FGD, if FGD is present. These sulfur compounds can be used for denitrification in the presence of certain sulfur oxidizing bacteria as ponted out by Cheremisinoff [13]. Also there is the possibility of the OLAND process where in case of oxygen limitation, nitrifiers switch from nitrification to

Table 6.4: Summary of Monod kinetic model for nitrification

Concentration of NH_4^+-N, mg/l	Half Saturation Constant K_s, mg/l	R^2 value from plot of kXt+S vs $\ln(S_0/S)$	k in equation 4.5 from Table 6.1	X in equation 4.5, from Table 6.1
2	81.021	0.9132	2.33	4.97
10	87.805	0.866	0.79	6.13
100	85.852	0.459	1.432	5.6
0	82.76	0.845	0.68	4.02
Average	84.36	0.7708	1.308	5.18

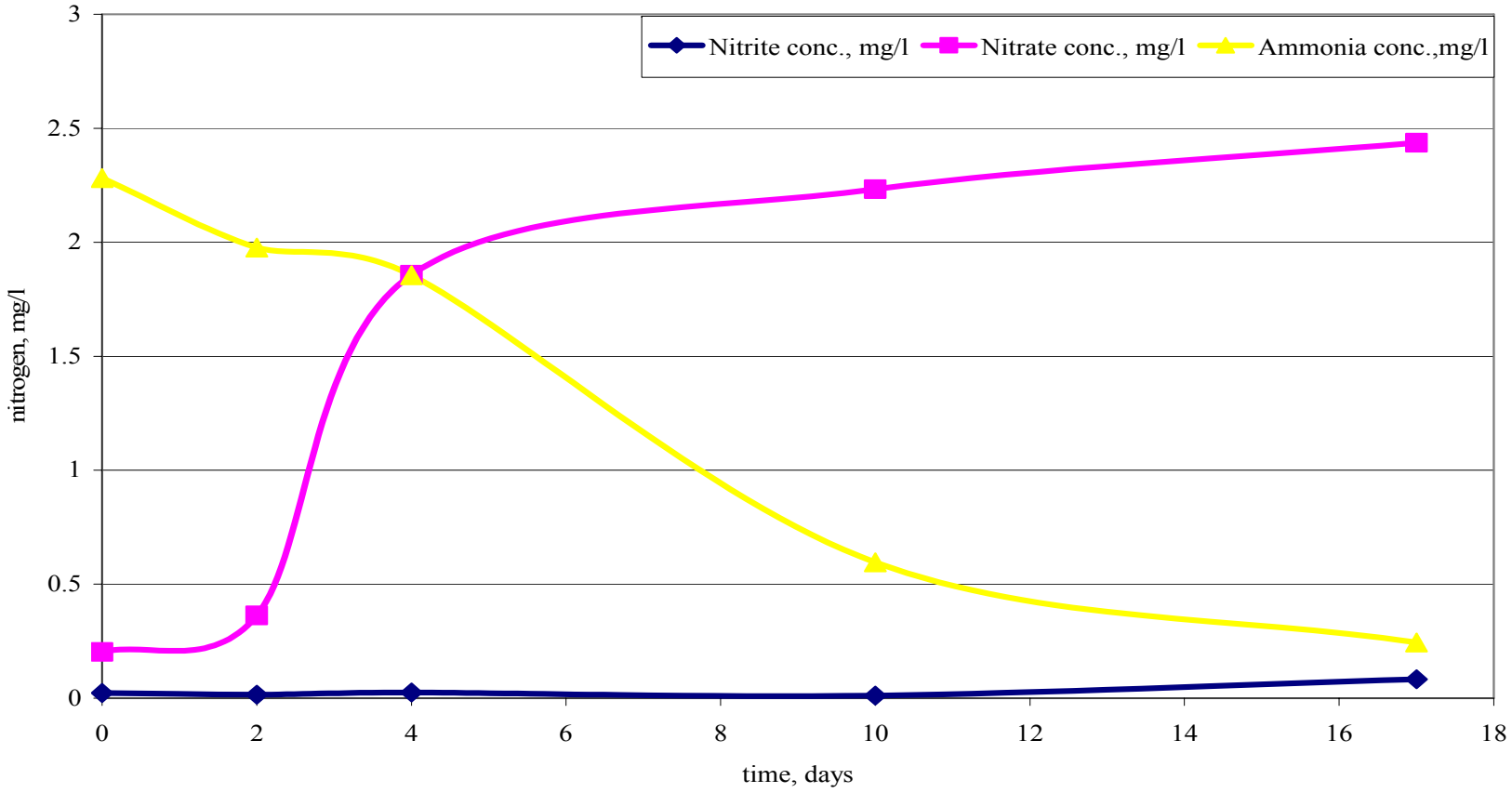

Figure 6.8: Nitrogen balance with 2 ppm NH_4-N injected in ash pond water

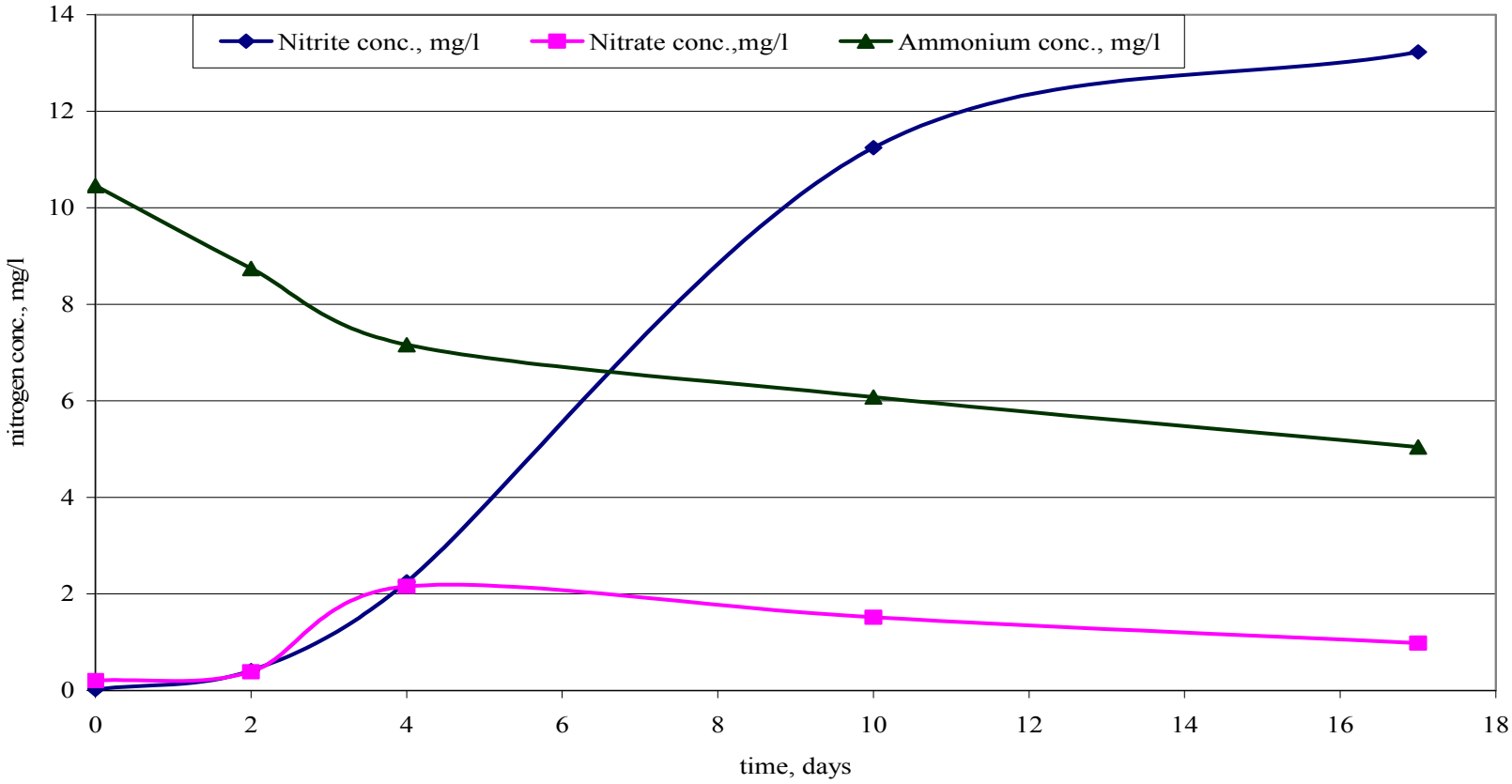

Figure 6.9: Nitrogen balance with 10 ppm NH_4-N injected in ash pond water

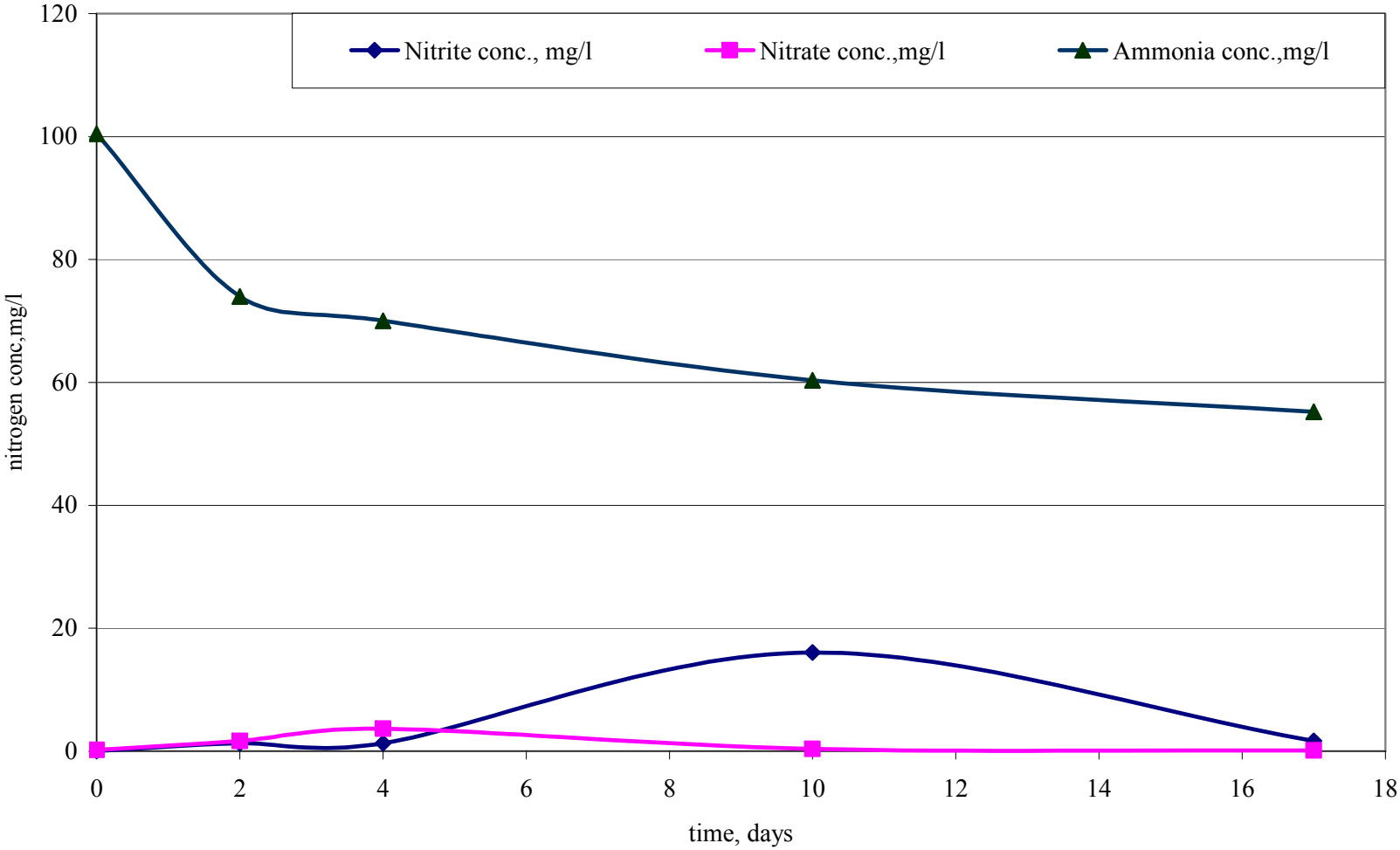

Figure 6.10: Nitrogen balance with 100 ppm NH_4-N injected in ash pond water

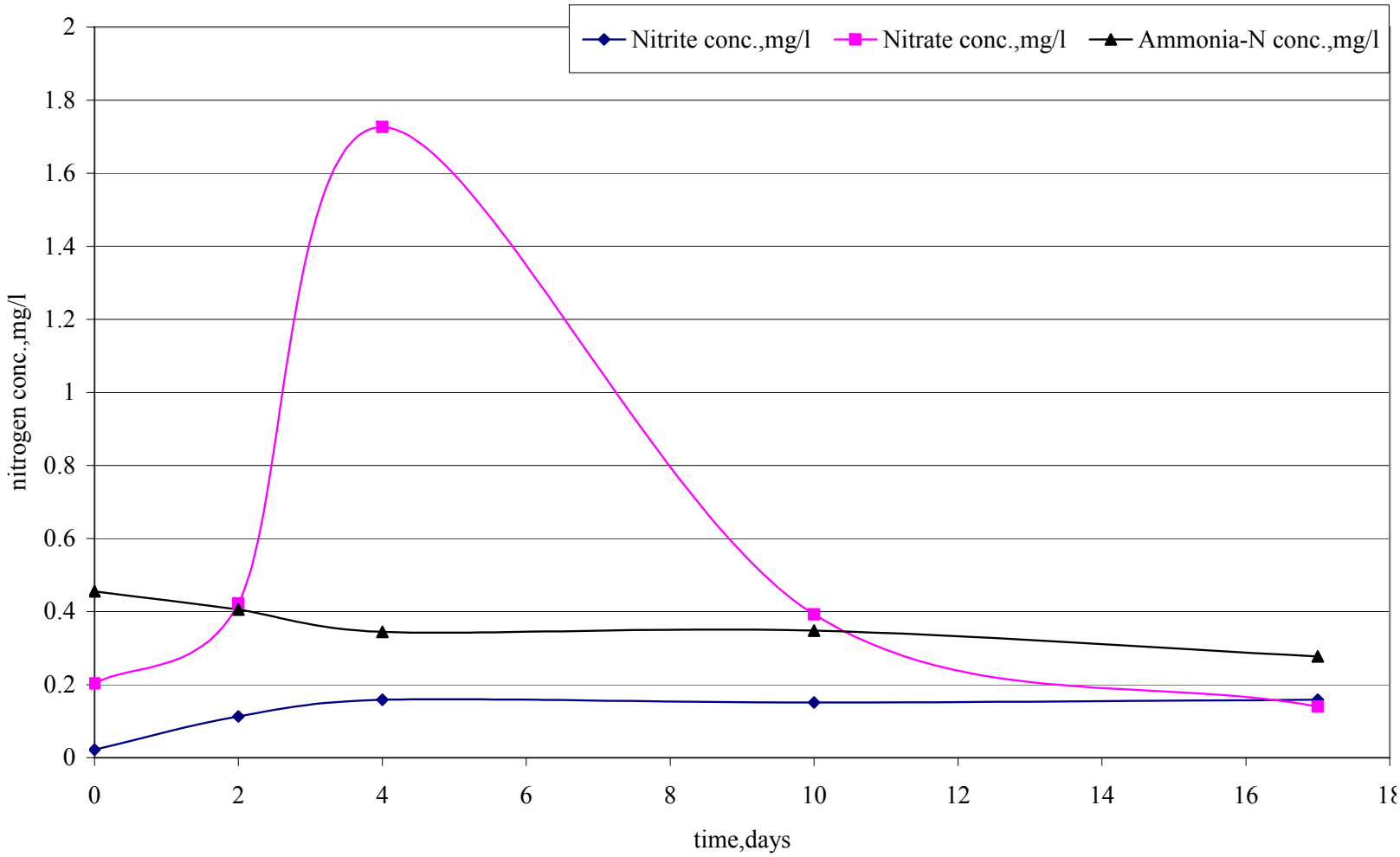

Figure 6.11: Nitrogen balance with no external addition (~ 0 ppm) NH_4-N injected in ash pond water

oxygen-limited autotrophic nitrification-denitrification (OLAND) in order to survive and maintain activity. According to Philips[42] et al, during OLAND, ammonium is oxidized using nitrite as electron-acceptor to form dinitrogen and nitrogen gas. In this work, both the OLAND process and denitrification by sulfur oxidizing bacteria process has been combined and the Monod equation calibrated.

6.1.3 Conclusion from nitrification experiments

The nitrification experiments when evaluated based on first order kinetic reaction and one following Monod kinetic equation, the results can be used to derive the following conclusions;

- The first order kinetic coefficient suggests that the reaction is fastest in the case of 2 ppm injected in the ash pond water. It slows down as the ammonium concentration goes up. However, there is a wide variation in the first order reaction constant at 2 ppm case and 10 ppm and 100 ppm cases. Hence, the nitrification reaction in the ash pond will not be modeled as a first order reaction.
- The Monod kinetic equation model for nitrification in the ash pond came up with more accurate description of the reaction. The k term in table 6.4 and equation 4.5 are very close to each other in the various cases. As a matter of fact, k term also incorporates the μ_m – maximum sp growth rate of bacteria, besides other constants (as explained before). Hence, the Monod kinetic model will be used to model the nitrification in ash pond. The average of the constants in table 6.4 will be used in ChemCAD to model nitrification in the ash pond.

- The k found experimentally is 1.308 day^{-1}(Table 6.4), which combines the temperature factor, the DO factor, pH factor and maximum specific growth rate, treating all of these factors as constants. In order to have temperature as a variable in the model, the k is divided by the constant temperature factor Exp (0.098*(20-15)), and then multiply the resulting constant (0.033 hr^{-1}) with Exp (0.098*(Temp-15)) in the model, where temp is the temperature of the pond. The K_s obtained experimentally is 84.36 mg/l (6.02 mol/m^3). The nitrification user rate expressions is shown as Figure 6.12.
- Since the BOD of the ash pond water is too low (~ 2 ppm), the organic content is also too low. This implies that denitrification by denitrifying bacteria with an organic carbon source is impossible.

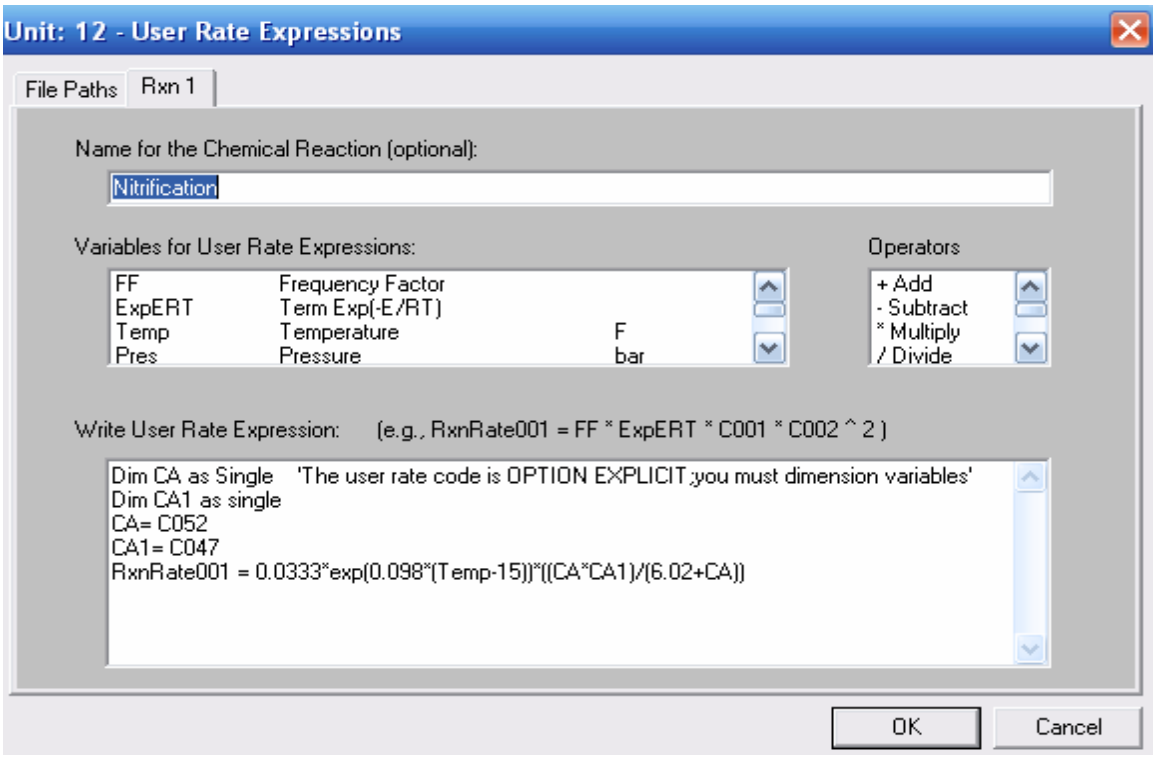

Figure 6.12 Nitrifier rate expression with experimentally determined constants

- The denitrification reaction is occurring either by OLAND process or by sulfur oxidizing bacteria, the kinetic study of which can be taken up as further study.

6.2 Results from Mercury experiment

Preliminary study with the ash pond water and the ash mercury content lead us to the following;

1 g ash in 100 ml ash pond water, mercury measured after 2 days: 3.7 ng/l

$$= 3.7 \times 10^{-12} \text{ g/ mL}$$

Mercury in ash : 31.5 ng/g = 31.5×10^{-9}

Hence, the distribution coefficient = $31.5 \times 10^{-9} / 3.7 \times 10^{-12} = 8513.5$ mL/g

In 2 days, the ash pond water mercury concentration increases from 2.9 ng/l (dechlorinated tap water mercury concentration) to 3.6 ng/l. From this data, the ash pond mercury desorption can be modeled in ChemCAD. However, these figures are so small that any small noise in data cannot be easily detected. So, it was decided to first increase the concentration in ash pond water by injecting mercury externally and then study the desorption kinetics.

6.2.1 Mercury adsorption Experiment

Mercury adsorption on ash followed a pattern suggesting mercury reached equilibrium with ash almost instantly. Table 6.5 shows the mercury in ash with respect to time when the starting concentration of mercury in water was 0.25 ppb (henceforth called case 1). It is evident that after 7 hours, as soon as it crossed 50 ng/g, mercury is in near equilibrium with ash. The mercury adsorption kinetics has no real significance in the model development, as the mercury comes adsorbed with the ash to the ash pond.

Table 6.5: Mercury adsorbing on ash with time at 0.25 ppb starting concentration (case 1)

time, hrs	mercury in ash, ng/g (ppb)
0	31.5
3	47.5
7	52.9
11	52.3
27	58.2
31	54.5
51	55.4
78	58.0
83	56.5
99	56.9
103	58.4

The adsorption experiment was performed to arrive at a reasonable mercury concentration in the ash, so that desorption experiment can be performed. The mercury as such in the ash collected from the plant is too low to detect any mercury during desorption. When the same adsorption experiment is repeated with 10 ppb starting concentration (henceforth called case 2), the same pattern is noted, which is after 17 hours, the mercury in the ash reaches a near equilibrium concentration as shown in Table 6.6. This suggests that mercury reaches equilibrium with ash almost instantly (within couple of hours), which is also confirmed by Figure 6.13.

Table 6.6: Mercury adsorbing on ash with time at 10 ppb starting concentration (case 2)

time, hrs	mercury in ash, ng/g
0	32
17	972.4
21	984.1
43	1037.5
45	1068.5
67	1102.5
76	1100.9
102	1102.7

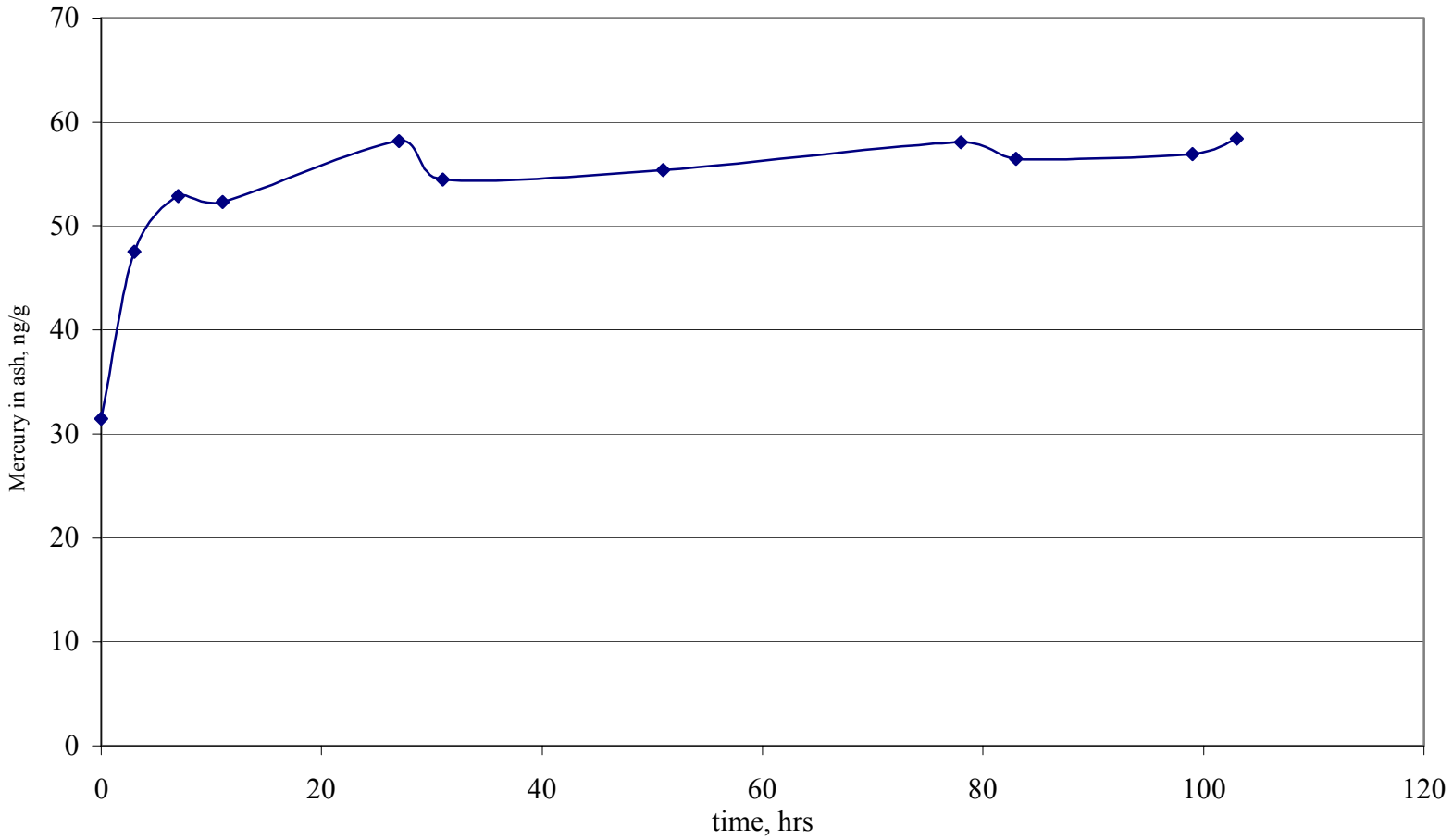

Figure 6.13: Mercury adsorption in ash with time (Case 1)

6.2.2 Mercury desorption Experiment

As explained before in chapter 4, mercury desorption from ash will follow the following equation;

$$t = \frac{m_3 * K_D}{{}^3K_{A2} * A} ln \frac{w_A^0}{w_A} \quad \text{..... 4.6}$$

Where,

m_3 = total mass of ash, kg (a constant neglecting mass loss due to mercury desorption)

w_A = mass fraction of mercury in ash at time t

w_A^0 = mass fraction of mercury at time, t=0

${}^3K_{A2}$ = overall liquid-phase mass transfer coefficient across a ash-water interface, m/hr

K_D = Partition or distribution coefficient for mercuric chloride between ash phase and water phase, m^3/kg

A = desorption area of ash, m^2

In the batch experimental process, all the above except mass fraction of mercury in ash remains constant. In the real life case of an ash pond also, all the above except mass fraction can be safely assumed to be a constant, as the net increase of mass of ash (m_3) with time will be offset by the desorption area (A) increase in the denominator. So, the equation 4.6 may be modified as,

$$t = k \ln \frac{w_A^0}{w_A} \quad \text{.....6.2}$$

Table 6.7 : Mass fraction of mercury with time in case 1

time, hrs	mercury conc., ng/l	w_A	$\ln(w^0_A/w_A)$
0	130	1.0431E-07	0
8	203	9.64694E-08	0.07813748
24	151	1.0211E-07	0.02130897
32	222	9.50198E-08	0.09327881
48	235	9.40008E-08	0.10406033
69	235	9.43444E-08	0.10041141

With known w^0_A, if the mass fraction of mercury in ash is plotted against time, t, equation 6.2 gave a straight line for case 1 (0.25 ppb starting concentration). Table 6.7 tabulates the mass fraction of mercury in ash with time for case 1. The overall mercury mass balance for case 1 is shown in table 6.8. Figure 6.14 is the plot of $\ln(w^0_A/w_A)$ versus time, hours for case 1. The total mercury at beginning of desorption (940 ng) is greater than at time, t=0. This is possible only if the amount of mercury in the test sample was less than the mercury in the ash used for experimentation. This is probable, as the mercury is not homogeneously distributed on the ash surface, as it gets adsorbed on the ash during its passage through the flue gas duct and gets captured along with the ash in the Electro Static Precipitator.

Table 6.9 shows the mass fraction of mercury in ash with time for case 2 (10 ppb starting concentration). Table 6.10 shows the overall mercury balance and figure 6.15 is the plot of $\ln (w^0_A/w_A)$ versus time, hours for case 2.

Table 6.8: Overall mercury balance for case 1

mercury at time 0			
1	in ash	261	ng*
2	in water	250	ng
3	mercury lost in adsorption sampling	13.26	ng
	Total	524.26	ng
mercury beginning of desorption			
1	in ash	938.786667	ng
2	in water	1.2	ng
	Total	939.986667	ng
mercury at completion of desorption exp			
1	in ash	528	ng
2	in water	207.196	ng
3	mercury lost in sampling	208.6751	ng
	Total	943	

* ng – nano gram

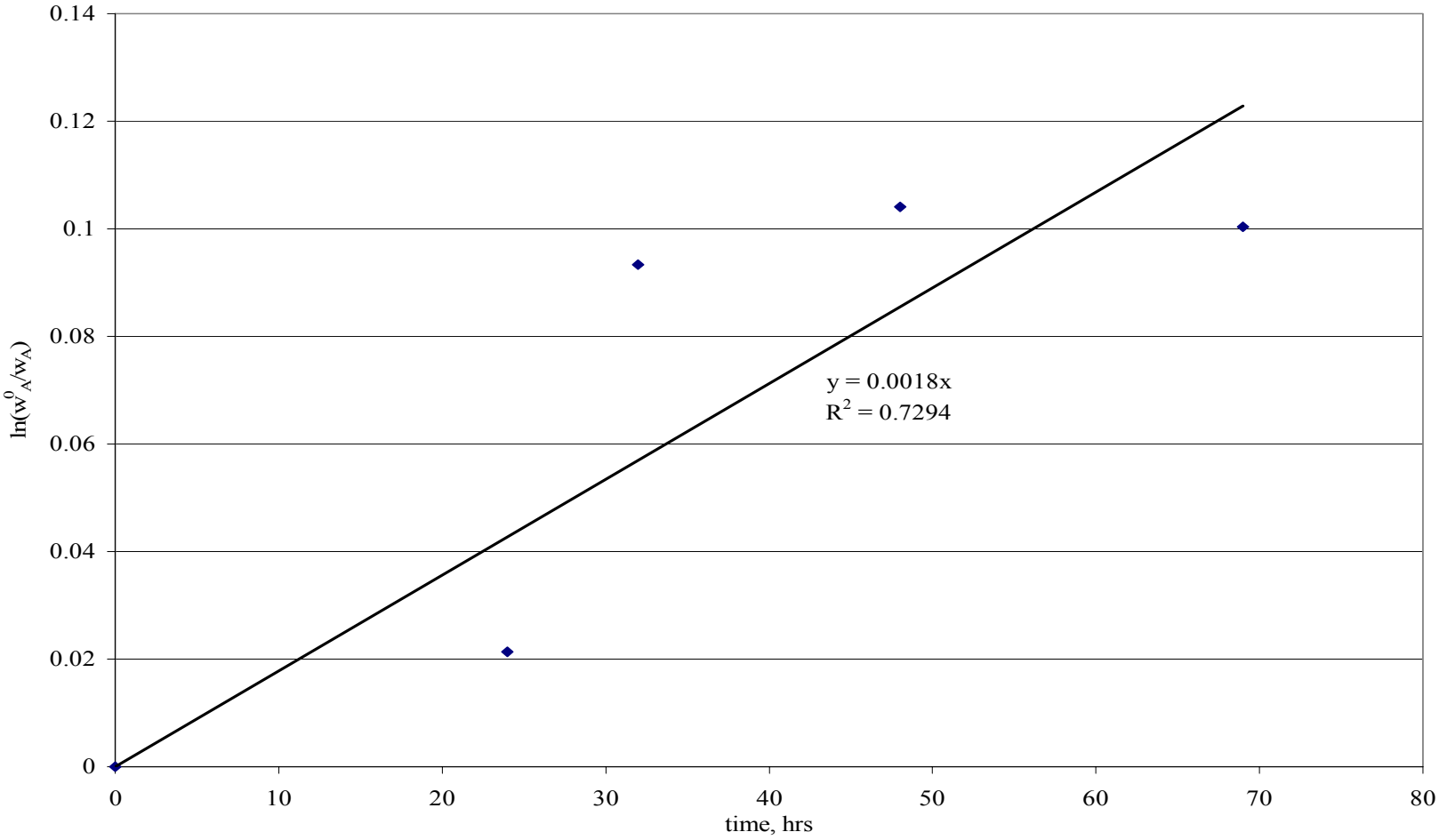

Figure 6.14: Desorption curve for Case 1

Table 6.9 : Mass fraction of mercury with time in case 2

time, hrs	mercury conc., ng/l	w_A	$\ln(w^0_A/w_A)$
0	22	7.24254E-07	0
14	27	7.23734E-07	0.00071812
24	42	7.22163E-07	0.00289198
49	29	7.2353E-07	0.00100074
64	30	7.2347E-07	0.00108351
69	21	7.24373E-07	-0.0001636
91	18	7.25907E-07	-0.00228

Table 6.10: Overall mercury balance for case 2

mercury at time 0			
1	in ash	261	ng
2	in water	9657	ng
3	mercury lost in adsorption sampling	261.419576	ng
	Total	10179.4196	ng
mercury beginning of desorption			
1	in ash	6518.28667	ng
2	in water	1.2	ng
	Total	6519.48667	
mercury at completion of desorption exp			
1	in ash	5616	ng
2	in water	14.001615	ng
3	mercury lost in sampling	977.743	ng
	Total	6607	ng

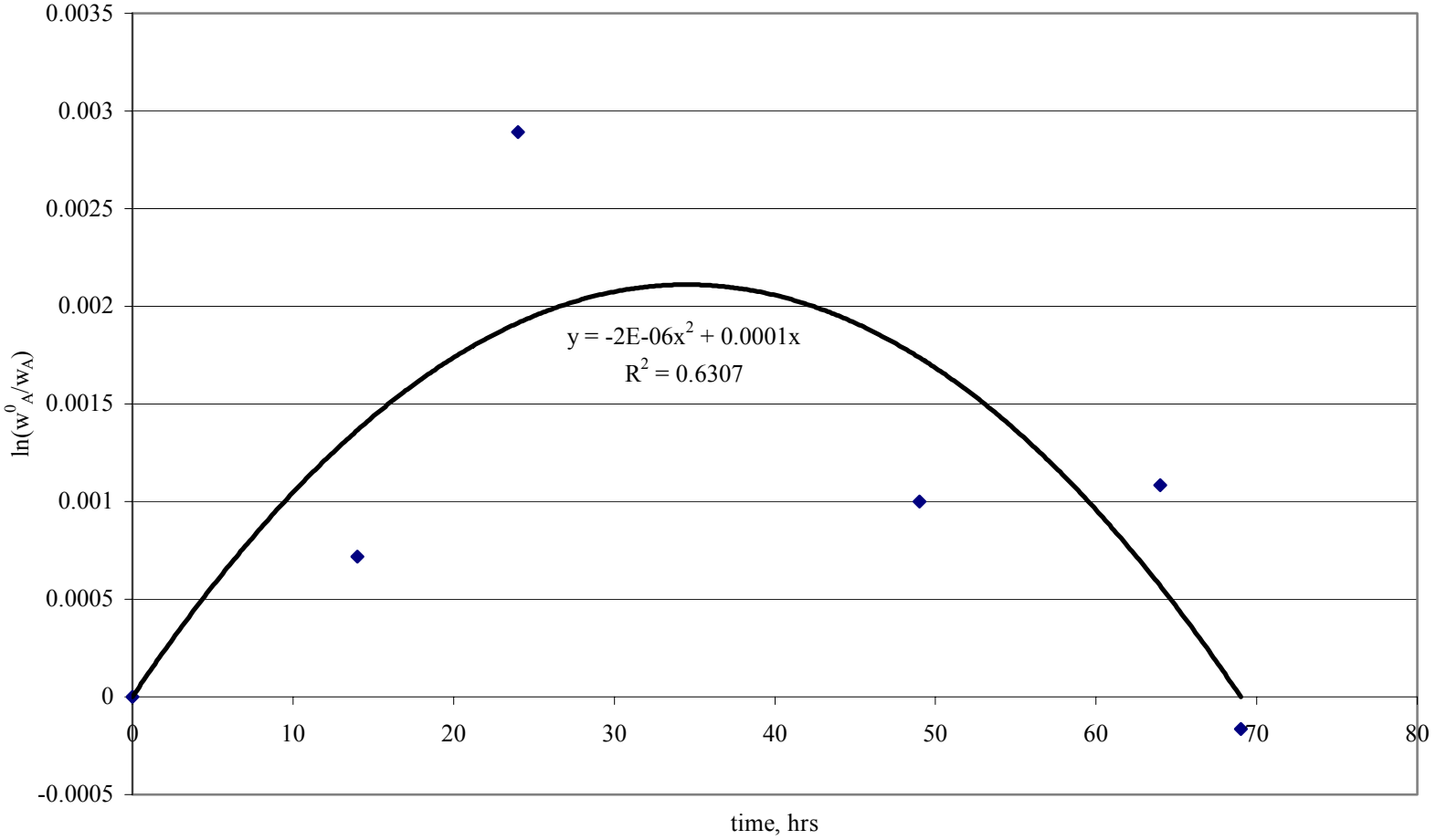

Figure 6.15: Desorption curve for case 2

6.2.3 Conclusion from mercury experiments

The following conclusion can be drawn from the experiments.

Case 1:

- Total mercury at the beginning is about half of that at the end.
- Mercury is possibly not homogenously distributed in the ash. Hence, actual mercury is higher in the ash in experiment than the ash analysed.
- Total mercury at the beginning of desorption matches quite closely with that at end.

Case 2:

- Total mercury at the beginning is almost 50% more than at the end.
- Some mercury vaporised during the experiment, causing lower total mercury at the end.
- Total mercury at the beginning of desorption matches quite closely with that at end.

In both cases the material balance at the beginning and end of desorption experiments is quite close to each other. This indicates that very little or no mercury lost during desorption experiment. The overall conclusion from the experiments are as follows;

1. The distribution coefficient from case 1 is 10430 mL/g, calculated from the equilibrium concentration of mercury in ash pond water and ash before desorption started.
2. Similarly, the distribution coefficient from case 2 is 37590 mL/g. The higher distribution coefficient in case 2 suggests, at higher aqueous concentration the

mercury has a tendency to adsorb more strongly with the ash, which is indicated by Figure 6.14 also. The mercury desorbs in the first 30 hours and adsorbs back to the ash in Figure 6.14.

3. As the ash mercury concentration is expected to be in the range of case 1 (0.25 ppb initial concentration), the desorption coefficient, k in equation 6.2, can be considered as 0.0018 hour in ChemCAD model for mercury desorption. However, the next section deals with ammonia-mercury interaction, which will predict accurate kinetic equation to be used in the model.

6.3 Ammonia-mercury interaction

The ammonia mercury interaction is studied with varying concentration of mercury and ammonia in ash. Nine experiments were performed as described in chapter 4 with mercury and ammonia laden ash suspended in autoclaved (sterilized) deionized water. The desorbed mercury from the ash in the nine cases were analysed and presented as Table 6.11. The ln (ω^0_A/ω_A) is negative in several instances indicating $\omega_A > \omega^0_A$, i.e, the mercury adsorbing back into ash from the aqueous phase. This is more prominent as the ammonia-N concentration increases to 14 ppm. This indicates mercury forms complex molecules with ammonia just like arsenic, selenium, nickel, etc indicated by EPRI[30]. Refer to appendix-2 for change in ammonia concentration with time. Volatilization of ammonia is not evident from the ammonia analysis. A drop of 1-2 ppm in ammonia concentration is noticed, which is due to the complex molecules formation with mercury. Ammonia in aqueous phase tends to increase the pH also, which helps in precipitating the complex molecules of mercury. The 9 cases of ammonia-mercury

Table 6.11: Rate of mercury desorption from ash

Desorption -2 ppm NH_3-N / 0.25 ppb Hg			
time, hrs	mercury conc., ng/l	ω_A	$\ln(\omega^0_A/\omega_A)$
0	16 (21)*	1.5969E-07	0
5	32	1.5783E-07	0.011721821
20	22	1.5898E-07	0.004507182
43	36	1.5748E-07	0.013984828
70	25	1.5874E-07	0.005985102
Desorption-5 ppm NH_3-N / 0.25 ppb Hg			
time, hrs	mercury conc., ng/l	ω_A	$\ln(\omega^0_A/\omega_A)$
0	16	1.5969E-07	0
5	30	1.5809E-07	0.01011528
20	25	1.5875E-07	0.0059329
43	29	1.5831E-07	0.00872611
70	16 (12)*	1.5971E-07	-0.0001047
Desorption-14 ppm NH_3-N / 0.25 ppb Hg			
time, hrs	mercury conc., ng/l	ω_A	$\ln(\omega^0_A/\omega_A)$
0	16	1.5969E-07	0
5	23	1.5894E-07	0.00470773
20	50	1.5598E-07	0.02352444
43	25	1.5877E-07	0.00580894
70	12 (13)*	1.6005E-07	-0.0022021

* Numbers inside parenthesis is a repeat measurement to ensure negligible measurement error

Table 6.11: Continued

Desorption-2 ppm NH_3-N / 0.5 ppb Hg			
time, hrs	mercury conc., ng/l	ω_A	$\ln(\omega^0_A/\omega_A)$
0	37	9.1053E-08	0
5	21	9.2858E-08	-0.01962505
20	30	9.1827E-08	-0.00845794
43	35	9.127E-08	-0.00237342
70	31	9.1636E-08	-0.00637527
Desorption-5 ppm NH_3-N / 0.5 ppb Hg			
time, hrs	mercury conc., ng/l	ω_A	$\ln(\omega^0_A/\omega_A)$
0	37	9.1053E-08	0
5	78	8.6577E-08	0.05040974
20	52	8.9414E-08	0.01816725
43	64	8.8194E-08	0.03191051
70	57	8.9015E-08	0.02264486
Desorption-14 ppm NH_3-N / 0.5 ppb Hg			
time, hrs	mercury conc., ng/l	ω_A	$\ln(\omega^0_A/\omega_A)$
0	37	9.1053E-08	0
5	24	9.2446E-08	-0.0151819
20	70	8.7523E-08	0.03954761
43	29	9.1846E-08	-0.0086704
70	13 (10)*	9.3507E-08	-0.0265961

* Numbers inside parenthesis is a repeat measurement to ensure negligible measurement error

Table 6.11: Continued

Desorption-2 ppm NH_3-N / 1 ppb Hg			
time, hrs	mercury conc., ng/l	ω_A	$\ln(\omega^0_A/\omega_A)$
0	129	1.8194E-07	0
5	140	1.8076E-07	0.006507556
20	216	1.7218E-07	0.055149604
43	241	1.6967E-07	0.069780492
70	514	1.4058E-07	0.257908227
Desorption-5 ppm NH_3-N / 1 ppb Hg			
time, hrs	mercury conc., ng/l	ω_A	$\ln(\omega^0_A/\omega_A)$
0	129	1.8194E-07	0
5	227	1.7129E-07	0.06032343
20	129	1.82E-07	-0.0003353
43	68	1.8833E-07	-0.034532
70	67	1.8837E-07	-0.0347412
Desorption-14 ppm NH_3-N / 1 ppb Hg			
time, hrs	mercury conc., ng/l	ω_A	$\ln(\omega^0_A/\omega_A)$
0	129	1.8194E-07	0
5	30	1.9277E-07	-0.057831
20	65	1.8883E-07	-0.0371945
43	35	1.9176E-07	-0.0525915
70	17 (16)*	1.9348E-07	-0.0614909

* Numbers inside parenthesis is a repeat measurement to ensure negligible measurement error

Table 6.12: Summary of Fit

RSquare	0.532934
RSquare Adj	0.44457
Root Mean Square Error	0.035159
Mean of Response	0.007535
Observations (or Sum Wgts)	45

interaction (full factorial) indicated in Table 6.11 were used for regression analysis using JMP version 6. The summary of fit is shown as Table 6.12. The R^2 value for the model equation from regression analysis is 0.533.This R^2 and the model can be accepted for the present work, given the complex nature of the ammonia mercury interaction. Table 6.13 shows the parameter estimates from JMP. The Probability estimates in the last column indicates the contribution of the parameter to the model. The smaller the probability, and anything less than 0.05, the greater is the contribution of the factor to the model. Hence, ammonia by itself or in conjunction with mercury has a significant effect on mercury desorption. Time or mercury concentration by itself has no significant effect on desorption. Figure 6.16 shows the leverage plot for ammonia, Figure 6.17 for mercury, Figure 6.18 for ammonia mercury and 6.19 for ammonia, mercury and time. The leverage plots graphically indicate the significance of an effect. The curves on either side of the horizontal line are the confidence curves. If the confidence curve crosses horizontal line, the effect is significant as in the case of ammonia in Figure 6.16. The mercury leverage

Table 6.13: Parameter Estimates

Term	Estimate	Std Error	Prob>|t|
Intercept	0.0192139	0.014275	0.1865
Ammonia	-0.008363	0.002802	0.0050
Mercury	0.0077816	0.016809	0.6461
(Ammonia-2.5)*(Mercury-0.58333)	-0.035093	0.008985	0.0004
Time	0.0001699	0.000202	0.4059
(Ammonia-2.5)*(Time-27.6)	-0.000286	0.000108	0.0119
(Mercury-0.58333)*(Time-27.6)	0.0009381	0.000648	0.1561
(Ammonia-2.5)*(Mercury-0.58333) *(Time-27.6)	-0.000981	0.000346	0.0074

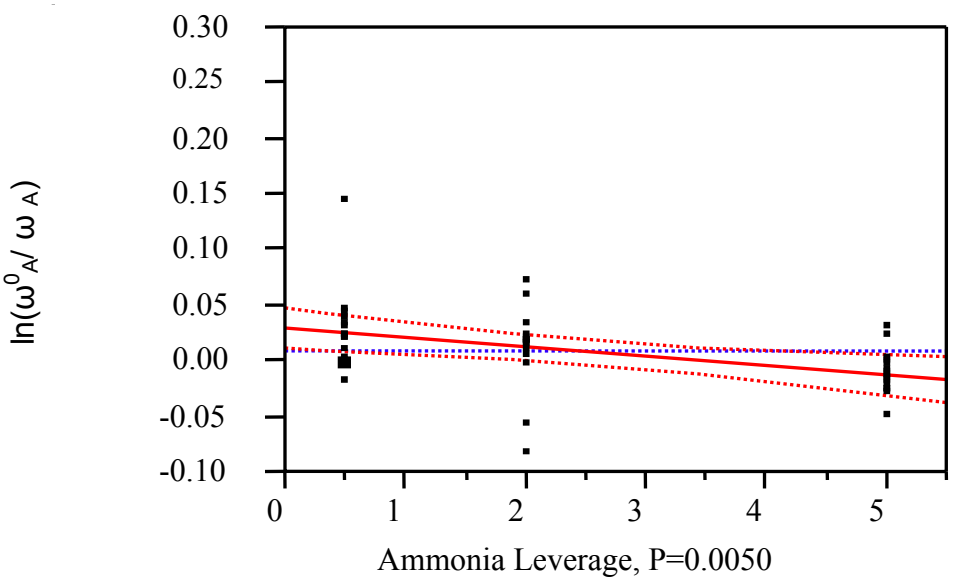

Figure 6.16: Ammonia Leverage Plot

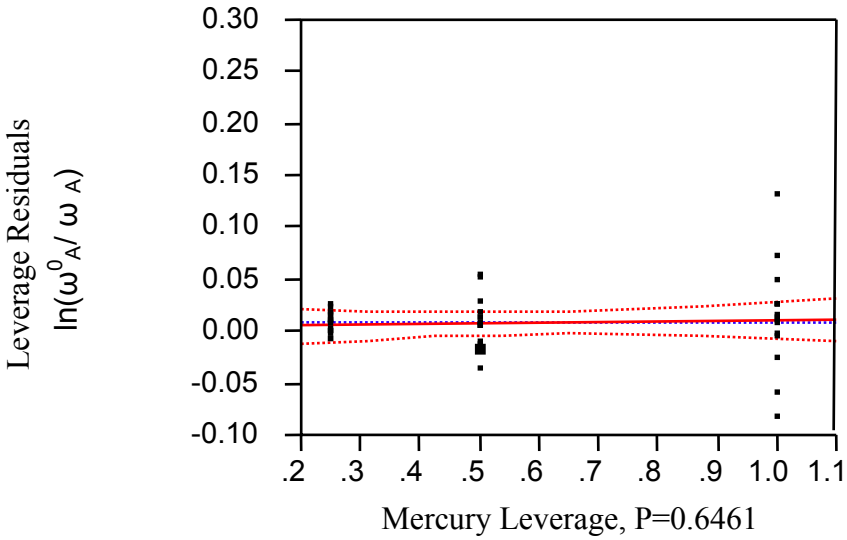

Figure 6.17: Mercury Leverage Plot

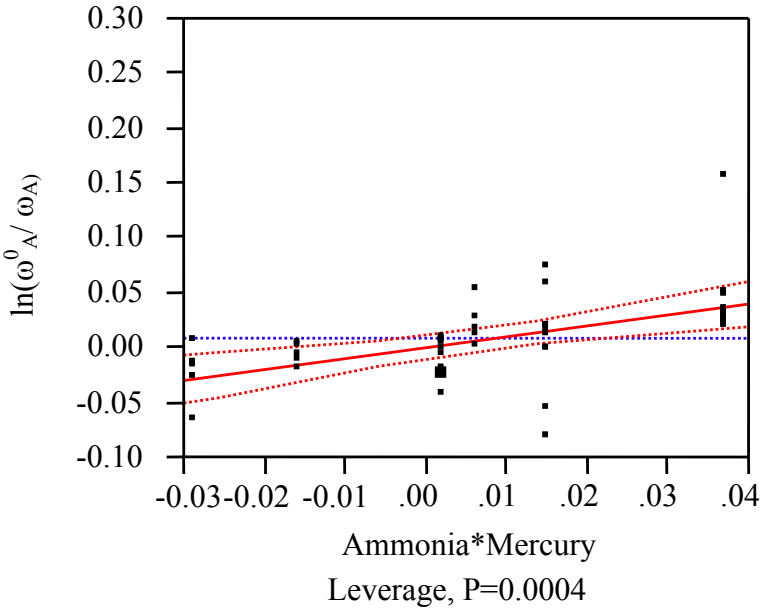

Figure 6.18 : Ammonia Mercury Leverage Plot

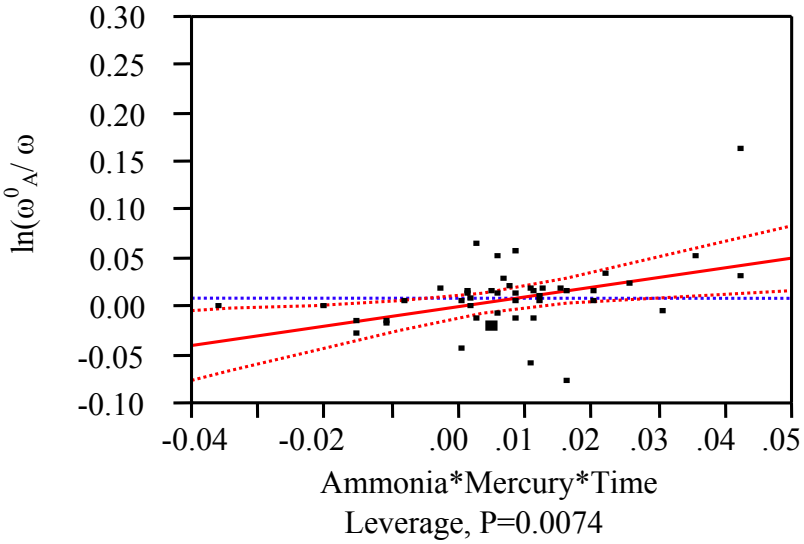

Figure 6.19: Ammonia *Mercury*Time Leverage Plot

plot in Figure 6.17 has the confidence curve not crossing the horizontal line, indicating mercury by itself is not significant. Figure 6.18 and 6.19 has the confidence curve crossing the horizontal line, indicating ammonia interaction with mercury is significant in causing or preventing mercury desorption. The parameter estimates in Table 6.13 gives the model fit equation for response, i.e., ln ω0A / ωA, which is as follows;

$$\ln \frac{\omega_A^0}{\omega_A} = 0.019 - 0.008\, C_{NH_3} + 0.008\, \omega_A - 0.035\, (C_{NH_3} - 2.5)(\omega_A - 0.58) + 0.00017\, t - 0.00029\, (C_{NH_3} - 2.5)(t - 27.6) + 0.00094\, (\omega_A - 0.58)(t - 27.6) - 0.00098\, (C_{NH_3} - 2.5)(\omega_A - 0.58)(t - 27.6) \quad \ldots\ldots 6.3$$

The rate form of equation 6.3 is as follows;

$$r_{\omega_A} = \frac{-.00017 + .00029\,(C_{NH_3} - 2.5) - .00094\,(\omega_A - .583) + .00098\,(C_{NH_3} - 2.5)(\omega_A - .583)}{.008 - .035\,(C_{NH_3} - 2.5) + .00094\,(t - 27.6) - .00098\,(C_{NH_3} - 2.5)(t - 27.6) + \frac{1}{\omega_A}} \quad \ldots 6.4$$

Equation 6.4 is integrated into the model equation for mercury desorption in the ash pond.

6.3.1 Conclusion from ammonia mercury interaction

The ash pond is simulated in the closest possible manner in the laboratory. However, on applying equation 5.2-74 of Thibodeaux to the experimental result, no fixed pattern emerges with respect to the ln (w0A/wA) vs t as shown in figure 6.20 and 6.21. The plot of ln (w0A/wA) vs t should be a straight line if the ammonia effect is negligible. Figure 6.20 further confirms that the mercury adsorption / desorption is highly dependant on the effect of ammonia concentration. Thus, the equation 6.3 developed from data analysis in JMP takes care of the ammonia effect with time. The‘t’ in the equation is the

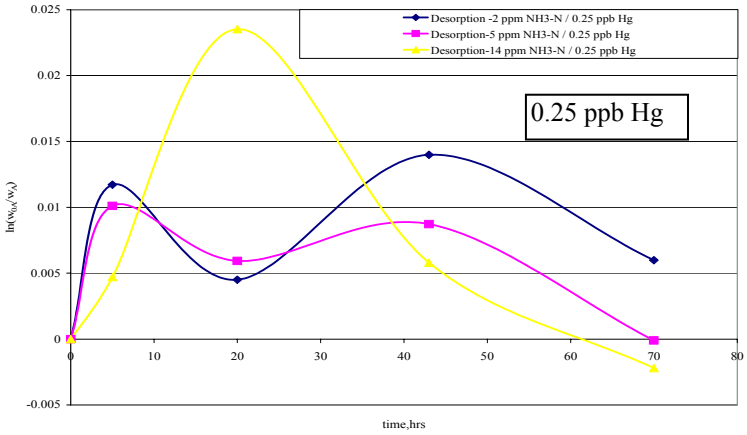

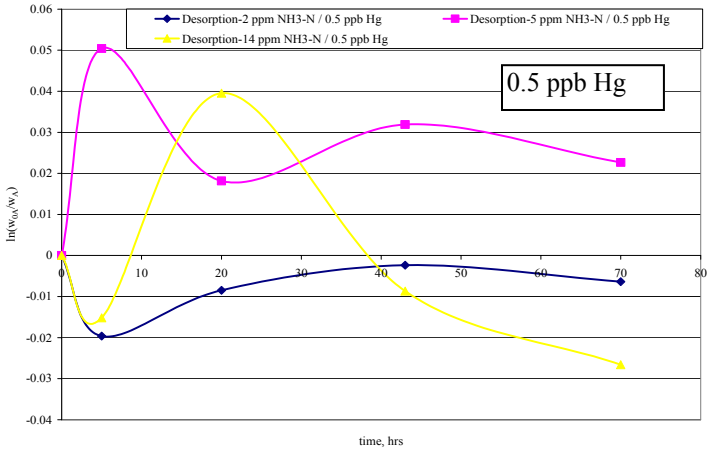

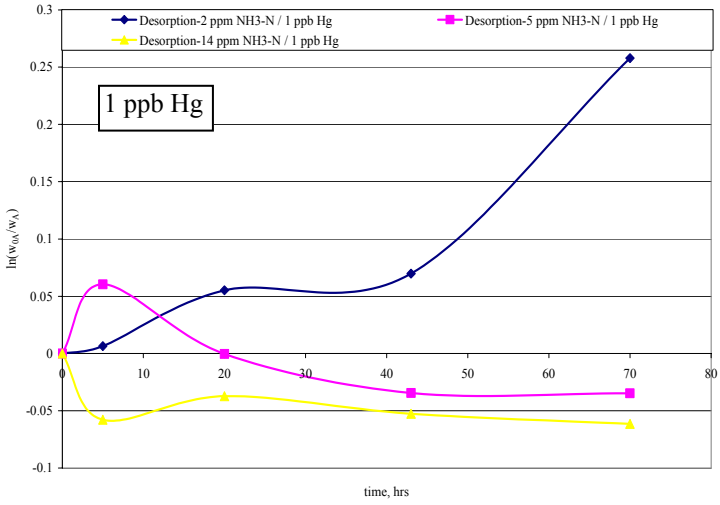

Figure 6.20: Effect of increase of ammonia on mercury desorption

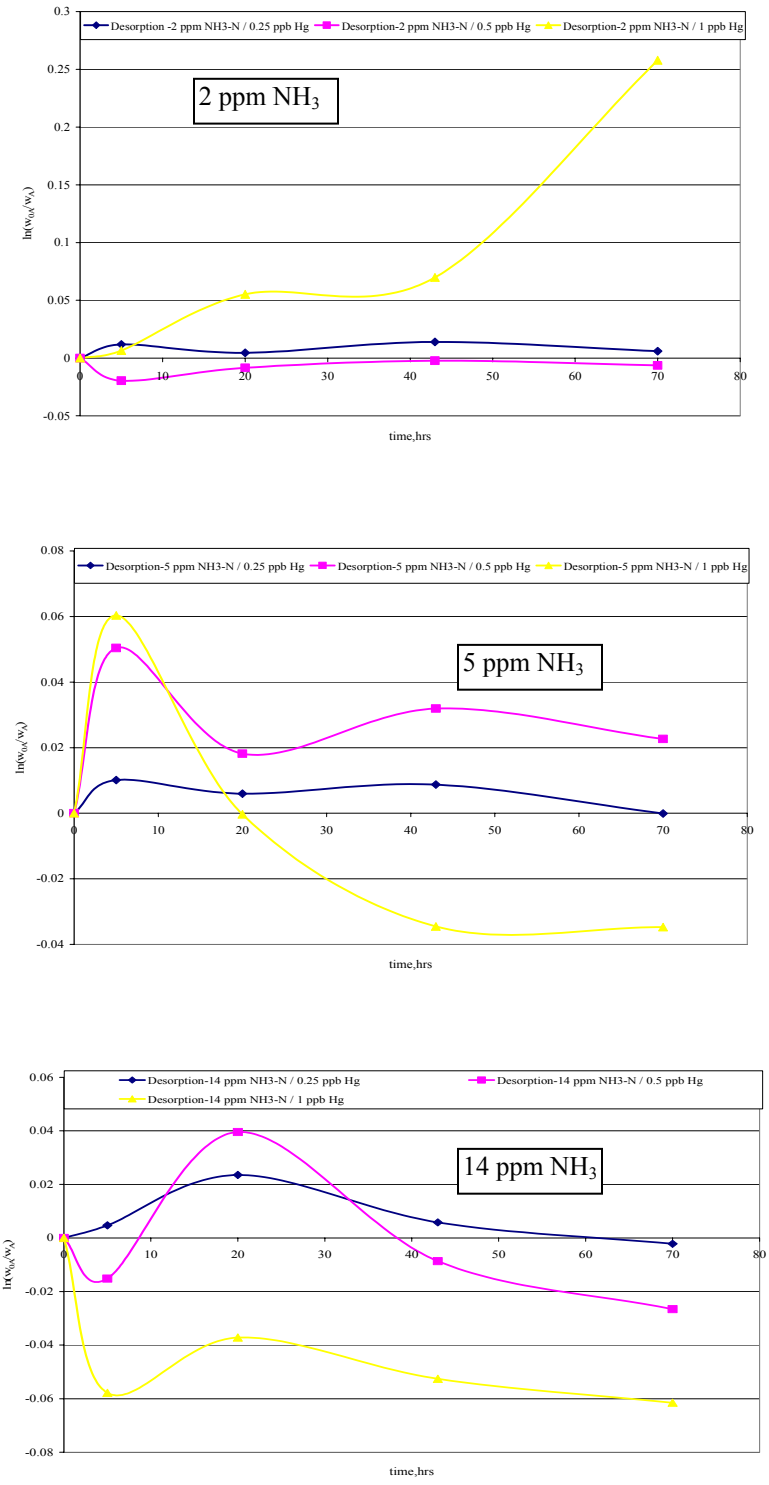

Figure 6.21: Effect of increase of mercury on constant ammonia

time to adsorb / desorb to/from the solids on a real time basis, as the parameter ln (w_{0A}/w_A) is analysed based on the varying concentrations of mercury in ash and ammonia in water with time, which is measured on a batch scale in the laboratory but that will also be nearly true for the continuous ash pond process since the ash and water residence times in ash pond are nearly equal. The ammonia mercury interaction experiment suggests that ammonia has a significant effect on mercury desorption from ash. The more the concentration of ammonia in the ash, the less is mercury desorption from ash. The exact nature of the mercury ammonia complexes formed due to interaction is not known, however the kinetic equation given by Equation 6.4 and incorporated into the model as part of this work assist in predicting accurately the mercury concentration at outfall for a given concentration of mercury in ash and ammonia in water.

CHAPTER 7.0

CHEMCAD MODEL

7.0 Introduction

A generic model of the flue gas side consists of the boiler, economizer, air preheater, SCR unit, ESP and the FGD unit. There is a separate model of the Kingston plant for model validation, where no FGD unit is present. The flue gas side is separated from the ash pond model because the ash pond is modeled as electrolyte model where each component is in ionic form and the reactions (nitrification and eutrophication reactions) are modeled in ionic form, and the flue gas side is modeled as NRTL where composition of components at equilibrium is determined by NRTL equation. Table 7.1 presents the sample analysis results from TVA Kingston plant, which is used as a guideline for model development. The percent nitrogen at the ESP and SCR outlet allows developing the model and designing experiments for nitrification and mercury ammonia interaction by giving an idea about the nitrogen and mercury at various equipment outlet.

7.1 Model of Flue Gas side

The generic flue gas model in ChemCAD is shown as Figure 7.1. The list of process conditions and assumptions used in the model are shown in Table 7.2. The source of the main process data is TVA. Wherever process data is not available from TVA or elsewhere, suitable assumption as listed in Table 7.2 is made. At the temperature of the SCR ammonia breaks down to nitrogen and hydrogen in Gibb's reactor.

Table 7.1: Samples from TVA's Kingston power plant - 19 August 2004(all values in ppm unless otherwise mentioned)

Smpl No.	Sample ID	Sample Description	Remarks	Result							
				Ammonia-N	NO_3-NO_2-N	TKN	%N	%S	Hg,ppm	TDS	TSS
1	1-coal I/L	Coal feed to the unit-1 boiler					1.42	0.79	0.0452		
2	7-coal I/L	Coal feed to the unit-7 boiler					1.39	1.49	0.1612		
3	Eco:1-1	Unit 1 economizer outlet 1st hopper					0.13	0.07			
4	Eco:8-1	Unit 8 economizer outlet 1st hopper					0.09	0.03			
	Economizer 5,6 & 9 doesn't have SCR installed. Hence, economizers are										
	bypassed to AAF. Unit 6 not operating										
5	SCR O/L#1-9	Unit 1 SCR outlet to AAF					0.09	0.06			
6	SCR O/L#7-11	Unit 7 SCR outlet to AAF					0.06	0.03			
7	Bottom Ash-1	Unit 1 boiler bottom ash					0.19	0.19			
8	Bottom Ash Water #1	Unit 1 boiler bottom ash water (results in ppm)		0.01	1.7	6.4		14	0.0024	4930	230
9	Bottom Ash#5-1	Unit 5 sec.1 boiler bottom ash	Unit 6 not operating				0.08	0.01			
10	Bottom Ash Water #5-1	Unit 5 sec.1 boiler bottom ash water(results in ppm)		0.02	0.64	1		9	<0.0001	2220	170
11	Bottom Ash#5-2	Unit 5 sec.2 boiler bottom ash					0.06	0.02			
12	Bottom Ash Water #5-2	Unit 5 sec.2 boiler bottom ash water(results in ppm)		<0.01	0.47	3.1		26	<0.0001	4420	240
13	Bottom Ash#7-1	Unit 7 sec.1 boiler bottom ash					0.22	0.09			
14	Bottom Ash Water #7-1	Unit 7 sec.1 boiler bottom ash water(results in ppm)		<0.01	0.36	5.4		13	<0.0001	####	180
15	Bottom Ash#7-2	Unit 7 sec.2 boiler bottom ash					0.27	0.15			
16	Bottom Ash Water #7-2	Unit 7 sec.2 boiler bottom ash water(results in ppm)		<0.01	0.49	0.45		8	<0.0001	800	160
17	Bottom Ash#9-1	Unit 9 sec.1 boiler bottom ash					0.1	0.26			
18	Bottom Ash Water #9-1	Unit 9 sec.1 boiler bottom ash water(results in ppm)		<0.01	0.5	0.62		8	<0.0001	810	160
19	Bottom Ash#9-2	Unit 9 sec.2 boiler bottom ash					0.11	0.08			
20	Bottom Ash Water #9-2	Unit 9 sec.2 boiler bottom ash water(results in ppm)		0.01	0.47	1.4		20	<0.0001	5280	210
21	AAF # 1-3	Ash from Electrostatic Precipitator(AAF), unit 1, hopper 3					0.11	0.42			
22	AAF # 1-6	Ash from Electrostatic Precipitator(AAF), unit 1, hopper 6					0.11	0.24			
23	AAF # 1-11	Ash from Electrostatic Precipitator(AAF), unit 1, hopper 11					0.22	0.13			
24	AAF # 1-15	Ash from Electrostatic Precipitator(AAF), unit 1, hopper 15					0.19	0.1			
25	AAF # 1-16	Ash from Electrostatic Precipitator(AAF), unit 1, hopper 16					0.17	0.09			
26	AAF # 5-1	Ash from Electrostatic Precipitator(AAF), unit 5, hopper 1					0.08	0.52			
27	AAF # 5-6	Ash from Electrostatic Precipitator(AAF), unit 5, hopper 6					0.08	0.28			
28	AAF # 5-11	Ash from Electrostatic Precipitator(AAF), unit 5, hopper 11					0.09	0.12			
29	AAF # 5-16	Ash from Electrostatic Precipitator(AAF), unit 5, hopper 16					0.22	1.13			
30	AAF # 7-1	Ash from Electrostatic Precipitator(AAF), unit 7, hopper 1	Unit 6 not operating				0.11	0.45			
31	AAF # 7-6	Ash from Electrostatic Precipitator(AAF), unit 7, hopper 6					0.12	0.28			
32	AAF # 7-11	Ash from Electrostatic Precipitator(AAF), unit 7, hopper 11					0.1	0.13			
33	AAF # 7-15	Ash from Electrostatic Precipitator(AAF), unit 7, hopper 15					0.39	0.46			
34	AAF # 9-1	Ash from Electrostatic Precipitator(AAF), unit 9, hopper 1					0.14	0.33			
35	AAF # 9-6	Ash from Electrostatic Precipitator(AAF), unit 9, hopper 6					0.17	0.25			
36	AAF # 9-11	Ash from Electrostatic Precipitator(AAF), unit 9, hopper 11					0.11	0.14			
37	AAF # 9-15	Ash from Electrostatic Precipitator(AAF), unit 9, hopper 15					0.2	0.84			
38	1&2 SCR to pond	Unit 1&2 SCR to pond(results in ppm)		0.01	0.48	0.2		6	<0.0001	260	150
39	SCR 3&4 to pond	Unit 3&4 SCR to pond(results in ppm)		<0.01	0.48	0.18		6	<0.0001	26	140
40	Unit 7&8 SCR to pond	Unit 7&8 SCR to pond(results in ppm)		<0.01	0.48	0.15		6	<0.0001	14	140
41	Unit 1&2 AAF to pond	Water from AAF(Elec. Precip.) of unit 1&2(results in ppm)		<0.01	0.72	2.6		43	0.0011	####	320
42	Unit 5&6 AAF to ash pond	Water from AAF(Elec. Precip.) of unit 5&6(results in ppm)		<0.01	0.43	1.3		15	0.0009	1910	180
43	Unit 7&8 AAF to ash pond	Water from AAF(Elec. Precip.) of unit 7&8(results in ppm)		0.01	1.2	5		72	0.0004	9640	340
44	Unit#9 AAF to pond	Water from AAF(Elec. Precip.) of unit 9(results in ppm)		<0.01	0.42	8.6		44	0.017	####	280
45	1 thru 5 Bottom Ash to pon	Bottom Ash wash water from Unit 1 thru 5(results in ppm)		<0.01	0.59	2		9	0.0002	520	160
46	6 thru' 9 Bottom Ash to pon	Bottom Ash wash water from Unit 6 thru 9 with bottom (results in ppm)		<0.01	0.56	0.32		6	<0.0001	36	150
	with bottom closed	closed, ie, no ash washing taking place									
47	Pond#1	Water from Pond#1(results in ppm)		<0.01	0.38	0.14		20	<0.0001	110	210
48	Pond#2	Water from Pond#2(results in ppm)		0.01	0.22	0.12		22	<0.0001	28	230
49	Pond O/L	Water outlet from ash pond to emory river(results in ppm)		<0.01	0.3	0.14		20	<0.0001	220	220

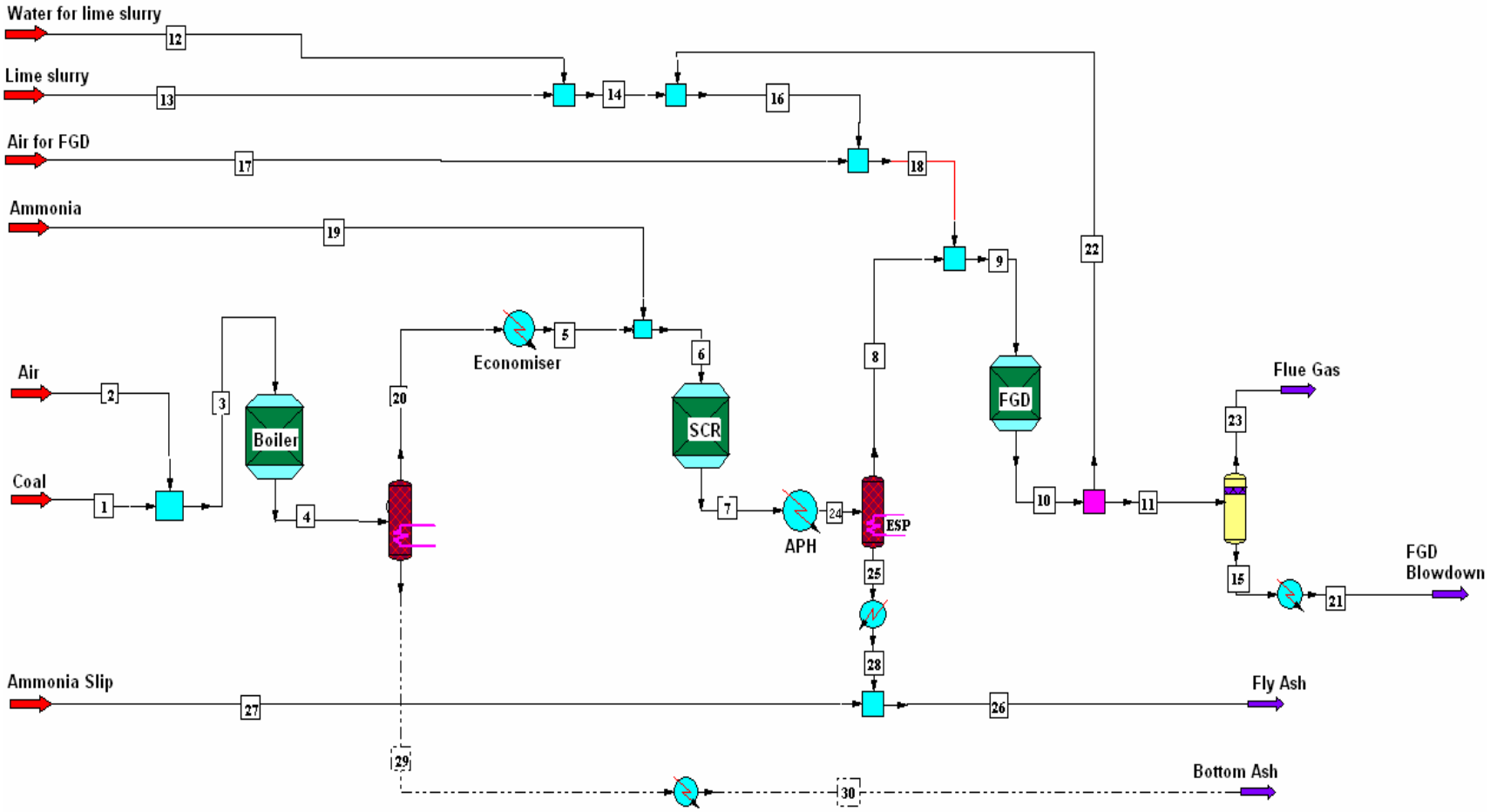

Figure 7.1: Generic Model of flue gas side in ChemCAD

Table 7.2: Process conditions and assumptions used in Model Development

	Case-1	Case-2	Case-3	Case-4
Description	Generic model of flue gas side (no FGD)	Generic model of ash pond (with FGD blow down)	Flue gas model of Kingston power plant (no FGD)	Ash pond model of Kingston power plant (no FGD blow down)
Boiler Temperature	1800^0F	1800^0F	N.A.	N.A.
Ambient/Ash pond Temp.	68^0F	68^0F	68^0F	68^0F
Excess Oxygen	11.1 %	11.1 %	N.A.	N.A.
Ammonia slip*, ppm	1.82	1.82	.08	.08
Mercury Separation, %	With Bottom Ash - 0.49 With Fly Ash-4.1	N.A.	With Bottom Ash** - 0.009 With Fly Ash** - 0.57	N.A.

*1. Ammonia slip for generic condition is specified from literature, which is about 2 ppm.

2. Ammonia slip in Kingston (case 3 & 4) is decided based on analysis of pond water (refer to Table 7.3).

**Mercury separation is evaluated from mercury analysis (Refer to Table 7.4)

Table 7.3: Analysis of mercury and ammonia as N

	Ammonia as Nitrogen, ppm*	Mercury
Bottom Ash	-	0.465 ng/g
Fly Ash	0.0031 %	15.05 ng/g
Pond inlet	0.126	9.8 ng/L
Pond outlet	0	3.2 ng/L

*-Source: Galbraith (appendix-3)

Table 7.4: Coal and lime slurry details

	Coal	Lime slurry
Feed rate, lb/hr	1356997 (TVA input for 9 units of Kingston)	354500 (TVA input for a unit operating FGD)
Coal /lime slurry composition (dry), %		
Carbon	69.35	11.55
Hydrogen	4.06	-
Nitrogen	0.1	-
Oxygen	17.55	-
Sulfur	0.6	0.06
Chlorine	200 ppm	43 ppm
Mercury	0.2 ppm	0.004 ppm
Ash / Solids	8.94	88.4

Hence, the ammonia slip is shown as a separate stream in Figure 7.1 to model the slip. The coal composition and feed rate in both generic model and Kingston plant model is kept same and presented as Table 7.4, the source of which is TVA. The lime feed rate and composition for the FGD unit of the generic model is from a plant of TVA having FGD unit.

7.2 Model of Ash pond

The ash pond receives sluiced fly ash, sluiced bottom ash and FGD blow down in the generic model. The ash pond is modeled for nitrification, eutrophication and mercury desorption from ash. Refer to Figure 7.2 for the Kingston ash pond model. The generic ash pond model has an additional stream for the FGD bow down into the ash pond. However, the ash pond volume is kept same as that in Kingston. The volume in the nitrifier, eutrophication reactor and mercury desorber will depend on the actual volume of the pond, in case the generic model is used for the ash pond.

Equation 4.3 with temperature, DO and pH correction is used for nitrification in the nitrifier. The average values of kinetic constants from Table 6.4 are used in Equation 4.3. Equation 2.24 is used for eutrophication. Equation 6.4 is used in modeling mercury desorption, which takes into account the ammonia mercury interaction also. Oxygen constantly dissolves into the water, as it is consumed during nitrification. The rate of oxygen dissolution is calculated as follows;

$$N_{O2,Z} = k'_{O2} A (\rho^*_{O2} - \rho_{O2}) \quad \text{.....7.1}$$

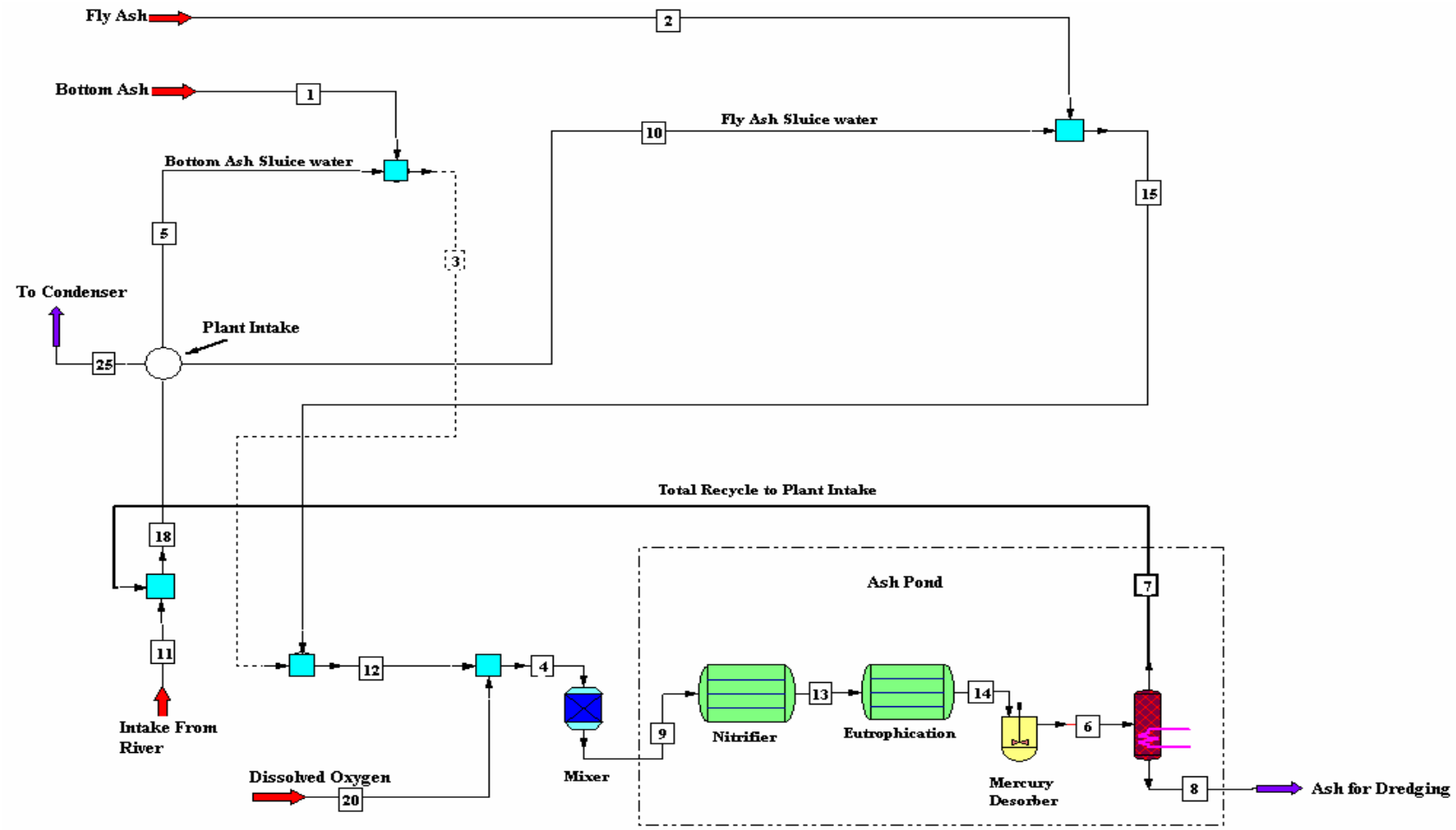

Figure 7.2: Kingston Ash pond model (Case-4)

Where,

$N_{O2,Z}$ = Flux of oxygen dissolution, kg/m^2-hr

k'_{O2} = mass transfer coefficient = 0.0625 m/hr (source: Thibodeaux [52])

A = Area of pond = 400000 m^3 (volume)/ 5m (depth)

ρ^*_{O2} = 12 mg/l = 0.012 kg/m^3 (concentration at air water interface)

ρ_{O2} = 0, assuming rapid consumption of oxygen due to nitrification

Hence, the oxygen dissolution rate is calculated as 60 kg/hr, which is shown as continuous intake in the model flowsheet as dissolved oxygen input to the pond. The carbon dioxide is assumed as 50 ppm in the pond water. The carbon as carbonate presentin the pond water is 600 ppm (source: Galbraith –appendix 4). The VSS of the pond water is 5 ppm and hence biomass in the pond is considered as 5 ppm. The ash pond model is validated and presented in section 7.2.1.

7.2.1 Model validation

The ash pond model is validated for ammonia-N and mercury and presented in Table 7.5. The model prediction for mercury at outlet is quite close, given the ppt (parts per trillion) level of measurement. The ammonia prediction at outlet is zero. However, the analysis result below 0.1 ppm is not reported by commercial laboratories like Galbraith because of the uncertainty in analysis at that level of concentration. The flue gas model is validated by the work done on mercury reemission by Handagama[21]et al (which includes this author). Refer to Figure 7.3 for detailed comparison of actual vs model mercury in flue gas. The entire flue gas system starting from the boiler to the stack was modeled in ChemCAD and the model mercury at various points were compared with actual plant

Table 7.5: Ash pond model validation

	Ammonia-N, ppm		Mercury, ppt	
	Pond Inlet	Pond Outlet	Pond Inlet	Pond Outlet
Actual	0.126	<0.1*	9.8	3.2
Model	0.126	0	9	2.72
Percent difference	0	*	-8.2	-15

- Analysis result by Galbraith at pond outlet is <0.1 ppm (appendix 3), which means anything below 0.1 ppm is not easily detected and reported

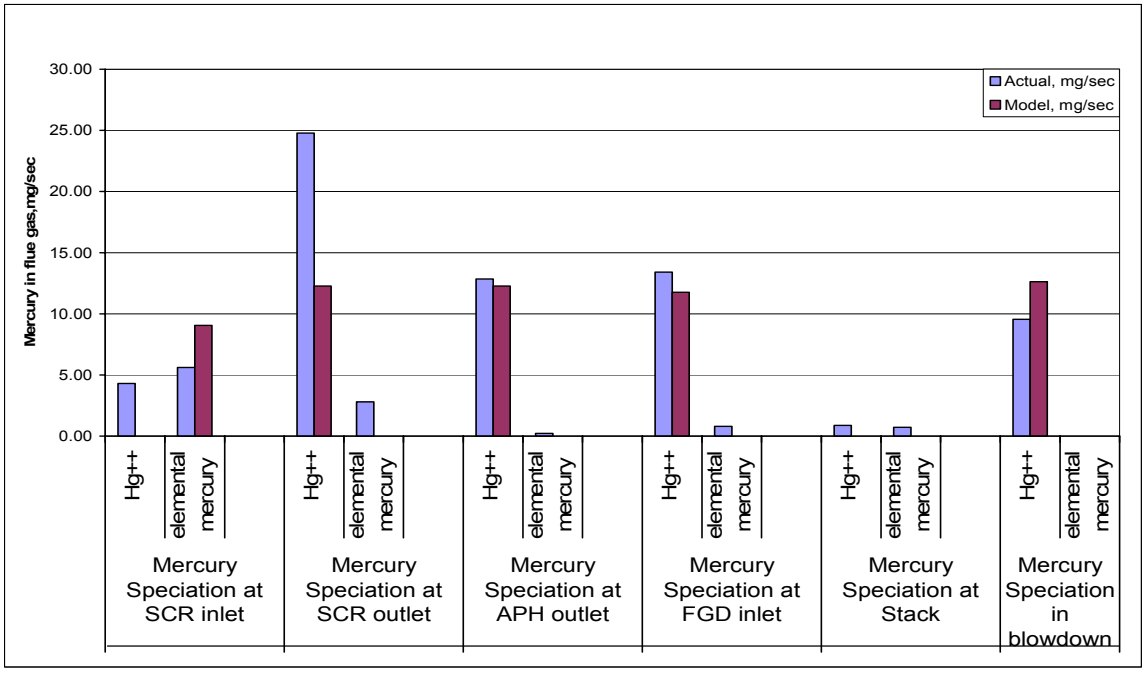

Figure 7.3 Comparison of flue gas mercury (reproduced from Handagama[21] et al)

data. From Figure 7.3, it is evident that except for the SCR outlet, at all other points the actual total mercury is reasonably (~ 15%) close to the model. The SCR outlet mercury in actual data seems erroneous as it is more than the inlet defying material balance principles. The other possibility is instantaneous carryover of deposited mercury from the catalyst bed in SCR.

The summary of the stream to condenser is shown in Table 7.6. The stream to condenser is first mixed with ash pond outlet water and then pumped to the condenser. It contains no mercury and ammonia, as the ash pond outlet water has very low mercury and apparently no ammonia (refer to Table 7.5). This stream after passing through the condenser is then released to the river. Only notable feature in the stream flow is the pH, which is lower (4.16) than normal ash pond water pH of about 6.5-7. The reason for this low pH is the appreciable amount of sulfuric and phosphoric acid formed during the coal burning and subsequently in the flue gas is assumed to condense totally on the fly ash surface. This anomaly in pH can be corrected with the further study of the ash pond with respect to pH. Refer appendix-1 for Kingston plant models and generic models.

7.3 Model Application

The model is applied to four different blends of coal as illustration of the model use. The block diagram shown in Figure 7.4 depicts the important flue gas and sluice water streams. The description of the four different coal blend that is fed to the boiler in the four simulation runs is shown in Table 7.7.

Table 7.6: Summary of flow to condenser (stream 25 in Figure 7.2)

FLOW SUMMARIES		
Stream No.	25.00	
Stream Name		
Temp F	68.00	
pH value	4.16	
Total MGD	1296	
Component mass fractions		
Carbon Dioxide	56	ppm
Water	99.99%	
Biomass	5	ppm
$SO4^{--}$	28	ppm
$H2PO_4^-$	6	ppm
K^+	4	ppm
Ca^{++}	6	ppm
Na^+	4	ppm

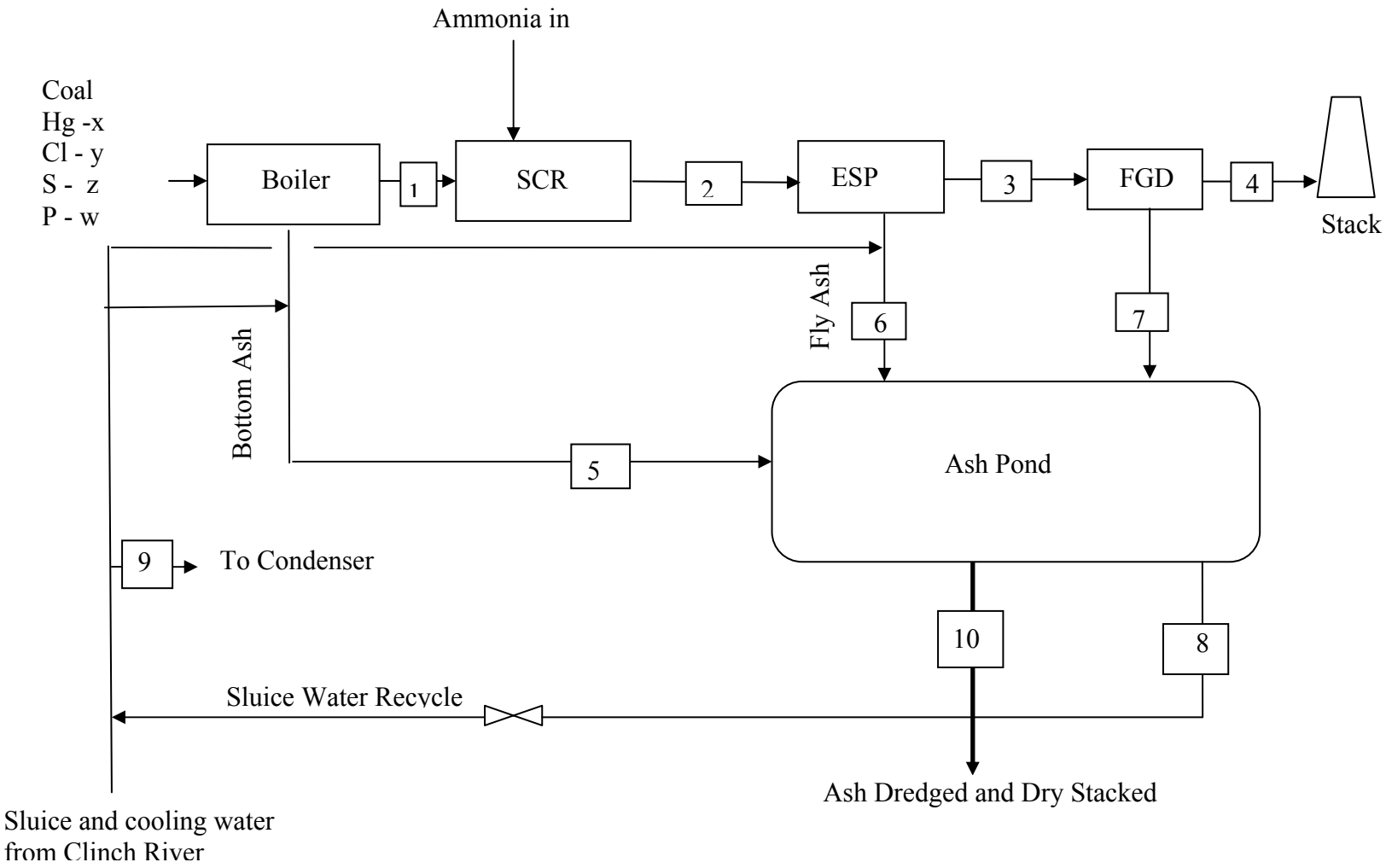

Figure 7.4: Block diagram of flue gas flow and ash pond

Table 7.7: Description of various coal blends simulated

	Blend1(PRB)	Blend2(PRB)	Blend3(Colorado)	Blend4(CAP)
Coal	68.31	67.98	79.19	78.22
Moisture	26.04	26.05	11.2	7.04
Sulfur	0.32	0.34	0.47	0.61
Ash	5.33	5.63	9.14	14.13
Coal Composition,%				
carbon,dry	69.1	68.8	73.3	68.5
hydrogen,dry	5.01	4.64	4.94	4.62
nitrogen,dry	0.94	1.04	1.62	1.05
oxygen,dry	17.3	17.4	9.33	16.4
chlorine,dry	0.006	0.011	0.04	0.007
phosphorus,dry	0.64	0.44	0.49	0.4
Mercury	0.000007	0.00000683	0.00000574	0.00000751
Ash, dry	7.004	7.669	10.28	9.023

The Colorado blend (Blend 3) is quite different from the other three in the carbon and moisture content. The moisture content of the CAP blend (blend 4) is also low but it is offset by the high ash content, resulting in near equal carbon content as the PRB coal. PRB coal (blend 1 and 2) are low sulfur, high moisture coal. These differences in the sulfur, chlorine and moisture content in the blends, has a bearing on the main components prediction shown in Table 7.8 as the mercury and ammonia kinetics are different. The stream numbers in Table 7.8 is to be read in conjunction with the stream numbers shown in Figure 7.4. The simulation runs with the four different coal blends highlights the applicability of the model in effectively predicting the constituents. In all the four runs, it is assumed that the FGD unit is present and that the FGD blowdown flows into the ash pond. The experimental work done in this work is based on neutral pH.

Figure 7.5 shows how the percent nitrification (predicted by the model) and DO varies with ambient temperature, demonstrating another application of the model.

Table 7.8: Stream Properties from simulation run of different coal blends

Stream No.	1				2				3				4			
Name	PRB-blend1	PRB-blend2	CAP	Colorado	PRB-blend1	PRB-blend2	CAP	Colorado	PRB-blend1	PRB-blend2	CAP	Colorado	PRB-blend1	PRB-blend2	CAP	Colorado
- - Overall - -																
Mass flow lb/h	19082476	19082246	2E+07	19042846	19220478	19220246	2E+07	19180846	19100646	19099542	2E+07	18911060	20414178	20420516	20323248	20209174
Temp F	650	650.0000439	650	650	329	329	329	329	329	329	329	329	135.4756	135.0701123	134.14366	132.61619
Pres psia	14.5038	14.50376797	14.504	14.50377	14.5037	14.503754	14.504	14.503754	14.5036	14.50362301	14.504	14.50362	14.5038	14.50376797	14.503768	14.503768
Vapor mass fraction	1	1	1	1	1	1	1	1	1	1	1	1	1	1	1	1
Liquid pH																
Component mass fractions,ppm																
Carbon Dioxide	132129.1476	131857.2015	168530	153473	131123.9004	130852.22	167162	152036.41	131946.519	131679.1773	168849	154205.4	120249.6961	119953.1332	154724.66	141046.15
Mercury	0.003291	0.003195	0.0031	0.004062	0.000011	0.000003	0	0.000005	0.000011	0.000003	0	0.000005	0	0	0	0
Mercuric chlorid	0	0	0	0	0.004539	0.00443	0.0043	0.005594	0.00438	0.004275	0.0042	0.005442	0.000001	0.000001	0.000001	0.000001
Mercuric oxide	0.000104	0.000102	8E-05	0.000116	0.000012	0.000003	0	0.000005	0.000012	0.000003	0	0.000005	0	0	0	0
Ammonia	0	0	0	0	0	0	0	0	0	0	0	0	0	0	0	0
mercury in Ash																
HgCl2 in Ash																
Eth Cyanoacetate																
Algae																
NH4+																
NO3-																
PO4---																

Table7.8: continued

Stream No.	5				6				7				8			
Name	PRB-blend1	PRB-blend2	CAP	Colorado	PRB-blend1	PRB-blend2	CAP	Colorado	PRB-blend1	PRB-blend2	CAP	Colorado	PRB-blend1	PRB-blend2	CAP	Colorado
- - Overall - -																
Mass flow lb/h	2393980	2394183	2E+06	2433724	8119984	8120863	8E+06	8269944	3473739.75	3469751.25	3E+06	3495440	13827925	13818027	1E+07	13846991
Temp F	67.66068848	67.8077832	67.735	67.92967	67.6872998	67.86778076	67.88	68.000166	68	68	68	68	68	68	68	68
Pres psia	14.50376797	14.50376797	14.504	14.50377	14.503768	14.50376797	14.5	14.503768	14.5037699	14.50376797	14.504	14.50377	14.5037699	14.50376797	14.5	14.50377
Vapor mass fraction				0				0				0				0
Liquid pH	6.0765	6.5041	6.2691	6.5662	6.125	6.5499	6.539	6.3924	10.5227	10.5528	10.488	10.4972	10.0567	10.1861	10.06	10.0956
Component mass fractions,ppm																
Carbon Dioxide	380.006648	212.286104	325.3	209.166	419.971067	224.574047	279.3	275.89922	0.000923	0.000796	0.001	0.000822	0.07891	0.04478	0.078	0.065159
Mercury	0.00013	0.000126	0.0001	0.000157	0.000002	0.000001	1E-06	0.000001	0	0	0	0	0.000024	0.000022	2E-05	0.000029
Mercuric chlorid	0.000005	0	0	0	0.000446	0.00043	4E-04	0.000532	0.047364	0.025228	0.0425	0.031195	0	0	0	0
Mercuric oxide	0.000004	0.000004	3E-06	0.000005	0.000001	0	0	0.000001	0	0	0	0	0.000001	0.000001	1E-06	0.000001
Ammonia	0.000038	0	0	0	0.002443	0.006362	0.006	0.004417	0	0	0	0	0	0	0	0
mercury in Ash	0	0	0	0	0	0	0	0	0	0	0	0	0	0	0	0
HgCl2 in Ash	0	0	0	0	0	0	0	0	0	0	0	0	0	0	0	0
Eth Cyanoacetate	4.899758	4.92318	4.8877	4.842885	4.887794	4.911046	4.868	4.822208	0	0	0	0	4.522024	4.524598	4.519	4.515158
Algae	4.786774	4.786473	4.752	4.708406	4.775085	4.774676	4.733	4.688303	0	0	0	0	0	0	0	0
NH4+	0.083338	0	0	0	4.776291	4.688175	4.647	4.605643	0	0	0	0	0	0	0	0
NO3-	0.006422	0.278787	0.2767	0.274266	0.006669	0.278363	0.276	0.273265	0.004261	0.004389	0	0.003436	9.21716	9.226986	9.211	9.208584
PO4---	0.000769	0.003275	0.0024	0.009992	0.001634	0.006603	0.014	0.009315	89.172674	64.202221	89.135	64.47679	432.068569	389.133551	438.9	438.3863

Table7.8: continued

Stream No.	9				10			
Name	PRB-blend1	PRB-blend2	CAP	Colorado	PRB-blend1	PRB-blend2	CAP	Colorado
- - Overall - -								
Mass flow lb/h	438381472	438371616	4E+08	438400576	159906.625	166901	244499	352252.16
Temp F	67.9999219	67.99992188	68	67.999922	68	68	68	68
Pres psia	14.503768	14.50376797	14.504	14.503768	14.5037699	14.50376987	14.504	14.503768
Vapor mass fraction				0				0
Liquid pH	10.4285	10.4733	10.433	10.456	0	0	0	0
Component mass fractions,ppm								
Carbon Dioxide	0.009768	0.008174	0.0097	0.00893	0	0	0	0
Mercury	0.000001	0.000001	1E-06	0.000001	0	0	0	0
Mercuric chlorid	0.000005	0	0	0	0	0	0	0
Mercuric oxide	0	0	0	0	0	0	0	0
Ammonia	0.072	0	0	0	0	0	0	0
mercury in Ash	0	0	0	0	0	0	0	0
HgCl2 in Ash	0	0	0	0	1.328202	0.705277	0.7999	0.406818
Eth Cyanoacetate	4.961028	4.985166	4.985	4.984847	0	0	0	0
Algae	4.846631	4.846737	4.8465	4.846426	327.890302	313.060707	214.23	148.01348
NH4+	0.00717	0	0	0	0	0	0	0
NO3-	0.006502	0.282297	0.2822	0.282306	0	0	0	0
PO4---	1.947224	1.566344	1.9833	1.929483	0	0	0	0

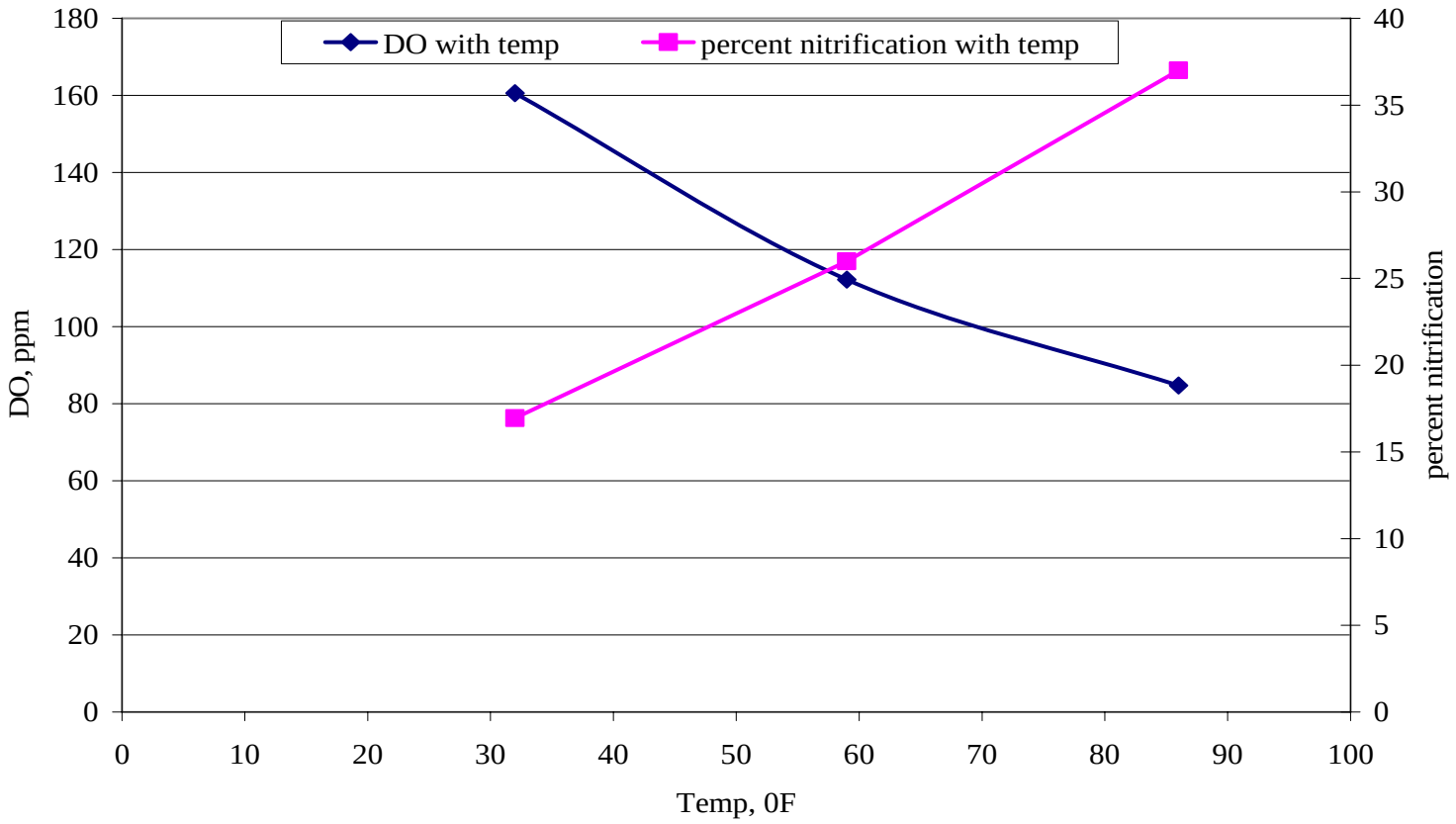

Figure7.5 : Effect of temperature on nitrification and DO

CHAPTER 8.0

WATER USAGE REDUCTION & WATER MANAGEMENT

8.0 Introduction

The water network as it exists in Kingston and shown in Figure 7.2 has the ammonia and mercury content very low in the stream to the condenser (stream 25). So, it is envisaged to do a pinch analysis on the key components such as ammonia and mercury, one component at a time. The pinch analysis is basically aimed at reducing the bottom ash and fly ash sluice water flow to the plant and maintaining the contaminant flow to the river under the level indicated by water quality criteria[1]; ammonia – 0.4 ppm, mercury – 50 ppb. Pinch analysis is first done on ammonia, the water usage evaluated and then it is done on mercury. The water usage is thus optimized. The generic ash pond model is used for pinch analysis and water usage reduction analysis. The generic model has the FGD blow down flowing into the ash pond. Refer Figure 8.1 for the generic ash pond model.

8.1 Pinch Analysis based on ammonia

The input detail for water pinch analysis in *Water Design* [17] based on ammonia is shown in Table 8.1. Fly ash is the only source of ammonia. However, lowest possible values of ammonia are assigned with bottom ash and FGD blow down to enable the program to execute. The notable feature in generic ash pond model is that the FGD blow down is fed in such a way that nitrification is not affected due to rise in pH to about 10.5. At a pH of 10.5, majority of ammonia is unionized and will inhibit nitrification (Cheremisinoff[13]). When FGD blow down is fed to the ash pond in Kingston, care must

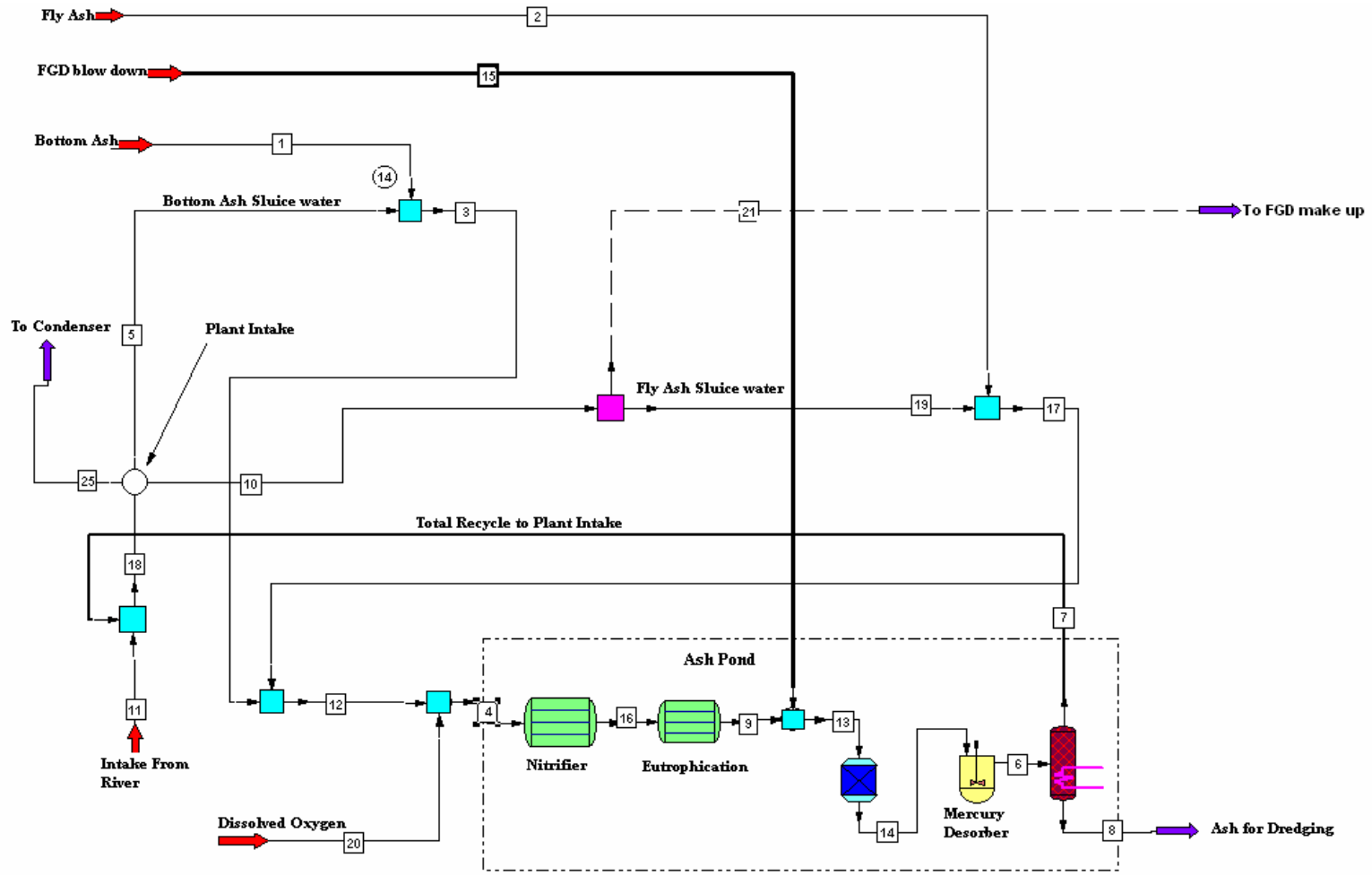

Figure 8.1: Generic ash pond model

Table 8.1: Input details for pinch analysis based on ammonia

Operation	Limiting Flowrate, te/hr	Limiting Inlet Concentration, ppm (Basis:nitrifier outlet in ChemCAD)	Limiting outlet Concentration,ppm	Mass load of ammonia kg/hr
Fly ash Sluicing	3973.63 (basis:Kingston)	0.02	4.6 (Basis: ChemCAD, stream 17, 2ppm at ash pond inlet)	18.2
Bottom ash Sluicing	1075 (basis:Kingston)	0.02	0.03*	0.01
FGD blow down	1322 (basis:TVA)	0.02	0.03*	0.01
Condenser cooling water	204000 (basis:Kingston)	0	0.01	2.04
Regeneration composition : 0.02 ppm (Basis: Nitrifier outlet composition from ChemCAD simulation of generic model)				

* Lowest value assigned to enable the program to run. There is no ammonia carryover with bottom ash, FGD blow down and condenser cooling water

be taken to ensure feeding at a point farthest away from the sluice water inlet to the pond. This may be supported with ash pond flow simulation in COMSOL, which may indicate the best point for feeding FGD blow down. The block diagram of the network will be as in Figure 8.2 with flow details in Table 8.2. The pinch analysis result summary is shown in Figure 8.3. With total regeneration of sluice water and FGD blow down in the ash pond and recycling, the outlet concentration is expected to be 0.1 ppm (as shown in Figure 8.3). Pinch analysis based on ammonia in the present case does not yield any significant result because the only source of ammonia is the fly ash, which is mixed the other streams in the ash pond and regenerated. As the contaminant laden sluice water is recycled totally, the only flow that can be reduced for water usage minimization is the condenser cooling water. The condenser cooling water flow cannot be reduced without compromising the heat duty. The pinch analysis based on mercury is done in the next section.

8.2 Pinch Analysis based on mercury

The pinch analysis based on mercury also suggests no fresh water usage reduction, as the contaminant laden water is recycled as shown in Figure 8.1. The fresh water pinch is suggested at 0.01 ppb, which means the cooling water can be mixed with the other streams after the condenser. However, it can be mixed before it enters the condenser because there is no mercury source in the condenser. Table 8.2 gives the input details for the pinch analysis based on mercury. Figure 8.4 shows the block diagram of pinch analysis based on mercury and Figure 8.5, the summary of result of pinch analysis.

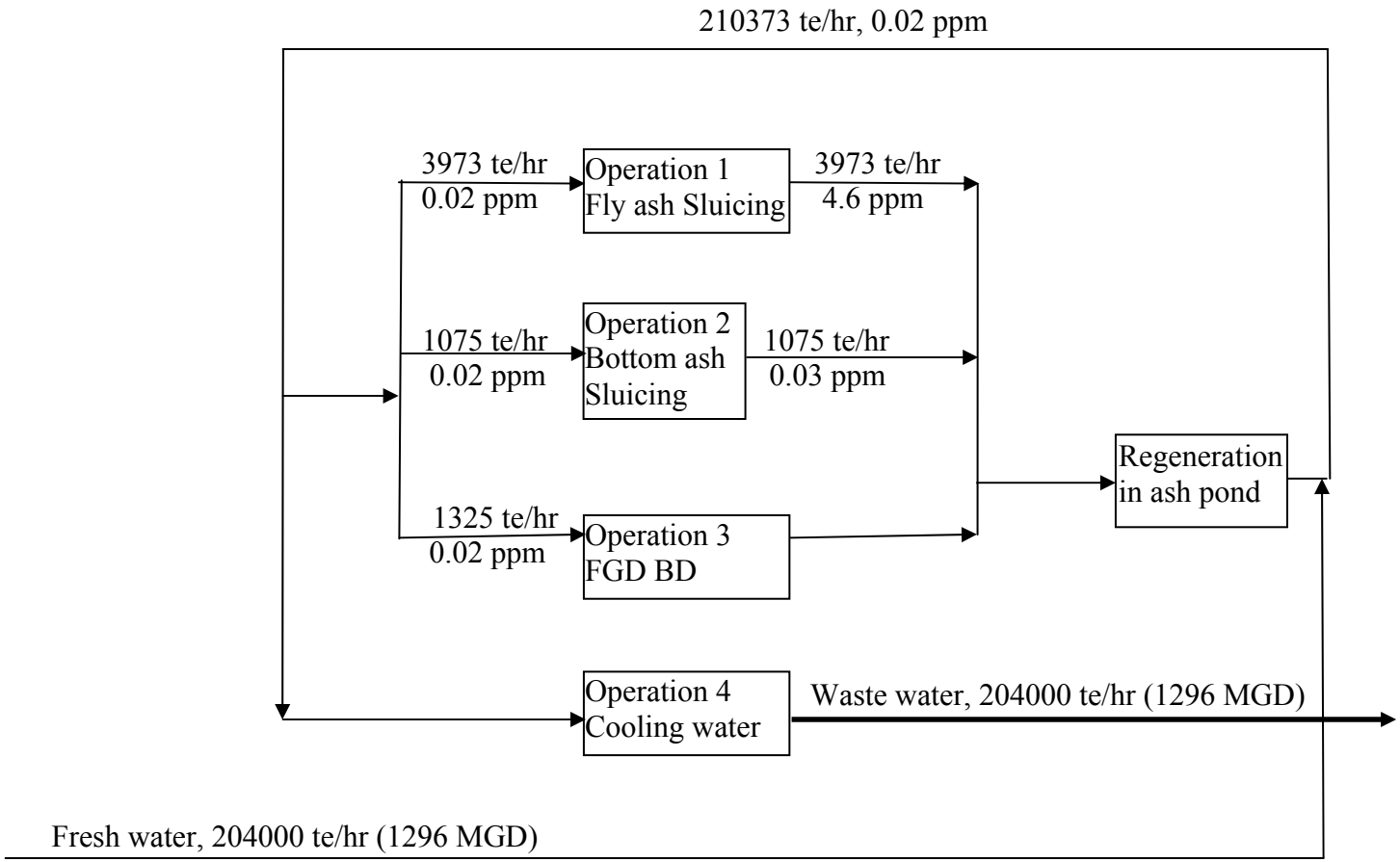

Figure 8.2: Block diagram for pinch analysis based on ammonia

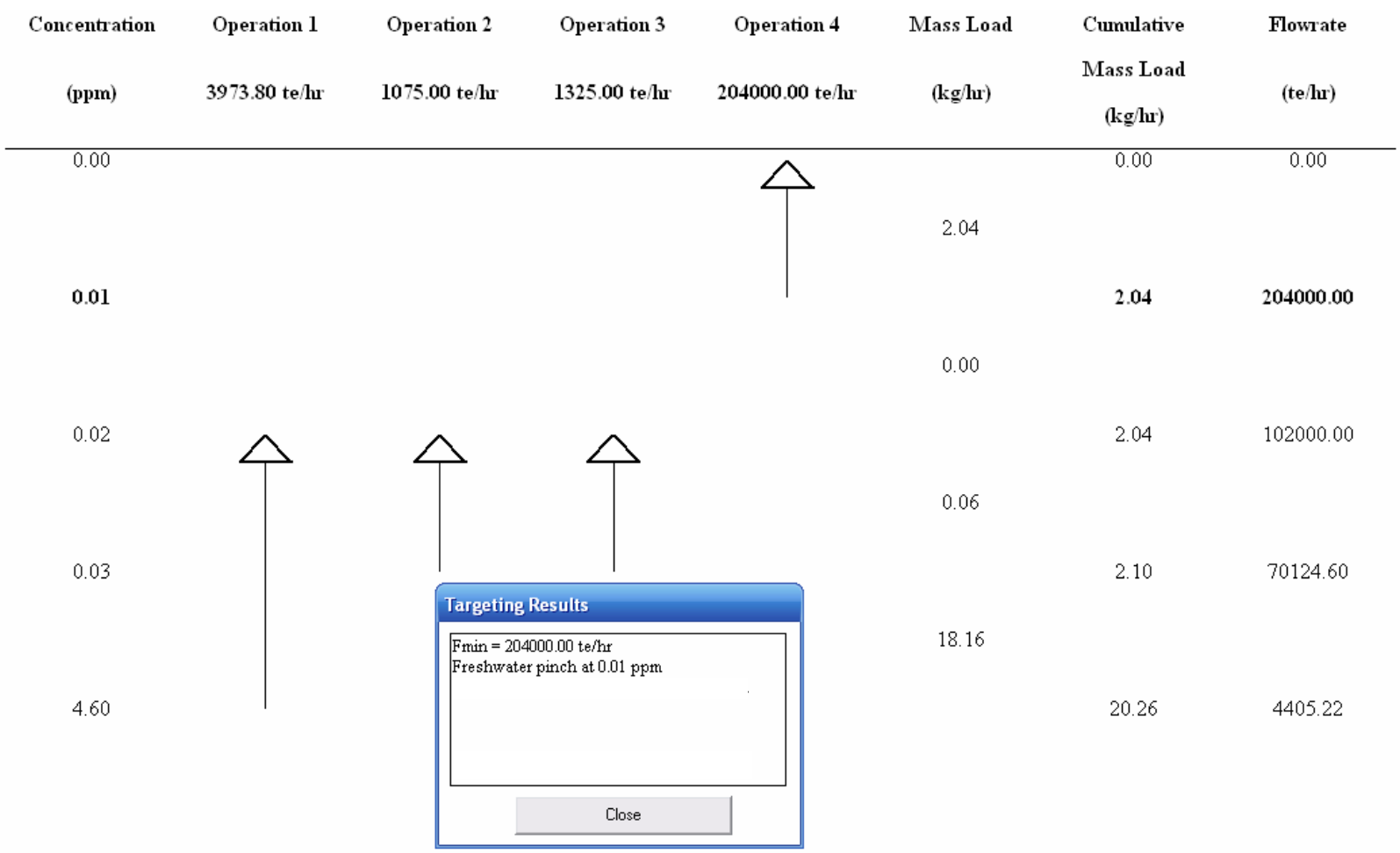

Figure 8.3: Pinch analysis result summary based on ammon

Table 8.2: Input details for pinch analysis based on mercury

Operation	Limiting Flowrate, te/hr	Limiting Inlet Concentration, ppb (Basis:Plant intake in generic model)	Limiting outlet Concentration,ppb	Mass load of mercury g/hr
Fly ash Sluicing	3973.63 (basis:Kingston)	0.03	2.43 (Basis: generic model stream 17)	9.53
Bottom ash Sluicing	1075 (basis:Kingston)	0.03	1.70 (Basis: generic model stream 3)	1.78
FGD blow down	1322 (basis:TVA)	0.03	82.30	108.6
Condenser cooling water	204000 (basis:Kingston)	0	0.01*	2.04
Regeneration composition : 0.83 ppb (Basis: Pond outlet composition from ChemCAD simulation of generic model)				

* Lowest value assigned to enable the program to run. There is no mercury carryover with condenser cooling water

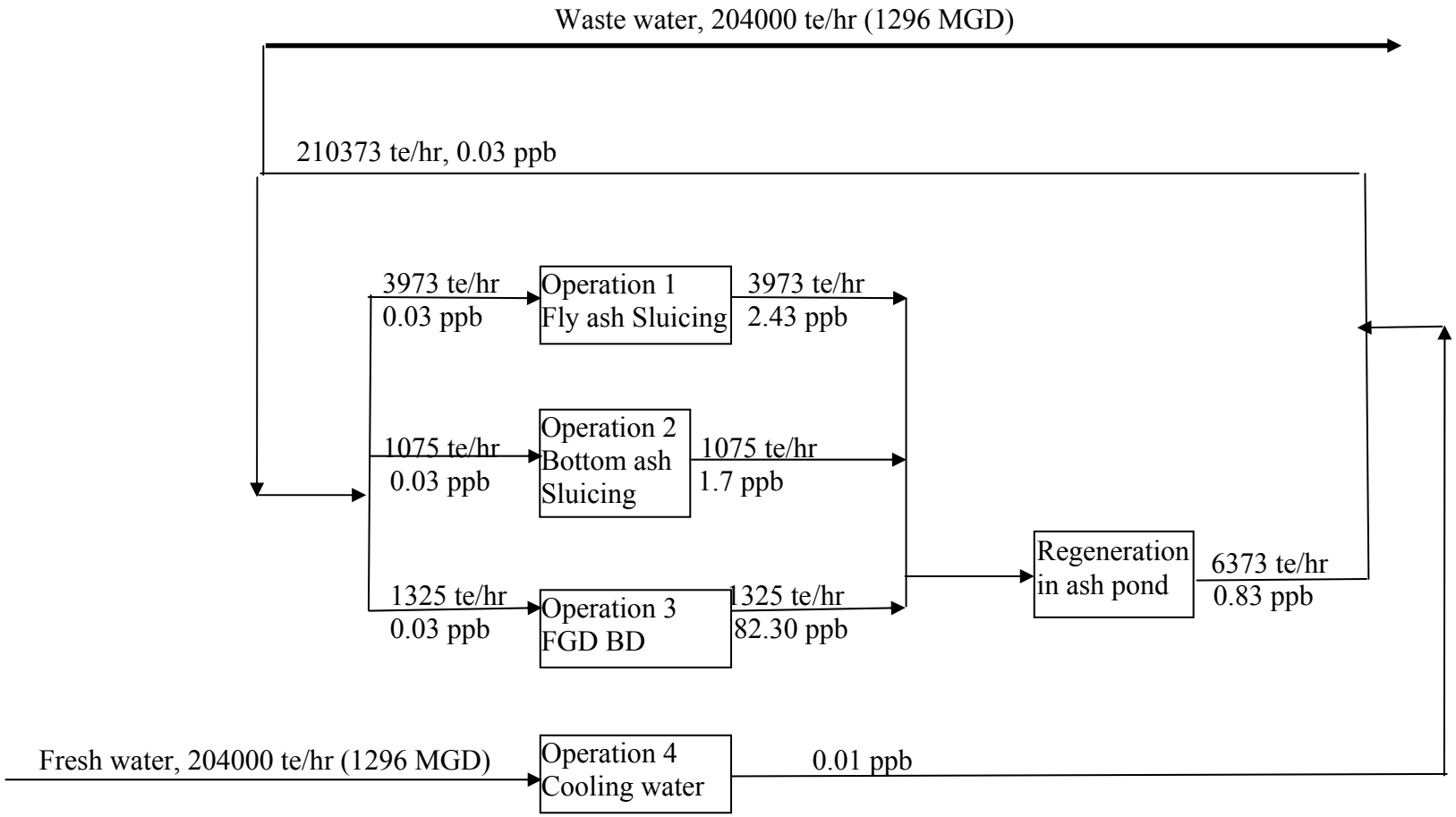

Figure 8.4: Block diagram for pinch analysis based on mercury

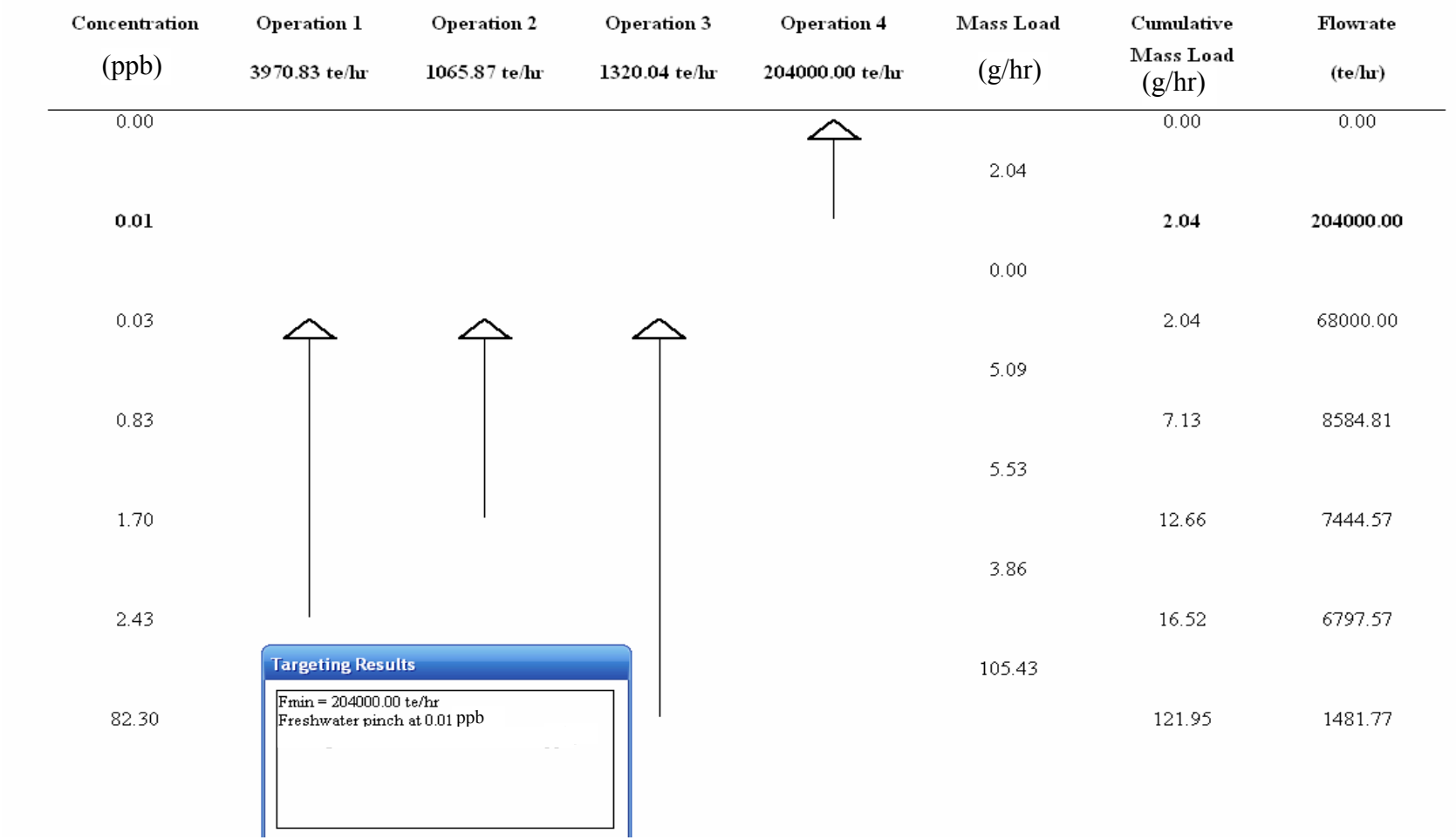

Figure 8.5: Pinch analysis result summary based on mercury

8.3 Sensitivity Study

The sensitivity study is performed based on varying the concentration of ammonia from 2-10 ppm at pond inlet. First, the ammonia sensitivity is studied by increasing the ammonia at pond inlet and see its effect on the ammonia concentration in the effluent. The effluent here is defined as the cooling water outlet from the condenser going into the river. The result is shown in Figure 8.6. The ammonia concentration in the effluent start rising steadily as the pond inlet concentration increases above 4 ppm. This is primarily due to oxygen depletion above 4 ppm, as shown by the simple oxygen balance calculation below;

Oxygen in with inlet water + Oxygen in by convective mass transfer into the pond = Oxygen consumed in nitrification process

Assuming, there is no oxygen accumulation in the pond and oxygen at outlet is zero.

Hence, $Q \times \rho^* + k \times A \times (\rho^* - \rho) = Q \times 4.57 \times (C_{NH4} - 0)$ ……..8.1

Where, Q = flow rate of water to pond = 6375 m^3/h

ρ^* = equilibrium concentration of oxygen in water = 12 g/m^3

ρ = bulk concentration of water = 0 (assuming total consumption)

A = Cross-sectional area of pond = Volume/depth = 400000/5= 80000 m^2

k = mass transfer coefficient = $1.5^{52}/24$ = 0.0625 m/hr

C_{NH4} = Inlet concentration of ammonia with 4.57 g of oxygen consumed per g of ammonium ion oxidized

On plugging all the known values in equation 8.1, C_{NH4} = 4.68 g/m^3 = 4.68 ppm, which

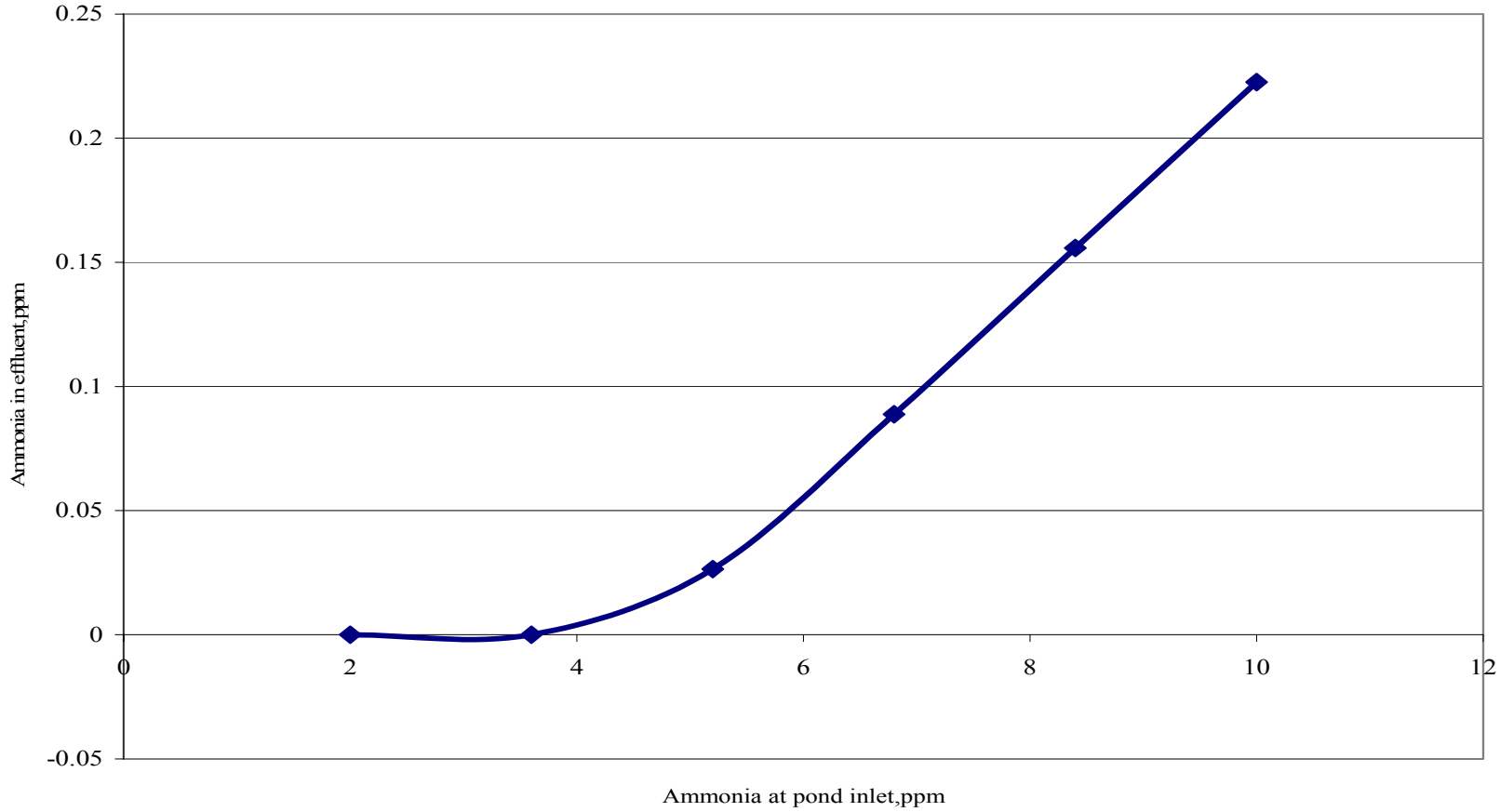

Figure 8.6: Ammonia sensitivity in the water cycle

explains why the ammonia in effluent starts increasing when the ammonia in the pond inlet is above 4 ppm .

The mercury sensitivity with increasing ammonia at the inlet is shown as Figure 8.7. The mercury increases as the ammonia at the inlet increases above 5 ppm, apparently due to increase in ammonia in the effluent which causes some mercury desorption. The mercury concentration in the effluent again start decreasing at ammonia concentration above 7 ppm, due to the achievement of equilibrium of mercury between ash and aqueous phase.

8.4 Conclusions

1. There is very little scope for water usage reduction in TVA's Kingston Power Plant. This is because the main water outlet from the plant is the condenser cooling water, which cannot be reduced without reducing the heat duty of the condenser. Part or the entire portion of the cooling water can be stored in a pond, dyke, etc for cooling and then recycled back. This avoids the dependence of the plant for cooling water from the river and also makes it a zero discharge plant, but requires huge plant area and investment for construction of a pond or a dyke.
2. The ammonia nitrification kinetics and mercury ammonia interaction kinetics accomplished through laboratory experiments and incorporated in the Kingston plant model predicts the ammonia and mercury at the pond outlet quite accurately (~15%). The model and its ability to predict the

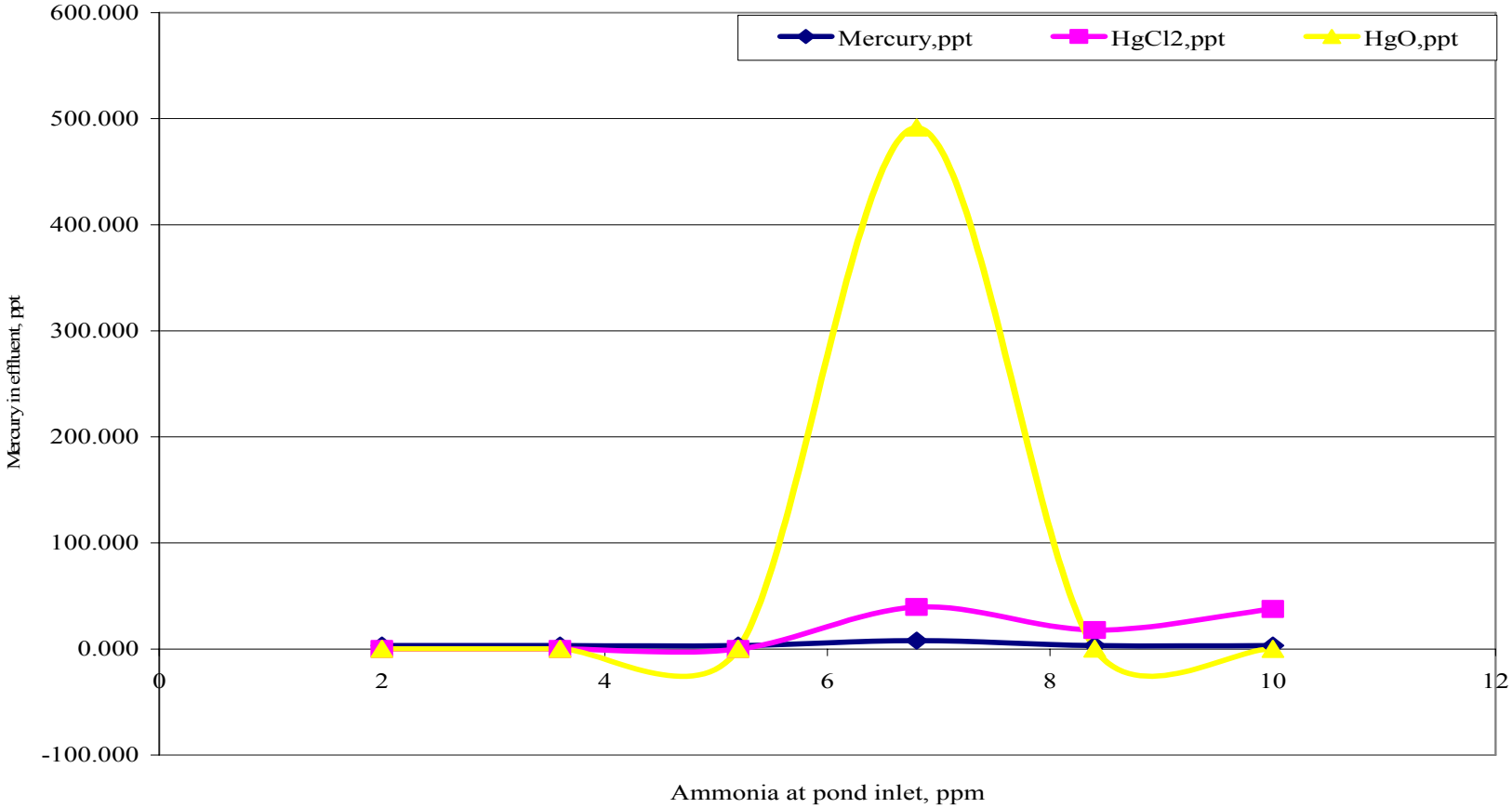

Figure 8.7: Mercury sensitivity with respect to ammonia at pond inlet

various constituents in water from the ash pond of a fossil fuel based power plant is the core of this work.

3. Oxygen is the controlling factor in the nitrification process in the ash pond. A conservative estimate shows that above 4 ppm of ammonia in the inlet, causes the oxygen depletion in the pond resulting in untreated ammonia in the effluent.
4. The ash pond model thus developed together with the laboratory experiments performed to evaluate the kinetic parameters to accurately predict the constituents from the ash pond is unique part of the work. This will be useful in modeling any power plant. The model can be used for studying any future remediation methodology required for the plant and the ash pond.

8.5 Future work

1. One of the future work concerning the ash pond is the introduction of FGD blow down in the ash pond. Since the pH of the blow down is about 10 or more, care must be taken so that nitrification is not affected by the high pH. The tentative point of the FGD blow down introduction is shown in Figure 8.8, which may be confirmed by CFD modeling of the ash pond in COMSOL.

   The ammonia at the outlet of the ash pond from the generic model is still 0 for an inlet $NH_4 - N$ concentration of 2 ppm. Howevr, further study of the

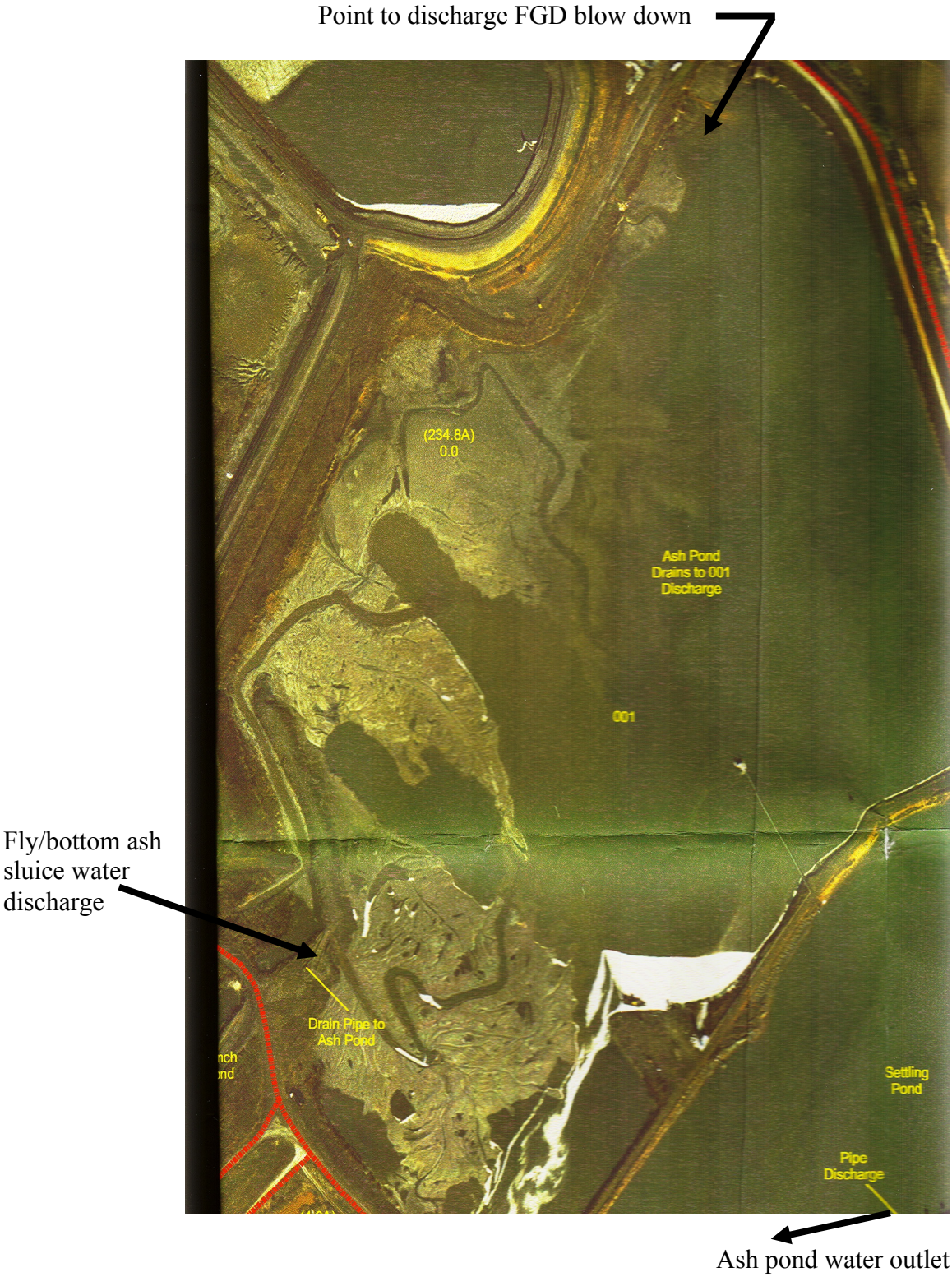

Figure 8.8: Aerial view of Kingston ash pond

2. higher concentration ammonia (> 5 ppm) elimination from ash pond need to be studied by:
   - Biomass addition externally
   - Promote denitrification in stilling pond by adding organic source externally
   - External aeration for nitrification
3. Study the mercury speciation and the remission due to change in:
   - Chlorine in coal
   - Sulfur in coal
4. Arsenic and selenium are the other two elements of concern in the ash pond. The desorption and ammonia interaction kinetics need to be studied and incorporated in the model for prediction of these constituents at the ash pond outlet.

LIST OF REFERENCES

References

1. General water quality criteria. In Tennessee Department of Environment and Conservation: 2004; Vol. Chapter 1200-4-3.

2. International programme on chemical safety environmental health criteria. In EHC, Ed. 1986.

3. Mercury information clearinghouse;quarter 4 - rerelease of mercury from coal combustion by-products; Canadian Electricity Association: October 2004.

4. A.Pollice; V.Tandoi; C.Lestingi, Influence of aeration and sludge retention time on ammonium oxidation to nitrite and nitrate. *Water Research* 2002, 36, 2541-2546.

5. B.Handagama, N., Coal composition and mercury speciation in flue gas. to Bagchi, Bratendu, 2005.

6. Burnett; Thomas, Personnel communication. In Research and Technical Applications,TVA: April, 2005.

7. C.Anthonisen, A.; C.Loehr, R.; S.Prakasam, T. B.; G.Srinath, E., Inhibition of nitrification by ammonia and nitrous acid. *Journal of the Water Pollution Control Federation* 1976, 48, 835-852.

8. C.Chapra, S., *Surface water-quality modeling*. WCB/McGraw-Hill: 1997.

9. C.Fux; K.Lange; A.Faessler; P.Huber; B.Grueniger; H.Siegrist, Nitrogen removal from digester supernatant via nitrite - sbr or sharon? *Water Science and Technology* 2003, 48, 9-18.

10. C.Hellinga; Schellen, A. A.; W.Mulder, J.; VanLoosdrecht, M. C.; J.Heijnen, J., The sharon process: An innovative method for nitrogen removal from ammonium-rich waste water. *Water Science and Technology* 1998, 37, 135-142.

11. C.N.Sawyer; P.L.McCarty, *Chemistry for environmental engineering*. McGraw Hill Inc.: New York, 1978.

12. Cardone, C.; Kim, A.; Schroeder, K., Release of ammonia from SCR/SNCR fly ashes. In NETL: 2005.

13. Cheremisinoff, N. P., *Biotechnology for waste and wastewater treatment*. 1996.

14. D.Allison, J.; L.Allison, T.; B.Ambrose, R. *Partition coefficients for metals in surface water, soil, and waste*; EPA/600/R-05/074; U.S. Environmental Protection Agency: July 2005.

15. D.Foerter; W.Jozewicz; K.Srivastava, R. *Cost of selective catalytic reduction (scr) application for nox control on coal-fired boilers*; EPA/600/R-01/087; U.S. Environmental Protection Agency: Washington D.C., 2001.

16. Dowling, C. B.; Poreda, R. J.; Basu, A. R.; Peters, S. L.; Aggarwal, P. K., Geochemical study of arsenic release mechanisms in the bengal basin groundwater. *WATER RESOURCES RESEARCH* 2002, 38.

17. G.Mann, J.; Y.A.Liu, *Industrial water reuse and wastewater minimization*. McGraw Hill: New York, 1999.

18. Garrido; Benthum, J. M. v.; J., W. A.; Loosdrecht, v.; M, M. C.; J.J.Heijnen, Influence of dissolved oxygen concentration on nitrite accumulation in a biofilm airlift suspension reactor. *Biotechnology and Bioengineering* 1997, 53, 168-178.

19. Gerke, S.; Baker, L. A.; Xu, Y., Nitrogen transformations in a wetland receiving lagoon effluent: Sequential model and implications for water reuse. *Water Research* 2001, 35, (16), 3857-3866.

20. Handagama, N., Re-emission of elemental mercury across FGD.to Bagchi, Bratendu, Ed. Tennessee Valley Authority: Knoxville, 2005.

21. Handagama, N.; Bagchi, B.; Bienkowski, P., A thermodynamic approach to analyze elemental mercury reemission across calcium-based wet scrubbers in coal-fired thermoelectric power plants. *Air & Waste Management Association (In review)* 2006.

22. Hansen, E.; Christ, M. *Suggested next steps to develop nutrient criteria for lakes and reservoirs in west virginia*; WV NUTRIENT CRITERIA COMMITTEE: West Virginia Rivers Coalition, June 20, 2003.

23. Hawkins, S. A. The rrnat/rdna ratio as a measure of nitrite oxidizing activity. Dissertation, University of Tennessee, Knoxville, 2005.

24. J.J.Biscogni; C.T.Driscoll, Denitrification using thiosulfate and sulfide. *Jour. Env. Eng. Div.* 1977, 103, 593.

25. J.M.Smith; H.C.VanNess; M.M.Abbott, *Introduction to chemical engineering thermodynamics*. Fifth ed.; McGraw-Hill: 1996.

26. K.Chandran. Biokinetic characterization of ammonia and nitrite oxidation by a mixed nitrifying culture using extant respirometry. University of Connecticut, Storrs, 1999.

27. K.Emerson; R.C.Russo; R.E.Lund; R.V.Thurston, Aqueous ammonia equilibrium calculations:Effect of ph and temperature. *Journal of Fish. Res. Board Can.* 1975, 32, 2379-2383.

28. K.Gale, T.; L.Merritt, R.; M.Cushing, K.; R.Offen, G., Mercury speciation as a function of flue gas chlorine content and composition in a 1 mw semi-industrial scale coal-fired facility. In *Proceedings of the Mega Symposium and Air & Waste Management Association's SpecialtyConference*, Washington, DC, 2003.

29. K.Hanaki; Wantawin, C.; S.Ohgaki, Nitrification at low levels of dissolved oxygen with and without organic loading in a suspended-growth reactor. *Water Research* 1990, (24:297-302).

30. K.Ladwig *Effects of ammonia on trace element leaching from coal fly ash*; 1010063; EPRI: December, 2005.

31. L.Shorney, F.; Grobmyer, W. P.; Taylor, G., Zero discharge water treatment design has high reliability. *Power Engineering* 1995, (October).

32. Leeman, L. *Ps200 automated mercury analyzer set-up and operating manual*; Part No. 150-00016; Massachusetts, 1991.

33. Licata, A.; Balles, E.; Schuttenhelm, W. In *Mercury control alternatives for coal-fired power plants*, Power Gen 2002, Orlando, Fl, December 2002; Orlando, Fl, December 2002.

34. M.Brick, C.; Moore, J. N., Daily variation of trace metals in the upper clark fork river, montana. *Environ. Sci. Technol.* 1996, 30, 1953-60.

35. Manan, Z. A.; Yee, D. F. C. In *Setting targets for water and hydrogen networks using cascade analysis*, AIChE Annual Meeting, San Francisco, Nov 16-21, 2003; San Francisco, 2003.

36. Metcalf; Eddy, *Wastewater engineering treatment disposal, and reuse*. Third ed.; McGraw-Hill Book Co: New York, 1995.

37. N.Bernet; P.Dangcong; J.P.Delgenès; R.Moletta, Nitrification at low oxygen concentration in biofilm reactor. *Journal of Environmental Engineering* 2001, 127, 266-271.

38. O.Turk; D.Mavinic, Benefits of using selective inhibition to remove nitrogen from highly nitrogenous wastes. *Environmental Technology Letters* 1987, 8, 419-426.

39. P.Chu, Pisces water characterization field study. In Manager, Project, Ed. EPRI: June 2000; Vol. Final Report.

40. P.Murarka, I.; J.Hassett, D.; F.Pflughoeft-Hassett, D.; V.Heebink, L. In *Leaching of selected constituents from ammoniated fly ash from a coal-fired power plant*, International Ash Utilization Symposium, Center for Applied Research, University of Kentucky, 2003; Center for Applied Research, University of Kentucky, 2003.

41. P.Wang, Y.; Smith, R., Design of distributed effluent treatment systems. *Chemical Engineering Science* 1994, 49, 3127.

42. Philips, S.; Wyffels, S.; Sprengers, R.; Verstraete, W., Oxygen-limited autotrophic nitrification/denitrification by ammonia oxidisers enables upward motion towards more favourable conditions. *Applied microbiology and biotechnology* 2002, 59, 557-566.

43. Richardson, C.; Machalek, T.; Miller, S.; Dene, C.; Chang, R., Effect of nox control processes on mercury speciation in utility flue gas. *Air & Waste Management Association* 2001, 52, (August), 941-947.

44. S.Diab; M.Kochba; D.Mires; Y.Avnimelech, Combined intensive-extensive (cie) pond system. A: Inorganic nitrogen transformations. *Aquaculture* 1992, 101, 33-39.

45. S.Prakasam, T. B.; C.Loehr, R., Microbial nitrification and denitrification in concentrated wastes. *Water Research* 1972, 6, 859-869.

46. Sharma, V. K., Zero water discharge systems a must for many waste-to-energy plants. *Power Engineering* 1989, (January).

47. Sigling, R.; Khalaf, C.; Healy, E. In *Enhance ammonia distribution for maximum scr performance*, Institute of Clean Air Companies Forum, Nashville,TN, October 14-15, 2003; Nashville,TN, 2003.

48. Southworth, G., Mercury measurement in ash and water samples. In Bagchi, Bratendu, Ed. Knoxville, 2006.

49. T.Wilburn, R.; L.Wright, T., Scr ammonia slip distribution in coal plant effluents and dependence upon so_3 2004. *PowerPlant Chemistry* 2004.

50. TheHongkongElectricCompany *Units l4 & l5 flue gas desulphurization plant retrofit project*; LAMMA POWER STATION: 2005.

51. Theis, T. L.; Wirth, J. L., Sorptive behavior of trace metals on fly ash in aqueous systems. *Environmental Science & Technology* 1977, 11(12), 1096-1110.

52. Thibodeaux, L. J., *Environmental chemodynamics*. Second ed.; John Wiley & Sons, Inc.: 1996.

53. TURNER, A.; MILLWARD, G. E.; M.LEROUX, S., Sediment-water partitioning of inorganic mercury in estuaries. *Environ. Sci. Technol.* 2001, 35, (23), 4648-4654.

54. U.Abeling; F.Seyfried, C., Anaerobic-aerobic treatment of high strength ammonium wastewater - nitrogen removal via nitrite. *Water Science and Technology* 1992, 26, 1007-1015.

55. W.Bae; S.Baek; J.Chung; Lee, Y., Optimal operational factors for nitrite accumulation in batch reactors. *Biodegradation* 2002, 12, 359-366.

56. Wang, J.; Ban, H.; Teng, X.; Ladwig, K. *The effect of ammonia on the leaching of cu(ii) and cd(ii) from fly ash*; EPRI.

57. Wang, Y. P.; Smith, R., Wastewater minimization. *Chemical Engineering Science* 1994, 49, 981-1006.

58. Webb, L.; Weiss, K., True zero discharge and wastewater design considerations. *Power Engineering* 1989, (July).

59. Yantarasri, T.; GarciaIII, A.; Brune, D., Thermodynamic model of nitrification kinetics. *Journal of Environmental Engineering* 1992, 118, (July/August), 568-584.

APPENDIX

Appendix-1

See attached files consisting of the following ChemCAD models used in this work;

1. Generic flue gas model
2. Kingston flue gas model
3. Generic ash pond model
4. Kingston ash pond model
5. Sensitivity study

These models need ChemCAD 5.5 or higher version installed in the system for viewing. Simply insert the CD in the CD ROM and wait. If the main page does not load automatically it can be opened via a file manager. If this document is being read electronically, simply click on the hyperlink of the model to be viewed. The following message will come while the file is being opened, click on no and then follow instructions.

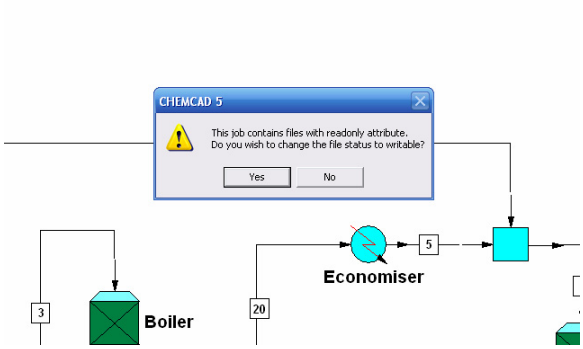

GALBRAITH LABORATORIES, INC.

LABORATORY REPORT

Bratendu Bagchi
University of Tennessee
Dept Of Chemical Engineering
419 Dougherty Engineering
Knoxville TN 37996

Report Date: 07/18/06

Purchase Order #: VISA,Holiway

Fax Number: 865-974-7076

SAMPLE ID	LAB ID	ANALYSIS	RESULT(S)		MATRIX SPIKE RECOVERY	
1	Z-5644	Ammonium	14	ppm	95.6	%
2	Z-5645	Ammonium	13	ppm		
3	Z-5646	Ammonium	12	ppm		
4	Z-5647	Ammonium	1.4	ppm		
5	Z-5648	Ammonium	1.4	ppm		
6	Z-5649	Ammonium	1.8	ppm		
7	Z-5650	Ammonium	5.0	ppm		
8	Z-5651	Ammonium	5.2	ppm		
9	Z-5652	Ammonium	4.8	ppm		
10	Z-5653	Ammonium	12	ppm		
11	Z-5654	Ammonium	13	ppm		
12	Z-5655	Ammonium	13	ppm		

Authorized Release of Data

Pat DeLozier, Production Coordinator

PD:yb D5

Mailing: P.O. Box 51610 | Knoxville, TN 37950-1610
Toll Free: 1.877.449.8797
www.galbraith.com
Shipping: 2323 Sycamore Dr. | Knoxville, TN 37921-1700
Fax: 865.546.7209

LABORATORY REPORT

Bratendu Bagchi
University of Tennessee
Dept Of Chemical Engineering
419 Dougherty Engineering
Knoxville TN 37996

Report Date: 07/27/06

Purchase Order #: VISA,Holiway

Fax Number: 865-974-7076

SAMPLE ID	LAB ID	ANALYSIS	RESULT(S)	
Pond Inlet	Z-6126	Ammonia	0.15	mg/L
Pond Outlet	Z-6127	Ammonia	< 0.1	mg/L
ESP Fly Ash	Z-6128	Ammonia	0.0031	%

Authorized Release of Data

_____
Pat DeLozier, Production Coordinator

PD: cb G8 Page 1 of 1

LABORATORY REPORT

Bratendu Bagchi
University of Tennessee
Dept Of Chemical Engineering
419 Dougherty Engineering
Knoxville TN 37996

Report Date: 08/08/06

Purchase Order #: VISA,Holiway

Fax Number: 865-974-7076

SAMPLE ID	LAB ID	ANALYSIS	RESULT(S)		MATRIX SPIKE RECOVERY	
Pond Inlet	Z-6129	Carbonate as Carbon	< 0.06	%		
Pond Inlet	Z-6130	Nitrate as Nitrogen	< 0.2	ppm	90.7	%
Pond Outlet	Z-6131	Nitrate as Nitrogen	< 0.2	ppm		
Pond Inlet	Z-6132	Sulfur (ICP)	10	ppm		
Pond Outlet	Z-6133	Sulfur (ICP)	26	ppm		
Pond Inlet	Z-6134	Phosphorus	< 2	ppm		
Pond Outlet	Z-6135	Phosphorus	< 2	ppm		

Authorized Release of Data

_____
Pat DeLozier, Production Coordinator

PD: cb H4

Page 1 of 1

Vita

Bratendu Bagchi was born in Ranchi, India on November 11th, 1968. He received a Bachelor of Science in Engineering with a major in Chemical Engineering in 1990 from Ranchi University. Mr. Bagchi worked 10 years in the design and engineering field, designing and engineering various kinds of chemical plant before entering the graduate program full time at the University of Tennessee in August, 2000. He graduated with a Master of Science in Chemical Engineering in December, 2002 and completed the requirements for a Doctor of Philosophy degree in Chemical Engineering in December, 2006.